



UiT

THE ARCTIC
UNIVERSITY
OF NORWAY

Faculty of Science and Technology, Department of Engineering and Safety

Feasibility study of Unmanned Aerial Vehicles (UAV) application for ultrasonic Non-Destructive Testing (NDT) of Wind Turbine Rotor Blades

Preliminary experiments of handheld and UAV ultrasonic testing on glass fibre laminate

Simon Kleppevik Skaga

Master thesis in Technology and Safety in the High North, June 2017



ABSTRACT

In this thesis, we have conducted a feasibility study on UAV application for ultrasonic pulsed non-destructive testing of wind turbine rotor blades. Due to the high initial cost of wind turbines, and their decreasing availability due to increasing size and offshore locations, it is imperative to properly maintain these structures over their 10-30-year lifetime. Operation and maintenance costs can account for 25-30% of the overall energy generation costs (Martinez-Luengo, et al., 2016), where the wind turbine rotor blade can be considered the most critical component, accounting for 15-20% of the manufacturing costs. Thus, an increase in O&M efficiency of wind turbine rotor blades through condition monitoring can yield substantial financial benefits.

Currently, Unmanned Aerial Vehicles (UAV) are in use for visual and thermography inspection of wind turbines. These techniques for structural condition monitoring does have serious limitations, as the condition of internal components in blades, built from glass fibre laminates, cannot be visually inspected. However, pulsed ultrasonic echo technique have proven highly efficient for wind turbine rotor blade inspection. The ultrasonic transducer requires surface contact with the examined material, and we investigated the potential of UAV implementation for fast, safe and reliable measurements of wind turbine rotor blades.

This feasibility study investigates the applicability of ultrasonic testing of glass fibre laminates, specifically glass fibre produced by Lyngen Plast A/S. Firstly, we conducted handheld ultrasonic tests on simulated delamination defects, looking for damage indications on a voltage-time graph. Secondly, we induced damage on a 27mm thick sample through a 3-point bending test and measured the echo response from the ultrasonic pulse. The second experiment was repeated using a Storm AntiGravity UAV, producing promising results with preliminary instrumentation.

A significant challenge to the feasibility of this study was the operational risks. We carried out a preliminary and qualitative risk assessment of the intended UAV operation by using the SWIFT-analysis and Bow-Tie method. The results were two important risk mitigating measures. Risk reductive: "Design UAV for impact with wind turbine rotor blades," and risk preventive: "Develop statistical data on wind conditions at wind turbine site, calculate low-risk dates for flight." The implementation of the said measures, quality of our results, experiences from the UAV flight and concept considerations are presented throughout this paper. In the end, a conclusion is drawn and topics for future studies is presented.

Keywords: *Unmanned Aerial Vehicles, Wind Turbines, Wind Turbine Rotor Blades, Non-Destructive Testing, Risk Analysis, Ultrasonic Pulsed Echo Technique, Feasibility Study, Ultrasonic Experiments*

PREFACE AND ACKNOWLEDGEMENTS

The submission of this thesis marks the completion of my master's degree in Technology and Safety in the High North at the University in Tromsø, Norway. This thesis has been written between February and May 2017, and is to be handed in on Thursday 1.06 2017.

I would like to thank my supervisor Jarle André Johansen for his efforts and enthusiasm during the writing of this thesis. He has been of great assistance in specifying the research objectives and developing the optimal approach. His influence in planning and executing the experiments, as well as coordinating with participating personnel at the University in Tromsø, facilitated the completion of this thesis. I would also like to thank Bernt Inge Hansen for providing the Storm AntiGravity UAV used in our experiments and his valuable UAV pilot experience.

The contribution of glass fibre laminates from Lyngen Plast A/S made our experiments possible, and their generosity is greatly appreciated. I would also like to thank KVS Technologies and Maneesh Singh for providing input during the development of our problem statement, and for their comments during the final review of this thesis.

Simon Kleppevik Skaga

Tromsø, May 2016

TABLE OF CONTENTS

| | | |
|-------|---|----|
| 1 | Introduction..... | 11 |
| 1.1 | Background and problem statement..... | 11 |
| 1.2 | Aim and objectives | 12 |
| 1.3 | Research questions | 12 |
| 1.4 | Scope of work and limitations..... | 12 |
| 1.5 | Structure of this thesis..... | 13 |
| 2 | Literature review..... | 14 |
| 2.1 | Wind Turbines | 14 |
| 2.1.1 | Wind turbine components..... | 15 |
| 2.1.2 | Metrological conditions at wind turbine sites | 17 |
| 2.2 | Wind turbine rotor blades | 19 |
| 2.2.1 | Basic Aerodynamics..... | 19 |
| 2.2.2 | Number of blades | 20 |
| 2.2.3 | Blade design | 21 |
| 2.2.4 | Glass fibre composite mechanical properties | 23 |
| 2.2.5 | Causes of rotor blade failure | 26 |
| 2.2.6 | Rotor blade failure modes..... | 29 |
| 2.3 | Non-destructive testing (NDT) | 33 |
| 2.3.1 | Condition monitoring and maintenance..... | 36 |
| 2.4 | Unmanned Aerial Vehicle (UAV) | 38 |
| 2.4.1 | Multicopter UAV..... | 38 |
| 2.4.2 | Fixed-Wing..... | 40 |
| 2.4.3 | Other designs..... | 41 |
| 2.4.4 | Norwegian Aviation Law and Regulations | 41 |
| 2.5 | Risk Management | 44 |
| 2.5.1 | Risk Analysis | 44 |
| 2.5.2 | SWIFT-Analysis..... | 47 |
| 2.5.3 | The Bow-tie Method | 48 |
| 2.6 | Ultrasonic Testing | 50 |
| 2.6.1 | Basic principles of soundwaves | 50 |
| 2.6.2 | Behaviour of ultrasonic waves | 52 |
| 2.6.3 | Ultrasonic instrumentation..... | 55 |
| 3 | Methodology..... | 58 |
| 3.1 | In depth literature review..... | 58 |

| | | |
|-------|---|----|
| 3.2 | Risk management | 58 |
| 3.3 | Ultrasonic non-destructive testing - ground experiments | 59 |
| 3.3.1 | Instrumentation..... | 59 |
| 3.3.2 | Experimental set-up..... | 60 |
| 3.4 | Ultrasonic non-destructive testing – UAV experiments | 60 |
| 3.4.1 | Experiment set-up | 60 |
| 3.5 | Criticism of methodology | 61 |
| 4 | Results..... | 62 |
| 4.1 | Risk analysis | 62 |
| 4.1.1 | SWIFT-analysis | 62 |
| 4.1.2 | Bow-tie analysis..... | 64 |
| 4.1.3 | Post-barrier risk matrix | 66 |
| 4.2 | Ultrasonic handheld measurements..... | 67 |
| 4.2.1 | Measurement of crack simulation..... | 68 |
| 4.2.2 | Measurement of induced damage | 70 |
| 4.3 | Ultrasonic measurement with UAV..... | 74 |
| 4.3.1 | Preliminary flight test | 74 |
| 4.3.2 | Ultrasonic measurements using UAV | 75 |
| 5 | Discussion..... | 78 |
| 5.1 | Review of UAV technology and flight challenges..... | 78 |
| 5.1.1 | Applicable UAV designs..... | 78 |
| 5.1.2 | Metrological conditions for UAV flight..... | 79 |
| 5.1.3 | UAV stability..... | 80 |
| 5.1.4 | RPAS Regulations | 80 |
| 5.1.5 | Future of UAV technology..... | 81 |
| 5.1.6 | Risk evaluation..... | 81 |
| 5.2 | Handheld ultrasonic experiments | 83 |
| 5.3 | UAV ultrasonic experiments | 85 |
| 5.3.1 | Transducer surface contact mechanism..... | 85 |
| 5.3.2 | Ultrasonic instrumentation..... | 85 |
| 6 | Conclusion | 86 |
| 7 | References | 88 |
| 8 | Appendix A..... | 93 |

LIST OF FIGURES

| | |
|--|----|
| Figure 2-1 Horizontal Axis Wind Turbine (HAWT) main components. (Layton, 9 August 2006) | 15 |
| Figure 2-2 HAWT Rotor hub pitch drive. (ifm, u.d.) | 16 |
| Figure 2-3 Wind Turbine Nacelle Structure. (The Worlds of David Darling, u.d.) | 17 |
| Figure 2-4 Probability distribution of hourly mean wind speeds (Dowell, et al., u.d.) | 18 |
| Figure 2-5 Lift and drag force induced over a wind turbine blade. (Learn Engineering, u.d.) | 19 |
| Figure 2-6 Bernoulli principle of pressure over a wind turbine rotor blade. (mpower, u.d.) | 20 |
| Figure 2-7 52.3m blade with cross section transition. (Xiao, et al., 2014) | 21 |
| Figure 2-8 Typical HAWT rotor blade configuration, components in a coordinate system. (Sørensen, et al., 2004) | 22 |
| Figure 2-9 Material composition of V52 wind turbine blade. (Sørensen, et al., 2004) | 22 |
| Figure 2-10 Unidirectional laminate (Wallenberger & Bingham, 2010) | 23 |
| Figure 2-11 Bi-directional laminate (Wallenberger & Bingham, 2010) | 24 |
| Figure 2-12 Crack growth in bi-directional laminate. (Wallenberger & Bingham, 2010) | 24 |
| Figure 2-13 Types of deformation in random short fibre laminates (Wallenberger & Bingham, 2010) | 25 |
| Figure 2-14 Complete structural failure of rotor blade due to excessive winds (Dongsheng, et al., 2015) | 27 |
| Figure 2-15 Damage on rotor blade tip due to lightning strike (Dongsheng, et al., 2015) | 27 |
| Figure 2-16 Flying ice due to atmospheric icing on rotor blade (Dongsheng, et al., 2015) | 28 |
| Figure 2-17 Structural failure due to faulty manufacturing (Dongsheng, et al., 2015) | 28 |
| Figure 2-18 Overview of wind turbine rotor blade failure modes (Sørensen, et al., 2004) | 30 |
| Figure 2-19 Type 7 & 5 rotor blade damage (Sørensen, et al., 2004) | 30 |
| Figure 2-20 Type 1 & 4 damage in skin and spar (Sørensen, et al., 2004) | 31 |
| Figure 2-21 Overview of main spar failure modes (Sørensen, et al., 2004) | 31 |
| Figure 2-22 Type 5, 3 & 7 failure modes in sandwich structure (Sørensen, et al., 2004) | 32 |
| Figure 2-23 UAV coordinate system. Roll, pitch and yaw. (Hansen, et al., 2014) | 39 |
| Figure 2-24 Roll and pitch, engine control (Learn Robotix, u.d.) | 39 |
| Figure 2-25 Yaw, engine control (Learn Robotix, u.d.) | 40 |
| Figure 2-26 Risk analysis procedure (Gjellestad, 2011) | 45 |
| Figure 2-28 Bow-tie diagram | 49 |
| Figure 2-29 Wave properties (CBSE Portal, u.d.) | 50 |
| Figure 2-30 Sound spectrum (Olympus, 2017) | 51 |
| Figure 2-31 Longitudinal soundwave propagation in air (Nave, 2016) | 51 |
| Figure 2-32 Transverse wave propagation (Nave, 2016) | 52 |
| Figure 2-33 Single element and dual element ultrasonic transducers (Olympus, 2017) | 56 |
| Figure 2-34 Block diagram of ultrasonic instrumentation (Olympus, 2017) | 56 |
| Figure 3-1 Ultrasonic pulser/reciever (left) and oscilloscope (right) | 59 |
| Figure 3-2 V397-SU 29mm element transducer (Skaga, 2017) | 60 |
| Figure 4-1 Triple echo response from ultrasonic pulse in 29.9mm thick glass fibre sample | 67 |
| Figure 4-2 Simulation of crack due to debonding in glass fibre sample (Skaga, 2017) | 68 |
| Figure 4-3 Echo response from ultrasonic pulse in simulated crack, first backwall echo | 69 |
| Figure 4-4 Echo response from ultrasonic pulse in simulated crack, second backwall echo | 69 |
| Figure 4-5 Set-up for 3-point bending test (Skaga, 2017) | 70 |
| Figure 4-6 Image of visual damage induced in 29mm glass fibre sample by 3-point bending test. Uncoated surface (left) and coated surface (right) | 71 |
| Figure 4-7 Position of ultrasonic measurements on damaged glass fibre sample (Skaga, 2017) | 71 |
| Figure 4-8 Echo response from measurement 1 | 72 |

| | |
|---|----|
| Figure 4-9 Echo response from measurement 2..... | 72 |
| Figure 4-10 Echo response from measurement 3..... | 73 |
| Figure 4-11 Small racing UAV (Helipal, 2017)..... | 74 |
| Figure 4-12 Medium UAV (Helipal, 2017)..... | 74 |
| Figure 4-13 Preliminary flight test with Storm Racing Drone 260 V2 (Skaga, 2017)..... | 75 |
| Figure 4-14 Preliminary flight test with Storm AntiGravity (Skaga, 2017)..... | 75 |
| Figure 4-15 Ultrasonic measurement using Storm AntiGravity (Skaga, 2017)..... | 76 |
| Figure 4-16 Echo response from ultrasonic measurement using Storm AntiGravity, test nr. 1.... | 76 |
| Figure 4-17 Echo response from ultrasonic measurement using Storm AntiGravity, test nr. 2.... | 77 |
| Figure 5-1 Example of UAV propeller guard (left) (DJI Store, 2017) and UAV propeller cage (right) (UAV Expert News, 2017)..... | 83 |

LIST OF TABLES

| | |
|---|----|
| Table 1 Wind speed profile at various heights (KNMI Hydra Project, 1998 - 2005)..... | 18 |
| Table 2 Component specific causes of wind turbine failure (Chia Chen, et al., 2008)..... | 26 |
| Table 3 Wind turbine rotor blade damage types (Sørensen, et al., 2004)..... | 29 |
| Table 4 Comparison of destructive and non-destructive testing (Baldev, et al., 2007)..... | 34 |
| Table 5 Review of common non-destructive testing techniques (Martinez-Luengo, et al., 2016)..... | 35 |
| Table 6 Description of UAV coordinate system (Learn Robotix, u.d.)..... | 39 |
| Table 7 5x5 risk matrix..... | 46 |
| Table 8 SWIFT analysis (Rausand & Utne, 2009)..... | 48 |
| Table 9 Velocity of sound in common gases, liquids and solids (Nave, 2016)..... | 53 |
| Table 10 Velocity of sound in glass fibre epoxy per glass fibre content..... | 53 |
| Table 11 Waveform measurements of oscilloscopes..... | 57 |
| Table 12 SWIFT-analysis "what-if" checklist..... | 62 |
| Table 13 Definition of consequence and probability parameters..... | 63 |
| Table 14 Risk matrix post SWIFT-analysis..... | 63 |
| Table 15 Identified ALARP risks..... | 64 |
| Table 16 Barriers identified from Bow-Tie method..... | 65 |
| Table 17 Post-barrier risk matrix..... | 66 |
| Table 18 3-point bending test, pressure, displacement and observations..... | 70 |
| Table 19 Brief review of 7 identified ALARP unwanted events with implemented barriers and comments..... | 81 |
| Table 20 Damage types visually observed in broken glass fibre sample..... | 84 |

LIST OF EQUATIONS

| | | |
|---------------|--|----|
| Equation 2.1 | Bernoulli equation..... | 20 |
| Equation 2.2 | Simplified Bernoulli equation..... | 20 |
| Equation 2.3 | Theoretical strength of composite by rule of mixtures..... | 24 |
| Equation 2.4 | Critical length of composite fibres..... | 25 |
| Equation 2.5 | Relationship of frequency and period..... | 50 |
| Equation 2.6 | Velocity of longitudinal waves..... | 53 |
| Equation 2.7 | Velocity of transverse waves..... | 53 |
| Equation 2.8 | Velocity of surface waves..... | 53 |
| Equation 2.9 | Soundwave reflection coefficient..... | 54 |
| Equation 2.10 | Soundwave transmission coefficient..... | 54 |
| Equation 2.11 | Snell's law..... | 54 |
| Equation 2.12 | Attenuation of soundwave..... | 55 |
| Equation 4.1 | Soundwave velocity derived from length and time..... | 67 |
| Equation 5.1 | Kinetic energy of rigid bodies..... | 82 |

:

1 INTRODUCTION

1.1 BACKGROUND AND PROBLEM STATEMENT

On the 4th of November 2016, the Paris Agreement entered force. The agreement is the result of the negotiations between nations to reduce emissions and protect the climate. The signed document covers many of the problems that are featured as dangerous consequences of fossil fuels, greenhouse gasses and deforestation. Among some of the goals in the agreement, the governments agreed to “A long-term goal of keeping the increase in global average temperatures to well below 2°C above pre-industrial levels “ (European Commission, 2017). The agreement marked a new effort in changing the faith of the planets ecosystem and diversity, in addition to reducing the increase in natural disasters such as floods and abnormally strong weather.

There is no doubt that the energy industry is changing. Renewable sources of energy are emerging as the new source of energy, and nations are striving to become “green”. For example, on June 10th, 2016, Sweden committed to a goal of 100% renewable energy by the year 2040 (Business Insider Nordic, 2016). To cover the demand of renewable energy across the globe, new and ambitious solutions must be developed. The price of solar panels has dropped rapidly over the last years, and according to The Guardian, prices of solar panels are predicted to fall by 10% per year (Darby, 2016). However, countries like Norway and Britain have limited and unreliable sun days. In addition to Norway’s huge water reservoirs and already established “green energy” production, wind turbines are being developed.

Profitability and power production is proportional with turbine size in the wind energy industry. Statoil, Norway’s leading energy company, is currently developing large offshore wind turbine projects (Statoil, 2017). To make these projects viable, the maintenance cost must be kept to a minimum due to the accessibility of these massive offshore structures. Repair can prove very costly, as replacing a rotor blade of 80-meters length at sea is not an easy task. Through basic reliability methodology, this calls for thorough inspection programs, which is where non-destructive testing becomes relevant. It is imperative to predict failures as accurately as possible to reduce the repair costs and maximize the uptime of the wind turbines. This requires innovative solutions and strong interdisciplinary competence in the field.

UAV’s, also known as drones, is another industry that is “in the wind” these days. The technology has rapidly been rising in the last decade, and the consumer market has exploded with design variety and models in all price ranges. The stability technology has reached a level where anyone can fly simple and small models with ease. This development has caught the eye of many maintenance and inspection branches and companies, and currently, UAV visual inspection of wind turbines is well developed. However, not all damages can be inspected visually or with thermography. “Delamination’s of the trailing edge are common and until now can’t be detected before they are visible at the blades surface” (Jüngert, 2008). The article by Anne Jüngert investigates the potential of ultrasonic echo testing to detect sub-surface defects in rotor blades, and suggests that the measurements can be carried out by industrial climbers or some form of robot.

Industrial climbers are costly and have a high associated risk when climbing at great heights. In addition, the wind can be strong and very uncomfortable at wind turbine sites, making climbers a costly and slow form of inspection. UAVs however, show exciting potential because surveys can be completed quickly and efficiently at any point of the blade. By investigating the technology of wind turbines, UAV technology regarding stability and payload capabilities, ultrasonic experimentation and operational risks related to UAV flight near wind turbine rotor

blades, this thesis aims to conclude on the feasibility of UAV application for NDT of wind turbine rotor blades.

1.2 AIM AND OBJECTIVES

The aim of this thesis is to study the feasibility of UAV application for ultrasonic non-destructive testing. Because ultrasonic testing requires direct contact with the surface of the tested specimen, a series of problems must be investigated.

- a) Review the current UAV technology regarding stability, high windspeed flight and risks associated with direct contact measurements of wind turbine rotor blades.
- b) Review the typical causes for wind turbine rotor blade damage and the resulting failure modes. Investigate the potential of the ultrasonic echo pulse technique for damage detection through literature review and handheld experimental studies.
- c) Conduct ultrasonic experiments using an UAV, identify advantages and challenges from the results.

1.3 RESEARCH QUESTIONS

The research questions have been developed to facilitate the aim and objectives of this thesis. They are directly related to the problem statement and will provide an understanding of how the author approaches the problem.

- a) Can UAVs fly near wind turbine rotor blades with acceptable risk?
- b) Is ultrasonic echo testing suitable for wind turbine rotor blades, built from fibre glass laminates?
- c) Can UAVs be used to carry out ultrasonic non-destructive testing?

1.4 SCOPE OF WORK AND LIMITATIONS

- To the extent of the authors knowledge, there are no commercially available UAV solutions for ultrasonic non-destructive testing. This thesis will investigate the potential for UAV application through a feasibility study, involving two sets of experiments.
- The current wind turbine technology was reviewed for a fundamental understanding of their working principles. Because this thesis focuses on non-destructive testing of rotor blades, only the basics of wind turbines and relevant factors such as environmental conditions are reviewed.
- Wind turbine rotor blades has been reviewed in detail, with specific focus on their construction, material selection, causes of failure and typical damage. This thesis is based on the most commonly used material, glass fibre. Thus, the emerging carbon fibre technology has been excluded.
- Due to the interdisciplinary nature of this thesis, details on aerodynamics, mechanics, electrical and economics are only presented in basics. This is to reduce the scope of work to an appropriate level, yet providing the fundamental understanding required for the study and experiments.
- The availability of equipment and funding for this thesis is very limited, and only UAV and ultrasonic instrumentation available at the University in Tromsø was used. The results may vary depending on the complexity of equipment and must be kept in consideration.

- The risk analysis is primarily oriented around safety aspects. Environmental and economic factors have informally been included, but should be considered in more detail in future studies.
- The full potential of ultrasonic testing has not been covered, only a single measurable parameter, echo response, was included in the experiments. The focus is oriented towards the use of UAV for close-proximity testing.
- The exact composition of the glass fibre samples is not known, and we do not attempt to identify material properties in this thesis. The topic of interest is the failure modes and general sound behaviour of the material, which may be very similar for a range of fibre composites.

1.5 STRUCTURE OF THIS THESIS

The interdisciplinary nature of this thesis requires a presentation of a series of topics. Wind turbines are presented in a standalone chapter to lay the groundworks for the extensive chapter on wind turbine rotor blades. In accordance with the aim of this thesis, a technical review of the rotor blades, in addition to recorded incidents and potential failure modes, is vital for our experiments. The philosophy of non-destructive testing is presented, including its influence on maintenance and operation. A basic presentation of UAV technology and regulations is presented before covering risk management, which is a crucial part of this feasibility study, and literature and methodology are presented to carry out a preliminary analysis. Lastly, the fundamentals and technology of ultrasonic testing is presented, in addition to an overview of the instrumentation used for our experiments.

The chapter on methodology presents how the data used in this thesis was acquired. It covers the approach towards the literature review as well as the experiments that were conducted. The chapter was split in 3 sections, whereas the first covers the literature review. The second chapter presents the reasoning behind our ground-level testing. The third subsection covers the UAV experiments with descriptions and setup drawings.

The results from the risk analysis and our experiments are presented in chapter 4, and chapter 5.1 presents a theoretical discussion on the use of UAVs for ultrasonic non-destructive testing and related challenges and potential solutions. Chapter 5.2 discusses the results related to the ground-level experiments, while the third chapter discusses the results from our UAV flight.

The conclusion will summarize the findings from the chapters on results and discussion.

2 LITERATURE REVIEW

This chapter presents the theoretical framework and will describe the major topics relevant to this interdisciplinary study.

2.1 WIND TURBINES

The power of the wind has been fascinating mankind for thousands of years. When the windmill was invented for grinding corn into flour early in the 2th millennium, it significantly boosted the efficiency of food production. Ever since, the energy potential in wind has been harnessed for our benefit. Over the last 50 years, the technology has taken huge steps in terms of cost-efficiency and power production. With the overhanging threat of global warming and politics pushing towards green energy, the power of wind is becoming increasingly relevant.

In 1980-1983, the size of commercial wind turbines were 15 meters in rotor diameter, which had a production capacity of 55 Kw. Since then, advanced computer simulation tools have become available. Combined with better production techniques, the size of commercial wind turbines increased to 66 meters in rotor diameter and a production capacity of 1500 kW in 1997 (D. C. Quarton, 1998). As simulation tools and engineering knowledge has continued to advance, wind turbines are built at ever larger scales. In 2014, engineering.com featured the V164 wind turbine manufactured by Vestas, which can produce 8-MW of power. The V164 is built for offshore use and has rotor diameter of 164 meters (Lombardo, 2014). Because wind turbines have a large initial installation cost, they are more cost effective in large scale. This has led to an increase in size, and opened for new locations of wind parks. For example, it is now considered viable to build offshore at shallow depths.

There are many attempts at harnessing the wind using different techniques, where designs range from the common propeller-like structure, to parachute based solutions. There are mainly two types of design principles which have proved successful. They have their strengths and weaknesses, and the core difference is that one rotates around a horizontal axis while the other rotates around a vertical axis.

The vertical axis wind turbine (VAWT) rotate around a vertically oriented shaft. It uses blades which runs from top to bottom to catch the wind. The major advantage of this design is that the power production is not dependent on the direction of the win. VAWTs are also capable of absorbing turbulence and gusty winds. Due to their design, the gearbox and generator is more easily accessible due to its placement on the ground. These turbines are unstable by nature, making them much hard to apply for large scale energy production (Dvorak, 2014). Because a substantial majority of the world's wind energy is produced by horizontal axis wind turbines, VAWT designs will not be considered further in this paper.

The horizontal axis wind turbine (HAWT) is by far the most popular commercial design. It uses a rotor which is forced into rotation by the wind, which in turn rotates a horizontally oriented shaft. The rotation of the rotor and shaft is relatively slow and will not produce sufficient power if connected directly to a generator. It is connected through a gearbox which converts torque to speed, or vice versa, to suit the generator's requirements. These windmills can reach high efficiency if the rotors are directed towards the wind.

2.1.1 Wind turbine components

Wind turbine design varies, to some extent, depending on the manufacturer, customer and turbine age. Most HAWT can be split into a set of main components that are included in the design variations. This chapter will briefly present the subsystems in a HAWT, while the wind turbine rotor blades will be presented in a separate chapter.

The rotor blades, typically 3 blades per rotor, absorb the kinetic energy of the wind. The blades are assembled onto a hub which transfers the loads onto a low-speed shaft. The rotation of the low-speed shaft is amped up through a gearbox, resulting in a much higher RPM (rounds per minute) on the high-speed shaft. The rotational energy in the high-speed shaft is converted into electrical current in the generator. The current is carried down through with cables running on the inside of the tower. At the bottom, the voltage of the current is increased in transformers to facilitate long-range electrical transfer. The image below shows the subsystems of a HAWT.

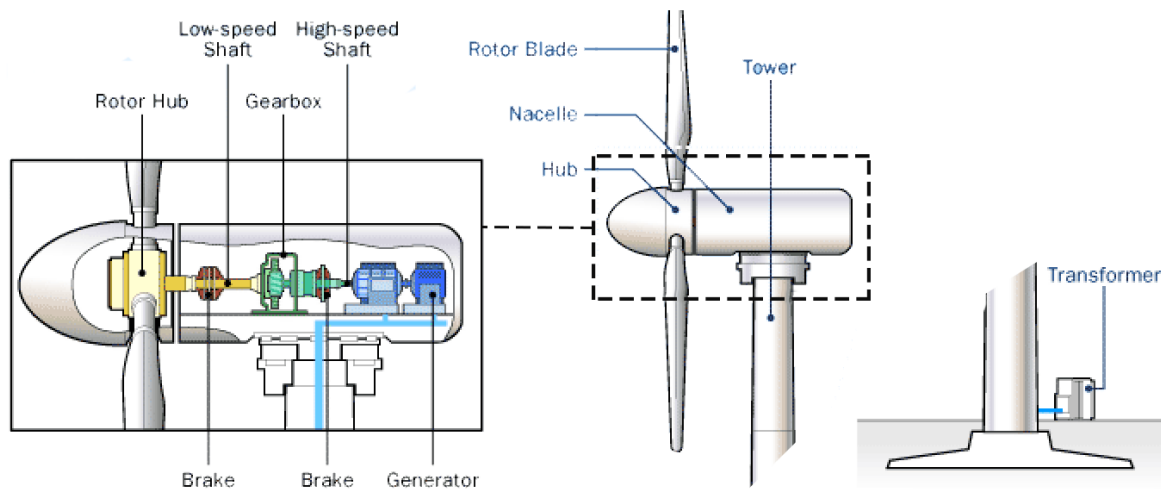


Figure 2-1 Horizontal Axis Wind Turbine (HAWT) main components. (Layton, 9 August 2006)

2.1.1.1 Rotor Blades

The blades of the wind turbine transform the kinetic energy in the wind to mechanical motion. These systems are available in a variety of designs, depending on factors such as the size of the wind turbine, wind conditions and desired power output. The rotor blades will be covered in detail in chapter 2.2 *Wind turbine rotor blades*.

2.1.1.2 Rotor Hub

The hub is the system that connects the blades of the wind turbine onto a rotating shaft. It takes the entire load of the blades and must be designed with high mechanical strength. In the early days of HAWT, the blades were simply bolted onto a rigid hub. This made the efficiency of the windmill entirely dependant on the direction of the wind. The most modern hub configurations allow the blades to be rotated to orient the blades into the optimal angle relative to the wind. This can greatly increase the power output of the wind turbine in changing winds. This system is referred to as a pitch system.

The pitch systems are strong electrically powered bearings that are controlled by an algorithm. Wind turbines are equipped with wind velocity and direction sensors, which allows the system to automatically rotate the blades into optimal positions. The image below shows a typical modern hub configuration, where we can observe the gears and actuator which powers the system.



Figure 2-2 HAWT Rotor hub pitch drive. (ifm, u.d.)

2.1.1.3 Turbine Shaft

The turbine shaft is one of the most critical components of a wind turbine. It must be designed to withstand the weight of the rotor, rotor thrust, torque and lateral forces (Spera, 2009). The combined effect of these forces causes fatigue loading on the shaft, which ideally must be designed for the entire lifetime of the wind turbine, as replacing a defect shaft will be very costly. In addition to taking massive loads, the turbine shaft must often include sensors, rotor breaks and rotor control measures. Because of the challenging service requirements of the turbine shaft, it must be designed with extreme care.

2.1.1.4 Gearbox

Due to the slow rotation of the rotor, the RPM (rotations per minute) has to be increased up in order to produce electricity. The gearbox has the input of the slowly rotating turbine shaft, and a high RPM shaft as output. The step-up in rotational speed can be as high as 100 times for large-scale HAWT (Spera, 2009). It can be beneficial to install the rotor breaks on the gearbox shaft for increased performance in breaking power.

2.1.1.5 Generator

The electrical generator converts the rotational speed of the gearbox shaft into electrical energy. All types of electrical generators are used in HAWT (Spera, 2009). In small rotor wind turbines, variable speed alternators and DV generators are often used. For medium and large scale wind turbines, AC generators are used.

2.1.1.6 The Nacelle Structure

The pitch system, which allowed the blade orientation to be optimized with respect to wind direction, does not help in case of large changes in wind direction. To cope with the issue, the HAWT often uses a nacelle structure. In the context of wind turbines, this means to build the previously mentioned turbine shaft, gearbox and generator inside a box-like structure. By placing the powertrain of the wind turbine inside a nacelle, the entire system can be rotated to face in the direction of the wind. This system is referred to as the yaw-drive (Spera, 2009).

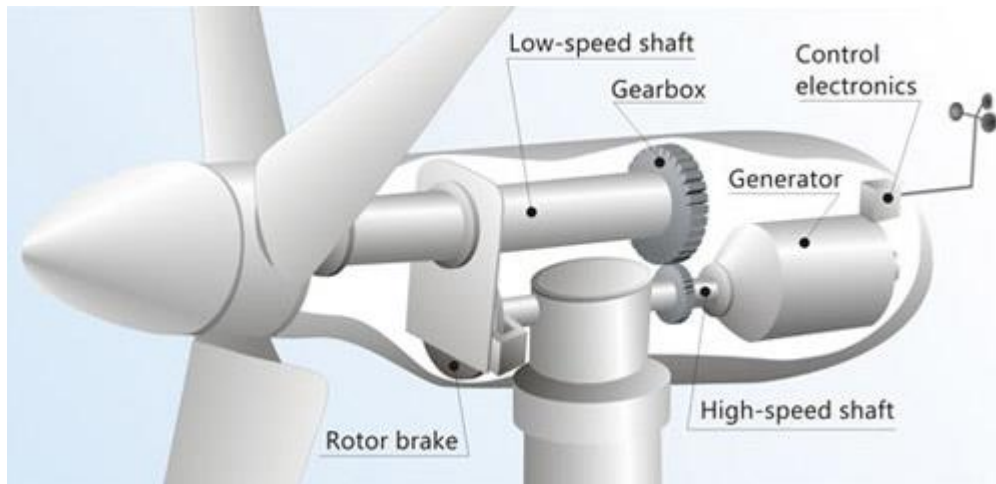


Figure 2-3 Wind Turbine Nacelle Structure. (The Worlds of David Darling, u.d.)

The nacelle structure is built on a strong bed plate with high static strength which provides the necessary structural support to carry all the components on top of the tower. Through strong yaw bearings, it can be rotated around a vertical axis. In addition to allowing more power production through the yaw system, the nacelle protects the components and maintenance personnel from environmental forces.

2.1.1.7 Tower

The tower of the HAWT raises the rotor and nacelle to the desired height. The minimum height of the tower depends on the ground clearance, which is the minimum distance from the swept area (lowest point of rotor blades) and the ground. The maximum height is a cost-related problem, where the aim is to find the optimal trade-off between increased construction costs and power production. Because the average wind velocity tends to increase with the height, detailed analysis must be carried out to calculate the optimal height (Spera, 2009).

A HAWT tower is typically constructed as a cylindrical shell, built with steel or reinforced concrete for large scale turbines. The hull of the shell can shelter ladders with floors at set intervals for rest during the climb or electrically powered elevators. Cables from the generator also run along the inside walls of the shell to transformers at the very bottom of the tower. This is where the ground station is placed, with transformers and other electrical utility systems. The equipment which does not have to be placed in the nacelle are positioned here for easy and sheltered access. The dimensioning of the towers height, shell width, weight and foundation will determine the fundamental system frequency of the wind turbine.

2.1.2 Metrological conditions at wind turbine sites

As commonly known, weather varies all over the globe. Where the wind ravages one day, may be completely still the next. Wind turbines are built on locations where the wind is at a suitable annual average, for optimal production. The optimal wind speeds are dependent on the size and technology of the wind turbine. For the wind turbine to start rotating and produce electricity, the wind speeds must reach a velocity known as cut-in wind speed. The cut in speed varies depending on the wind turbine design, and can require wind speeds of 10 m/s or more. In extremely windy conditions, the wind turbine must shut down to prevent excessive loads, this value is called cut-out wind speeds (DNV GL AS, November 2016).

A paper by (Dowell, et al., u.d.) processed wind and wave data from the FIN01 research platform to calculate the annual availability of offshore wind turbine farms located in the North Sea, which is comparable to many UK Round 3 sites. The paper derived a wind speed distribution for

hourly mean wind speeds, collected from 1/1/2004 to 1/10/2010, resulting in 59182 measurements. The distribution is presented in figure 2-4, and can to some degree, represent wind speed averages at offshore wind turbine sites.

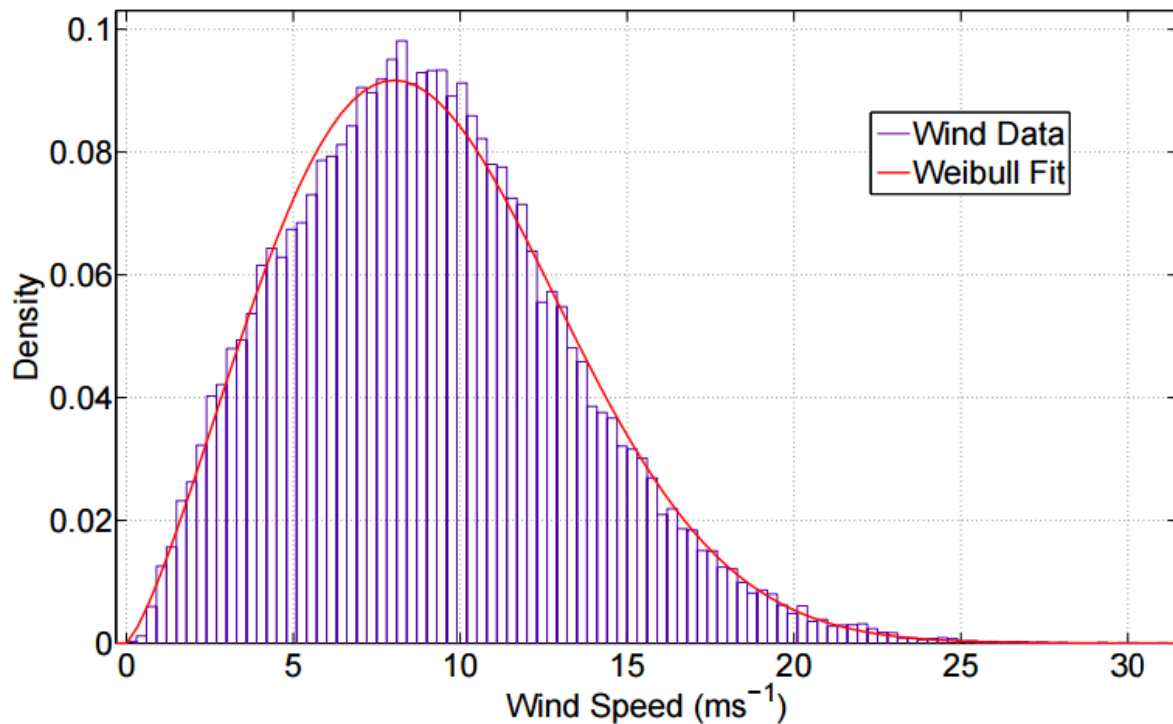


Figure 2-4 Probability distribution of hourly mean wind speeds (Dowell, et al., u.d.)

Wind speed increases with altitude, depending on the roughness of terrain and atmospheric stability. The Royal Netherlands Meteorological Institute (KNMI) presents the following table for wind speeds at various heights, given a cloudy day, a shiny day and clear nights (KNMI Hydra Project, 1998 - 2005).

Table 1 Wind speed profile at various heights (KNMI Hydra Project, 1998 - 2005)

| Height (m) | Cloudy day (m/s) | Shiny day (m/s) | Clear night (m/s) |
|------------|------------------|-----------------|-------------------|
| 1.0 | 1.8 | 1.9 | 1.7 |
| 1.5 | 2.3 | 2.4 | 2.2 |
| 2.0 | 2.7 | 2.9 | 2.6 |
| 3.0 | 3.3 | 2.4 | 3.2 |
| 4.0 | 3.7 | 3.8 | 3.6 |
| 4.8 | 4.0 | 4.1 | 3.9 |
| 7.1 | 4.5 | 4.6 | 4.5 |
| 10 | 5.0 | 5.0 | 5.0 |
| 15 | 5.5 | 5.4 | 5.6 |
| 21 | 6.1 | 5.8 | 6.3 |
| 29 | 6.5 | 6.1 | 6.9 |
| 42 | 7.0 | 6.5 | 7.7 |
| 60 | 7.5 | 6.8 | 8.6 |
| 88 | 8.1 | 7.1 | 9.8 |
| 117 | 8.5 | 7.3 | 10.9 |

2.2 WIND TURBINE ROTOR BLADES

Wind turbine rotor blades are considered the most critical component of the horizontal axis wind turbine. Especially with the ongoing trend of “larger is better”, the design and materials technology is in continuous development. Rotor blades account for a substantial part of the total wind turbine cost, and are designed for very long service life of 10-30 years. The forces subjected onto rotor blades are complicated and sometimes unpredictable, they are cyclic and in many cases difficult to compute. Damage or failure to the rotor blades can lead to very high repair or replacement costs, in addition to production downtime. Thus, it is imperative to continuously attend the structural integrity of wind turbine rotor blades.

2.2.1 Basic Aerodynamics

As the knowledge in aerodynamics rapidly developed towards the end of the 1800th century, powered by the aviation industry, the design of wind turbine blades changed in terms of working principle. Up until this point, the blades were mostly sails which were pushed into rotation through drag forces. The design of HAWT shifted towards utilizing the lift force by designing the blades similar to the wing of an aeroplane.

Figure 2-5 shows the wind flow and angle of attack over a curved blade. The principle of rotation is shown by the forces in play. As wind flows over the blade, two major forces occur. The lift force is the rotation-driving force, when seen from the cross-sectional perspective, lifts the blade upwards. Depending on the roughness of the blade, the wind induces a drag force along the surface of the blade. The drag force pushes the blade backwards and applies compressive and tensional loads in the blade.

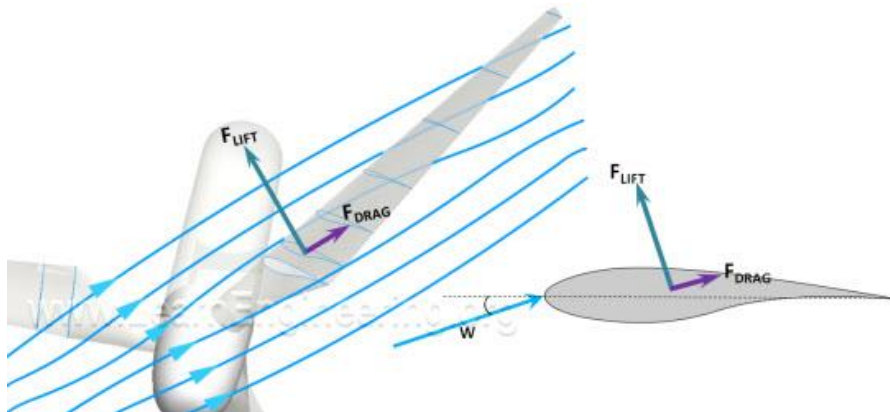


Figure 2-5 Lift and drag force induced over a wind turbine blade. (Learn Engineering, u.d.)

The lift force is caused due to a pressure difference on the top and bottom of the blade. When the wind flows onto the blade, as seen in figure 2-6, it has a longer path to travel over the top. The air has nowhere else to flow, thus it must increase the velocity to maintain the flow of mass.

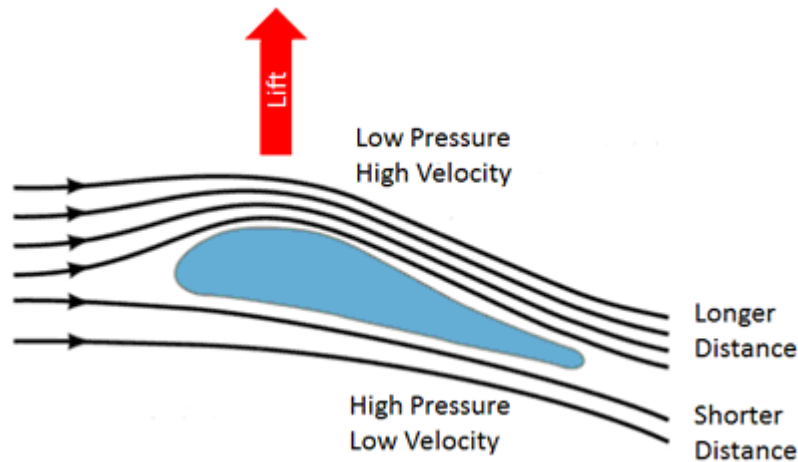


Figure 2-6 Bernoulli principle of pressure over a wind turbine rotor blade. (mpower, u.d.)

From the Bernoulli principle of pressure, we can see that the pressure on top of the blade will be lower than the pressure under the blade, due to higher velocity. This difference in pressure will create a lift force upwards (Eastlake, 2002).

$$P_1 + \frac{1}{2}\rho v_1^2 + \rho g h_1 = P_2 + \frac{1}{2}\rho v_2^2 + \rho g h_2 \quad (2.1)$$

Where P_1 and P_2 is the total pressures, ρ is the density of the air, v_1 and v_2 is the velocity of the air, h_1 and h_2 is the height and g is the gravity constant. The Bernoulli equation consists of three terms: total pressure (P_1 and P_2), kinetic energy ($\frac{1}{2}\rho v_1^2$ and $\frac{1}{2}\rho v_2^2$) and the static pressure ($\rho g h_1$ and $\rho g h_2$). Because the changes in static pressure over a relatively thin blade are very small, they can be neglected. After modifying the equation, we can use it to calculate the differences in pressure at the top and below the wind. When the pressure difference is known, we can apply the complex shape of the blade to calculate the actual lift force on the blade.

$$P_1 + \frac{1}{2}\rho v_1^2 = P_2 + \frac{1}{2}\rho v_2^2 \quad (2.2)$$

2.2.2 Number of blades

Commercial large-scale HAWT's are generally installed with a 3-blade configuration. Small and medium-scale wind turbines are gaining popularity with 2-blade configurations. Wind turbines with 1 and 4+ blades have been built and tested, but there are some serious considerations when determining the design. The aerodynamic efficiency of numerous rotor configurations has showed that going from 1 blade to 2 blades increases the aerodynamic efficiency by up to 7 percent (Spera, 2009). Adding another blade (3-blade configuration) yield an additional three percent improvement (Tangler, 2000).

Despite appearing like the most economical solution when considering the cost of rotor, blades and hub, which was estimated to about 26-27% of the cost of a wind turbine pp. 215 (Spera, 2009), 2-blade turbines has some disadvantages compared to the 3-blade turbine. The spacing of 120 degrees between the blades on a 3-blade configuration offers more dynamic balance,

which tends to have lower operating and maintenance costs (Tangler, 2000). In addition, the aesthetics of the 3-blade rotor appears more pleasing than the flickering appearance of the 1 and 2-blade rotors. Lastly, there are significant differences in noise production. The 2-blade rotors are often designed to rotate faster than the 3-blade rotors for better aerodynamic efficiency. The increase in noise due to the rotor is proportional to one fifth of the speed of rotor tip. Especially in the case of downwind rotors, the wake of the tower produces higher loadings on 1 or 2-blade rotors, which results in higher impulsive noise (Tangler, 2000).

2.2.3 Blade design

The design of wind turbine rotor blade varies depending on size, age, manufacturer and the materials used. For large-scale HAWTs, the most commonly used materials today are composite materials. Glass fibre has commonly been used with polyester and vinyl-ester to make glass fibre, a sort of fibre-reinforced plastic. However, many manufacturers have switched to epoxy due to better material properties. Carbon fibres for reinforcements are gaining increased interest, due to its strength to weight properties. However, carbon fibre is currently more expensive than glass fibre (Tangler, 2000).

The shape of wind turbine rotor blades follows some common characteristics, and can be split into three main regions. The first region connects the blade to the wind turbine hub. This section is commonly made from steel due to high mechanical strength requirements. The second region transitions the blade from a circular shape to an aerofoil. This region is commonly made from a combination of steel and glass fibre, and is often connected during the moulding of the blade. The last region consists of the aerofoil. This section transforms the energy of the wind into rotational movement through the lift and drag forces which were presented in chapter 2.2.1. Figure 2-7 shows an example of a 52.3m blade.

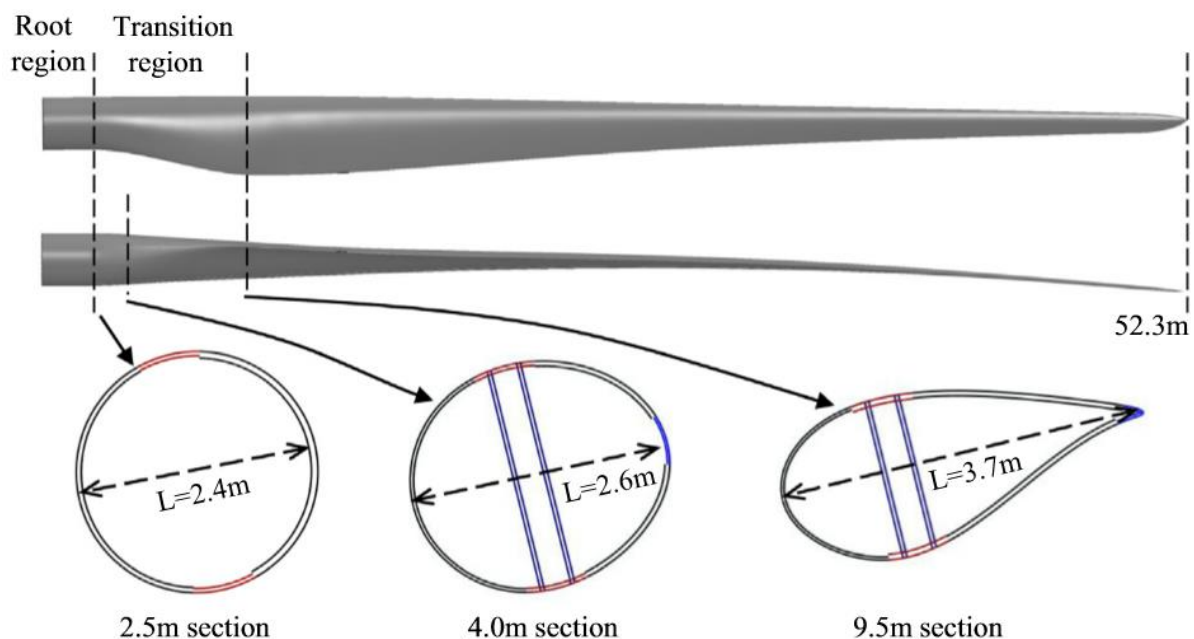


Figure 2-7 52.3m blade with cross section transition. (Xiao, et al., 2014)

Figure 2-8 shows the internal components of rotor blades in XYZ-coordinates. This is a typical large-scale wind turbine configurations. The wind hits the rotor blade at the leading edge, and due to the aerodynamic forces presented in chapter 2.2.1, the pressure differences between the upwind and downwind side creates lift on the blade. The forces from the wind are transferred

onto the aerodynamic shell which is commonly constructed in glass fibre epoxy. Due to the size of the blade and the magnitude of the forces, the blade is reinforced with a main spar. This beam carries the cumulative loads from the tip of the blade in towards the hub.

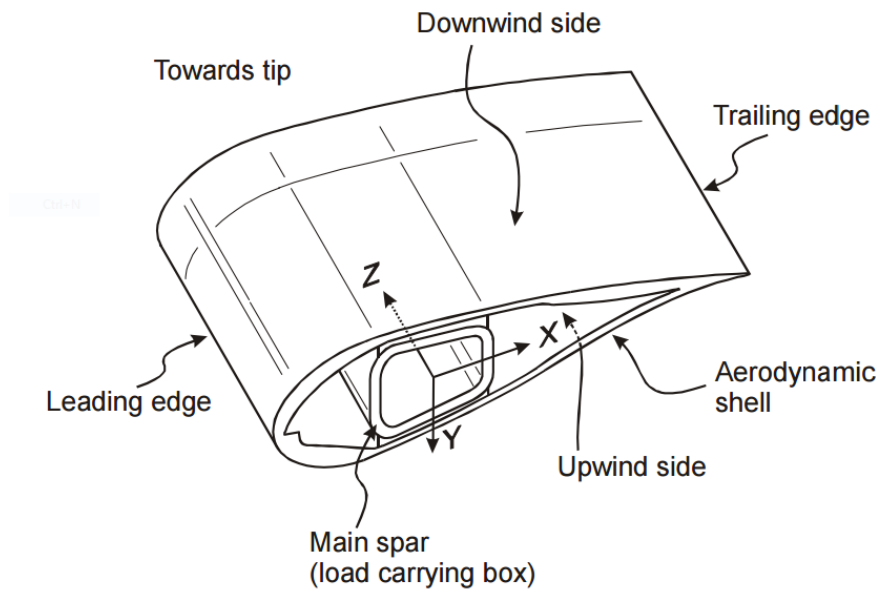


Figure 2-8 Typical HAWT rotor blade configuration, components in a coordinate system. (Sørensen, et al., 2004)

Figure 2-9 shows the structure of a V52 blade from Vestas Wind System A/S. The blade is constructed with a single load carrying spar. The spar consists of two laminate flanges, one for compression forces and one for tension forces. They are connected through two webs with sandwich structures. The blade is compiled by applying glue on the adhesive layers and joints, resulting in an intact and complete blade. (Sørensen, et al., 2004)

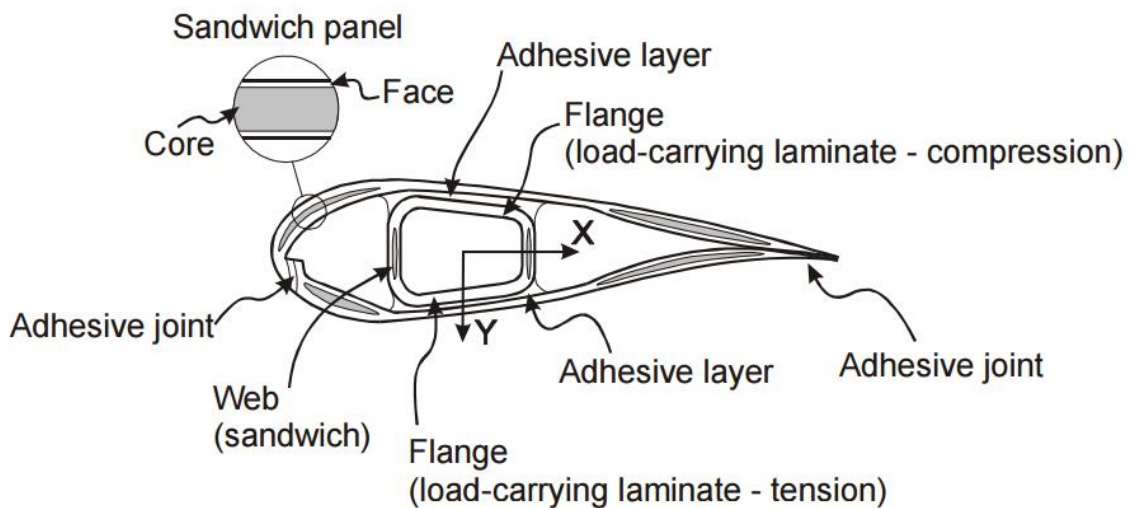


Figure 2-9 Material composition of V52 wind turbine blade. (Sørensen, et al., 2004)

2.2.3.1 Glass fibre composites

Most of wind turbine rotor blades are constructed from glass fibre composites. The concept of combining materials of different mechanical properties to create a combination which suits the intended purpose is widely used today. Through material engineering, materials of low weight and high strength can be produced for specific applications. Glass fibre is currently the largest segment of the composite industry, due to its low price and excellent mechanical properties. However, carbon, ceramic and metal fibres are also used for specific purposes. Glass fibre is mostly used due to its cost effectiveness and versatility. It's use ranges from offshore oil tanks to massive wind turbine rotor blades.

The process of combining the reinforcing glass fibres and the polymers (plastic) is called compounding, where the resulting material is called compound (Wallenberger & Bingham, 2010). A composite typically consists of a reinforcing fibre and an organic macromolecular matrix, often denoted resin, polymer or plastic. To understand how different compositions can yield vastly different mechanical properties, one must have a fundamental understanding of mechanical characteristics. The book on glass fibre (Wallenberger & Bingham, 2010) presents the following requirements for the reinforcing fibres to increase the strength of the polymer:

- The reinforcing fibre must have a significantly greater modulus of elasticity than the polymer.
- The reinforcing fibre must have a greater tensile (yield) strength.
- The reinforcing fibre must be compatible and have the best possible adhesion with the polymer.
- The reinforcing fibres must be chemically and physically resistant to the polymer and other additives, such as plasticizers and antioxidants.

2.2.4 Glass fibre composite mechanical properties

This chapter presents the mechanical properties of glass fibres composites. The core principle of composites is the transfer of loads from one component in the material to the other. Glass fibre composites gain their strength through the bond between the polymer matrix and the fibres. Mechanical loads such as stress are transferred from the matrix through the interface with the fibre, and fibres have the strength to withstand forces where the polymer would fail.

2.2.4.1 Unidirectional laminate

The strength of a composite is highly dependent on the orientation of the fibres. As seen in figure 2-10, we consider a unidirectional laminate, where the glass fibres run continuously in one direction.

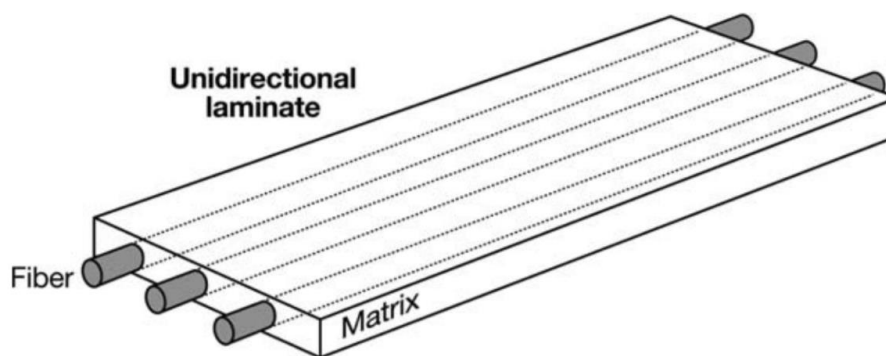


Figure 2-10 Unidirectional laminate (Wallenberger & Bingham, 2010)

Because the fibres are intended to take the mechanical loads, the fibres should be oriented in the direction of the load to maximize the strength of the composite. Theoretically, one may calculate the strength of the composite by a simple rule of mixtures where the strength of the composite is a function of fibre strength (σ_f), fibre volume (V_f), matrix strength (σ_m) and matrix volume (V_m) as seen in equation 2.3.

$$\sigma = V_f \sigma_f + V_m \sigma_m \quad (2.3)$$

This formula is however purely theoretical, and assumes perfect adhesion between the fibres and the matrix. It also assumes that the matrix can transfer stress to the fibres until the point of rupture, meaning that the matrix can sustain the same elongation as the glass fibre (Wallenberger & Bingham, 2010).

2.2.4.2 Bi-directional laminate

In the case of bi-directional laminates, as seen in figure 2-11, the behaviour of fibres in the direction of the load is the same as for the unidirectional example.

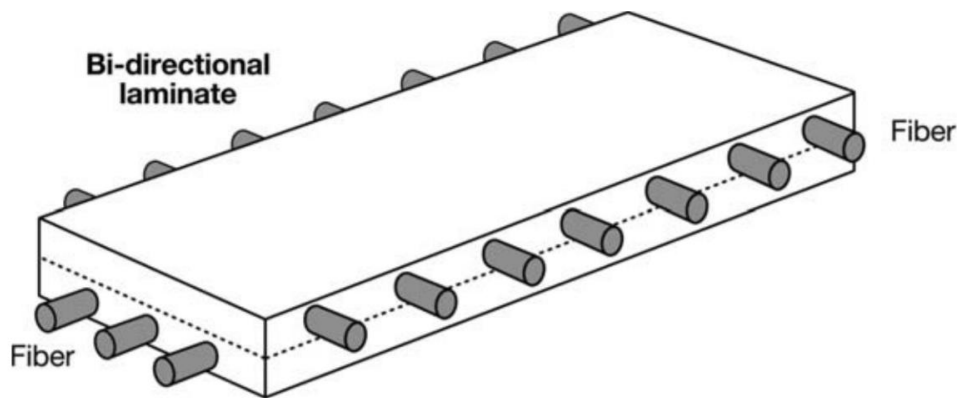


Figure 2-11 Bi-directional laminate (Wallenberger & Bingham, 2010)

In the layer with fibres oriented perpendicular to the applied force, we can observe a phenomenon called strain magnification. Because the fibres have a much greater modulus, it is more resistant to deformation. As seen in figure 2-12, the matrix will start cracking in between the fibres when the sample is elongated.

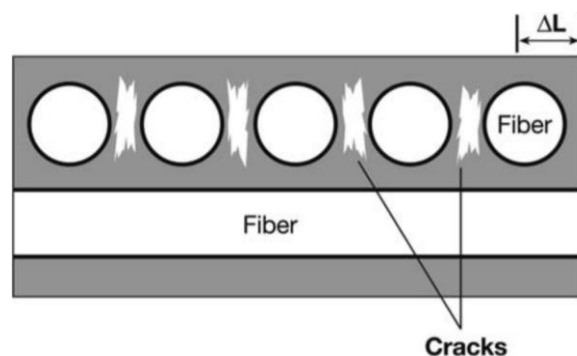


Figure 2-12 Crack growth in bi-directional laminate. (Wallenberger & Bingham, 2010)

These cracks can start to form at relatively low strains, where in experimental tests the sample will start to emit cracking sounds.

2.2.4.3 Random short fibres

To create a more homogeneous composite, many small fibres can be randomly distributed along two or three axes. This technique reinforces the composites in more than one or two directions. When these composites are subjected to strain, a complex deformation pattern occurs. Figure 2-13 shows the composite responses due to strain.

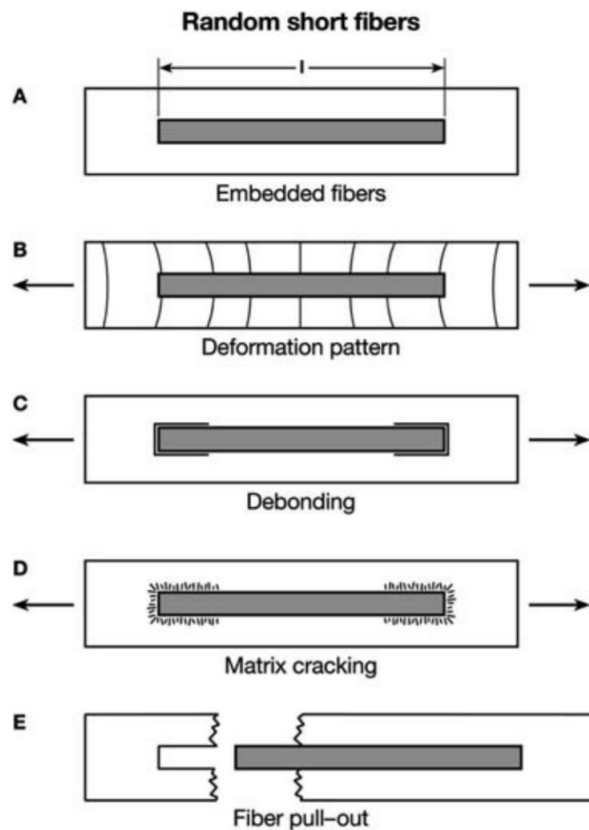


Figure 2-13 Types of deformation in random short fibre laminates (Wallenberger & Bingham, 2010)

Figure 2-13 (A) shows the fibre of length l under no strain. As strain is applied, the matrix will start deforming due to the low modulus relative to the fibres as seen in figure B. Depending on the matrix-fibre adhesion, either de-bonding or matrix cracking will occur. In the case of weaker adhesion, the matrix will start de-bonding with the fibres, beginning at the end of the fibres and growing in towards the centre of the fibre. Strong adhesion leads to matrix cracking, where the low modulus and strong adhesion starts tearing up the matrix.

Total failure can occur in two ways, fibre pull-out or fibre fracture. If the fibre length is above its critical length, enough stress can be transferred from the matrix and eventually fracture the fibre. If the fibre is below its critical length, the matrix cannot get the necessary “grip” to break the fibre, and it will be pulled-out of the matrix resulting in an empty cavity. The critical length can be derived using equation 2.4.

$$l_{critical} = \frac{(\sigma d)}{2\tau} \quad (2.4)$$

where $c_{critical}$ is the critical fibre length, σ is the fibre tensile strength, τ is the interfacial shear strength between fibre and matrix resin and d is the fibre diameter (Wallenberger & Bingham, 2010).

2.2.5 Causes of rotor blade failure

The term failure mode is commonly used in system integrity analysis and structural health monitoring systems. Failure is a broad term, which can vary depending on the system in question. For example, a load carrying beam may be subjected to bending, but is still able to carry the load. One could say the beam has failed because it has been deformed and has not maintained its original shape. Generally, failure can be defined as loss or reduction of intended function. In this thesis, we are looking for damage which occurs before the turbine completely fails, so that it can be prevented. We define damage as changes to the material or geometric properties. Some common causes of damage for wind turbines are fatigue, wind gusts, thermal stress, corrosion and moisture absorption.

This thesis focuses on the wind turbine rotor blades, but all parts of the wind turbine can be subjected to damage. The table 2 is presented in the paper by (Chia Chen, et al., 2008) and shows typical defects for a variety of wind turbine components.

Table 2 Component specific causes of wind turbine failure (Chia Chen, et al., 2008)

| Wind turbine component | Possible defects |
|--|--|
| Rotor blade | Surface damage, cracks, structural discontinuities, damage to the lightning protection system. |
| Drive train | Leakages, corrosion |
| Nacelle | Corrosion, cracks |
| Hydraulic and pneumatic system | Leakages, corrosion |
| Tower and foundation | Corrosion, cracks |
| Safety devices, sensors and breaking system | Damage, wear |
| Control system and electrics | Terminals, fastenings, function, corrosion, dirt. |

Damage occurs on the rotor blades and tower more frequently than other components. Because the rotor blades are a key component for the wind turbines function, and they can account for 15-20% of the total turbine cost, they are the prime focus in structural health monitoring. In addition, damaged turbine blades can create an unbalanced mass distribution which can make the fault propagate to other components. Wind turbines are exposed to a series of forces over its service life. In 10-30 years, it is likely to experience extremely high windspeeds, lightning storms, icing and even bird collisions. This section will present the potential causes of structural damage to the rotor blades.

2.2.5.1 Damage due to excessive wind

Usually, relatively fierce winds are wanted at wind turbine sites, as it leads to high production. However, wind turbines cannot operate in extreme windspeeds. Modern wind turbines can rotate the blades to reduce the angle of attack from the wind. This reduces the forces on the blades and allows the turbine to produce electricity in excessive winds. Once the wind exceeds the acceptable levels, production is shut down by applying brakes on the drive train. At this stage, there are no further measures to reduce the loads on the rotor blades, and the structural integrity of the blade is in the hands of the wind. There are a series of reported cases where the wind leads to complete turbine failure. In 2009, an industrial wind turbine was destroyed by fierce winds which threw parts of the turbine 150m away from the site (Dongsheng, et al., 2015).

Winds are powerful forces, and in addition to the expected cyclic loading it provides, extreme cases can lead to unexpected damage or complete failure, as shown in figure 2-14.



Figure 2-14 Complete structural failure of rotor blade due to excessive winds (Dongsheng, et al., 2015)

2.2.5.2 Damage due to lightning

Modern wind turbines are built with lightning strike protection systems, consisting of internal aluminium conductors running the length of the blade, leading to exterior copper air termination disks. However, rotor blades can be damaged despite the protection system. Due to the extreme temperatures caused by lightning strikes, internal moisture in the blade can transit into an expansive state, resulting in excessive stresses in the blade. These stresses subsequently lead to structural failure (Dongsheng, et al., 2015). Figure 2-15 shows a typical case of damage due to lightning strikes on the blade.



Figure 2-15 Damage on rotor blade tip due to lightning strike (Dongsheng, et al., 2015)

2.2.5.3 Damage due to ice accumulation

During specific weather conditions, atmospheric icing can form on the rotor blades. Icing changes the surface roughness of the blade, which in turn, changes its aerodynamic properties. In addition, icing leads to safety concerns. Large wind turbines have high rotational speeds at the rotor blade tip, thus large centrifugal forces. Large chunks of ice can be thrown off the blade, posing a serious threat to people and property within the area. Uneven ice formation can lead to bad mass distribution, which in turn can produce hazardous loadings on the blades and hub (Dongsheng, et al., 2015).



Figure 2-16 Flying ice due to atmospheric icing on rotor blade (Dongsheng, et al., 2015)

2.2.5.4 Failure due to faulty manufacturing

As with all products, insufficient quality management can lead to defect products in service. Rotor blades have complicated structural properties, and if not tested properly before deployment and installation, faulty products can be put into production. Ultrasonic non-destructive testing is a common method for post-production testing and has proved suitable for detecting internal faults. Figure 2-17 shows an example of a defect rotor blades in service, which lead to structural failure.



Figure 2-17 Structural failure due to faulty manufacturing (Dongsheng, et al., 2015)

2.2.6 Rotor blade failure modes

In 2002, (Sørensen, et al., 2004) carried out a post mortem analysis of a Vestas A/S V52 wind turbine blade. They identified 7 different failure modes that occurred in the blade during the test. The post mortem investigation was carried out by cutting out the failed compartments of the rotor blade for inspection. The identified failure modes were as follows:

Table 3 Wind turbine rotor blade damage types (Sørensen, et al., 2004)

| Type | Description | Failure mode |
|---------------|---|--|
| Type 1 | Damage formation and growth in the adhesive layer joining skin and main spar flanges. | Skin/adhesive debonding and/or main spar/adhesive layer debonding. |
| Type 2 | Damage formation and growth in the adhesive layer joining the up- and downwind skins along leading and/or trailing edges. | Adhesive joint failure between skins. |
| Type 3 | Damage formation and growth at the interface between face and core in sandwich panels in skin and main spar web. | Sandwich panel face/core debonding |
| Type 4 | Internal damage formation and growth in laminates in skin and/or main spar flanges, under a tensile or compression load | Delamination driven by a tensional or a buckling load |
| Type 5 | Splitting and fracture of separate fibres in laminates of the skin and main spar | Fibre failure in tension: laminate failure in compression |
| Type 6 | Buckling of the skin due to damage formation and growth in the bond between skin and main spar under compressive load | Skin/adhesive debonding induced by buckling, a specific type 1 cause |
| Type 7 | Formation and growth of cracks in the gel-coat; debonding of the gel coat from the skin | Gel-coat cracking and gel-coat/skin debonding. |

Some of the failure modes presented in (Sørensen, et al., 2004) is shown in figure 2-18. The illustration shows the damages on the downwind side of the section after compression load. Adhesive joint failure can occur at both the leading and/or trailing edge of the blade. The solid piece of skin experienced delamination and splitting along fibres as seen in type 4 and type 5 respectively. The gelcoat that is applied on top of the laminate skin experienced cracks which exposes the laminate to the environment. Type 1 failure also occurred, where the adhesive layer between the skin and main spar failed, which significantly affects the structural integrity of the rotor blade.

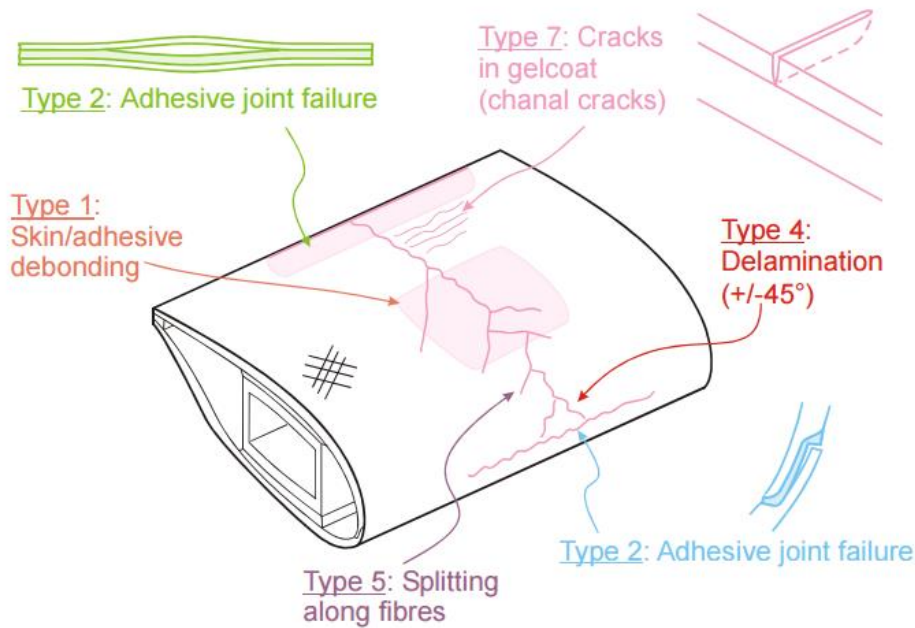


Figure 2-18 Overview of wind turbine rotor blade failure modes (Sørensen, et al., 2004)

The paper by (Sørensen, et al., 2004) also presents photographs of the damages. Some damages can be visually observed at the surface. In figure 2-19, type 7 and type 5 damages is shown. In this example, a compressive load caused damage to the downwind skin. The gel-coat started cracking along the failure. Laminate failure in the skin can be observed where the gel-coat has been removed.

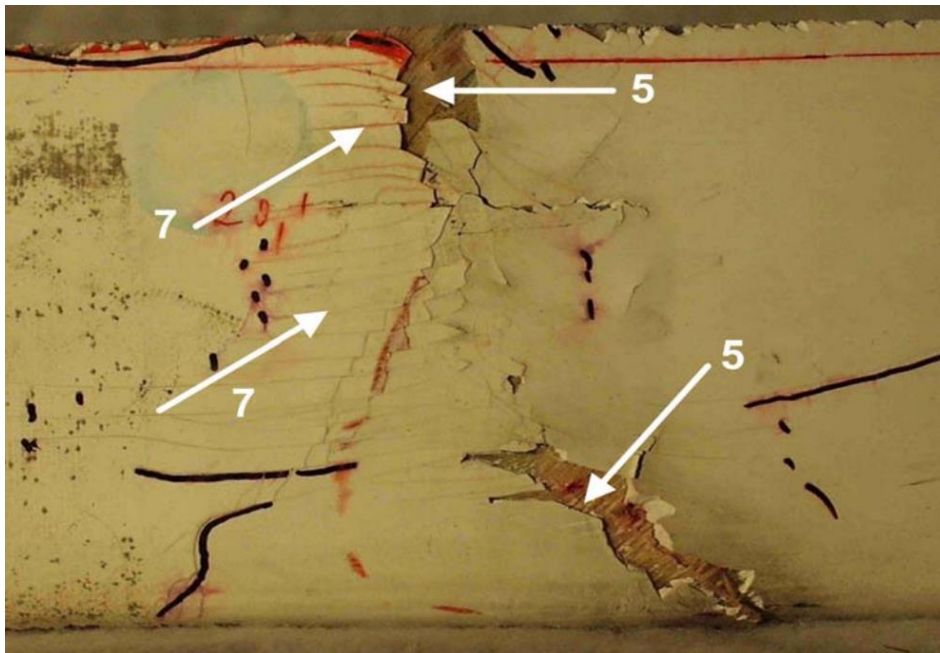


Figure 2-19 Type 7 & 5 rotor blade damage (Sørensen, et al., 2004)

In figure 2-20, type 1 and 4 damages can be observed. Debonding between the skin and spar cap leads to empty cavities in the materials. In undamaged condition, the material is dense and does not contain air due to its vacuum moulding. However, in damaged conditions, clear pockets occur. We can also observe that the direction damages occur parallel to the surface, this is because the fibres are moulded in planes, and damages are likely to occur in this direction. The image also shows an example of internal debonding (type 4) of the spar. This fault also propagates in the same direction as the surface and occurs in the same plane as the glass fibres. These failures are of high critically because the main spar carries the loads applied to the skin. Internal failure of the spar or adhesive damages can lead to a significant reduction in rotor blade strength. These faults cannot be detected through visual surface inspection because they form in between the layers of glass fibres.

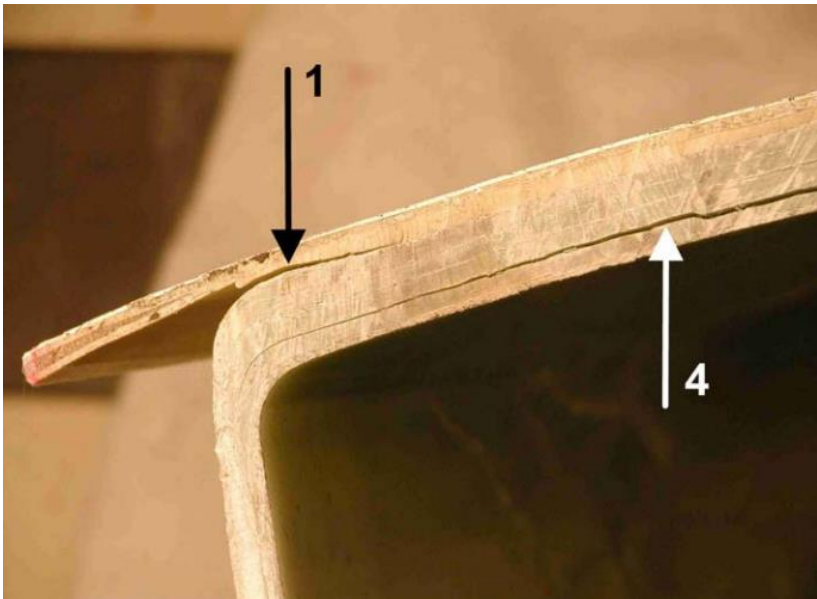


Figure 2-20 Type 1 & 4 damage in skin and spar (Sørensen, et al., 2004)

Figure 2-21 shows where type 4, 5 and 3 failure occurs. The spar is commonly constructed in a sandwich structure, consisting of glass fibre laminate and foam.

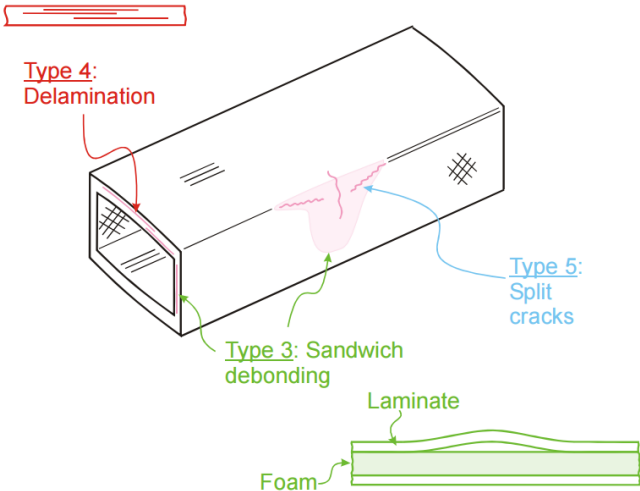


Figure 2-21 Overview of main spar failure modes (Sørensen, et al., 2004)

Figure 2-22 shows an example of type 3, 7 and 5 failures. We can observe internal delamination (type 5) in the core of the spar. The cracking of the gel-coat (type 7) can be observed on top of the sandwich structure. The bending of the laminate sandwich structure debonds from the main spar web (type 3).

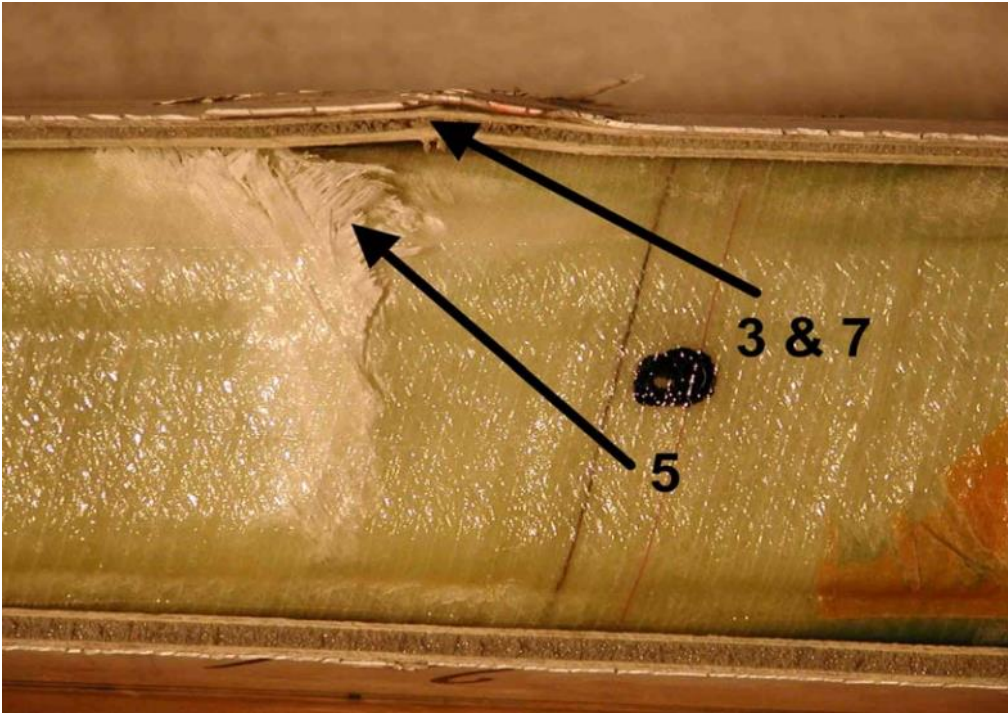


Figure 2-22 Type 5, 3 & 7 failure modes in sandwich structure (Sørensen, et al., 2004)

2.3 NON-DESTRUCTIVE TESTING (NDT)

This chapter will cover the reasoning and methodology behind Non-Destructive Testing (NDT), Non-Destructive Evaluation (NDE) and Non-Destructive Inspection (NDI). These concepts are used in most industries today because it can prolong the lifetime of process facilities and products. Nothing lasts forever, and in most cases, it is beneficial to approximate how long. Successful businesses design their products for a specific lifetime, depending on the function of the product. Thus, it is in many cases beneficial to evaluate the degree of degradation of the product over time. This evaluation can be carried out in a variety of ways, depending on the material and the availability of the product.

How long a product is expected to last is often referred to as the product's reliability. The reliability is a function of the design of the component, material selection and its intended purpose. A product often consists of a range of components, where each component has its own reliability. If a component is critical for the system, failure of the component will cause a system failure. It is therefore important that the critical components of the system are designed with high reliability. Even though the design of a component is of high reliability, production processes have a probability of creating a faulty product. In some cases, the finished product may not be of the intended quality. If these components are installed in a large system, we may experience system failure sooner than expected. This can potentially lead to major costs, and in some cases, loss of lives. To ensure that a product is produced according to a certain standard, most companies have implemented quality control in their processes. Quality control typically use a variety of methods to test either all products or randomly selected samples, depending on the criticality of the component. For example, oil pipelines must have a much higher quality than a furniture chair because the consequences of failure are vastly different.

The methods of testing a component can be split into two main categories, destructive and non-destructive testing. The basic concept of NDT is that the test does not alter or damage the object in question. Destructive testing is based on sampling of a product with the assumption that the rest of the object is of the same properties and condition. NDT may be used for in-service components, while destructive testing may not. In many cases, the system does not require to be shut down for NDT, which have significant economic advantages. This has caused non-destructive testing to be a common practise in most industries today, ranging for testing of commercial aircrafts to nuclear powerplants.

“Practical Non-Destructive Testing” by (Baldev, et al., 2007) has created a comparison between destructive and non-destructive testing, as seen in table 4.

Table 4 Comparison of destructive and non-destructive testing (Baldev, et al., 2007)

| | Destructive tests | Non-destructive tests |
|--------------------|--|--|
| Advantages | <ul style="list-style-type: none"> ▪ The measurements are direct and reliable. ▪ The measurements are usually quantitative. ▪ The correlation between the test measurements and material properties are direct. | <ul style="list-style-type: none"> ▪ The tests are made directly on the object. A 100% test of the object is possible. In-service testing is possible. ▪ In many cases, more than one NDT technique can be applied to the same object, allowing for testing of many or all material properties of interest. ▪ The same non-destructive test can be carried out several times on the same object. ▪ Most of the tests are rapid and require little preparation. |
| Limitations | <ul style="list-style-type: none"> ▪ The tests are not conducted directly on the entire object, thus the correlation between the object sample and the object must be proven. ▪ A single test may yield limited information. ▪ In-service testing is not possible. ▪ Destructive tests usually take longer time than NDT. ▪ It may be impossible to measure over time. ▪ Test preparations is expensive. | <ul style="list-style-type: none"> ▪ The measurements of NDT are indirect. Thus, the reliability of the test must be verified. ▪ The measurements are usually qualitative, but can in many cases be done quantitatively- ▪ NDT often require skilled personnel, as results may be hard to interoperate. |

There is a range of available techniques for non-destructive testing. Some require surface contact with the test object, some require access from multiple sides, and some techniques can only be applied to conductive materials, such as eddy-current testing. Specific methods can also be used for continuous monitoring, such as acoustic emission monitoring and strain gauges, which can be permanently installed. A paper by (Martinez-Luengo, et al., 2016) called “Structural health monitoring of offshore wind turbines: A review through the Statistical Pattern Recognition Paradigm” presented a table listing a series of advantages and limitations of common non-destructive testing techniques applicable for offshore wind turbines. The comparison is presented in table 5.

Table 5 Review of common non-destructive testing techniques (Martinez-Luengo, et al., 2016)

| Technology | Advantages | Limitations |
|---|--|---|
| Acoustic emission monitoring Type of sensors: - Piezoelectric transducers | Very effective at detecting failure mechanisms down to microscale. Allows for a simple, rapid and cost-effective inspection or monitoring of a structure. Good response at low frequencies. Multifunctional character of piezoelectric sensors. | Limited application offshore. Variable damage characterization and assessment effectiveness depending on the algorithm. Optimization for data processing needed as it still takes up much time and computational effort. High sensitivity to background noise. AE systems can only qualitatively gauge how much damage is contained in a structure. Determining acoustic signature of the structure is very difficult. |
| Thermal imaging method Type of sensors: - Impedance tomography - Thermography (infrared cameras) | Fast and cost effective. Trials using drones are currently being conducted, which will detect cracks up to 0.3 mm based on technology limitations, avoid the necessity of having personnel inside the turbine and be even more cost effective. Moreover, time required would be less than traditional sensors. | Limited implementation in offshore structures. Camera resolution for detecting cracks Laborious Image processing Cracks detection needs more automation from footage. |
| Ultrasonic methods Type of sensors: -Piezoelectric transducers | It is sensitive to both surface and subsurface discontinuities. The depth of penetration for flaw detection or measurement is superior to other NDT methods. Only single-sided access is needed when the pulse-echo technique is used. It is highly accurate in determining reflector position and estimating size and shape. Minimal preparation is required. Electronic equipment provides instantaneous results. Detailed images can be produced with automated systems. It has other uses, such as thickness measurement, in addition to flaw detection. | Surface must be accessible to transmit ultrasound. Skill and training required is more extensive than other methods. Coupling medium to promote the transfer of sound energy into the test specimen is required. Difficulty of inspection of rough, irregular, very small, exceptionally thin or not homogeneous materials. Difficulty of inspection of cast iron and other coarse-grained materials. Linear defects oriented parallel to the sound beam may go undetected. Reference standards are required for both equipment calibration and the characterization of flaws. |
| Fatigue and modal properties monitoring Type of sensors: - Accelerometers - MEMS Plastic optical-fibre based accelerometers -Velocimeters | High reliability, mature technology Easy installation. There are many different techniques available for this purpose. Recent developments in Operational Modal Analysis solve some limitations. Stable performance. | Difficult analysis in operating conditions. High number of uncertainties when applied in the offshore environment. Environmental and Operational Conditions changes have to be accounted in the results. Difficulties in wind and wave loads measuring. |
| Strain monitoring Type of sensors: - Strain gauge (capacitance, inductance, semiconductor and resistance) -Fibre optic cables Fibre Bragg Grating (FBG) | Easy installation process once appropriate training has been undertaken. Mature technology. Optical fibre might be the future of strain monitoring as it is less prone to fatigue, eliminates wiring issues and allows more points to be monitored with the same cable. | Not very robust system. The installation is very sensitive to misalignments. Reduced service life. Distance between the sensor and the Data Acquisition System influences accuracy and limits sensor location. Mechanical properties limitations Can be affected by EMI noise. |

2.3.1 Condition monitoring and maintenance

In all major manufacturing and production plants, maintenance represents a substantial portion of the total operating cost. Maintenance is carried out to ensure that the facilities are working efficiently for the highest production possible. For example, if the bearings in a generator are insufficiently lubricated, maintenance will prolong the life and production capacity of the generator. However, it can be hard to accurately predict exactly when the oil or bearings, should be changed. Production must be shut down and the system disassembled to change critical components. This leads to large costs that are unnecessary if the system has no faults, in addition to loss of production. Since the second world war, knowledge of maintenance techniques and philosophies have exploded. Back then, maintenance was viewed as a “necessary evil” and the costs of keeping systems running was considered impossible to reduce. Today, maintenance is viewed as an opportunity to achieve lower operating costs than your competition, resulting in lower prices and higher profits.

2.3.1.1 Maintenance techniques

There are several different maintenance techniques in use today. Companies prioritize maintenance of critical components, while other components may be completely ignored. Cost-effective maintenance is calculated based on the impact a component failure will have on the system. These calculations will not be covered in this thesis, but this chapter will present the main principles of maintenance. We can define maintenance in three categories: reactive, preventive and predictive maintenance.

2.3.1.1.1 Reactive maintenance

Reactive maintenance, also known as run-to-failure, is the way of the old days. Systems and components are run until they fail and causes a system-wide halt. This way of maintenance may seem very primitive. However, for simple system with easy access to spare parts, it may be the most cost-effective method. Because there is no effort to predict system failures, large downtime and high spare part storage or delivery costs can be expected. Today, few to none apply this kind of philosophy to industrial equipment. Because systems have become more advanced, it is in most cases beneficial to invest in detailed analysis to predict what is likely to fail, and when. This type of maintenance is called preventive maintenance.

2.3.1.1.2 Preventive maintenance

Preventive maintenance is one of many definitions for time-driven maintenance programs. The basic idea is to identify the most critical components and prioritize costs based on probabilities. By calculating the statistical probability of failure of equipment and components, and combining the results with the consequence of failure, the most maintenance heavy parts can be identified. This method prevents the excessive costs related to unexpected failure, in addition to reducing unnecessary maintenance of low-criticality components.

The application of preventive maintenance varies greatly from industry to industry. For example, nuclear power plants and airplanes have a substantially more detailed maintenance program than a wind turbine. This is the result of risk analysis, where failure of airplanes mid-air is unacceptable.

Although preventive maintenance appears like an effective method of maintenance, it does have its limitations. As it is based on probability, unexpected failures may still occur, and some repair will be reactive maintenance. Some repair may even be unnecessary, as components may be changed even though they are working perfectly fine. One of the greatest advantage of preventive maintenance is the ability to schedule the downtime of the system. A good example

of this is the maintenance of airplanes. They are grounded and disassembled at set intervals. This reduces the amount of delays and greatly increases the safety and reliability of airplanes.

2.3.1.1.3 Predictive maintenance

Like preventive maintenance, predictive maintenance is supported by statistical probabilities. It does however, introduce the concept of condition monitoring. From risk analysis, the most critical components of a system are identified. Instead of relying on the probability of failure, these components are monitored, either continuously or at calculated intervals. A comprehensive maintenance program often includes a combination of reactive, preventive and predictive maintenance to achieve the most cost-effective solution. It has become a common factor in the most successful and competitive industries because the company who does the best maintenance, often has the most profit.

There are many ways of monitoring a system through NDT. With the revolution of microprocessors and controllers, a wide array of sensors has become available to accurately measure the condition of a system or component. For example, the vibration of a powertrain in a wind turbine can be measured continuously with vibration transducers. This allows the maintenance personnel to identify wear of bearings and shafts in real time because each component has its own vibration signature. Deviation from the normal and expected vibration is easily identified by signal processors as it trends towards failure. This allows maintenance personnel to quickly replace or repair the components that are failing, resulting in minimal downtime and cost (Mobley, 1990).

2.4 UNMANNED AERIAL VEHICLE (UAV)

In the 20th century, the terms drones and UAVs were mostly connected to military usage and technology (Nex & Remondino, 2013) because drones could give a significant advantage in the battlefield, and carry out military strikes without endangering allied lives. However, due to technological growth in the area and a strong reduction in costs over the last decade, UAVs have become common in the hobby communities. According to a report from Tractica, consumer drone sales are expected to continue with an exponential growth over the coming years. Global annual unit shipments are predicted to increase tenfold from 2015 (6,4 million) to 2021 (67,9 million). While sales increase, average selling prices are predicted to decline, making aerial technology available and affordable to just about everyone (Tractica, 2016).

The potential in consumer UAVs expand way beyond the entertainment value, and the applications of UAVs are rapidly expanding. Today, it is common to use drones with cameras to take overview pictures for house listings. It is widely used for shooting movies, and industries such as oil and gas are starting to implement drones in monitoring and maintenance activities. In the consumer market, the term “drone” is commonly used for unmanned aerial vehicles (UAVS). Per the unmanned vehicle system (UVS) international definition, a UAV is “a generic aircraft design to operate with no human pilot on board” (Nex & Remondino, 2013). Other common definitions are Remotely Piloted Vehicle (RPV) and Remotely Piloted Aircraft Systems (RPAS). In this paper, the term drone, UAV and RPAS will be used together for the same purpose. This is to maintain the consumer everyday speech, while sticking to the definitions used in the regulations for RPAS flight.

The industry is currently flourishing with UAV designs, where each of them has its own strengths and weaknesses. Factors such as payload, flight time, safety, reliability, launch and landing, complexity and prices are some of them. This chapter will compare the two most popular solutions, multi-rotor and fixed-wing, as well as look in to new and emerging designs.

2.4.1 Multirotor UAV

Multirotor UAV's are the most favoured design in the current consumer market. These drones are great for putting a small and lightweight camera in the air for a brief time. Due to the principle of flight in multirotor designs, the pilot can have very good control over the drone. These UAVs are known for their stability and manoeuvrability, and an inexperienced pilot can take-off and land most consumer-market drones with ease. There are different controllers and auto-pilots available, and the drones come in many shapes and sizes.

2.4.1.1 Principles of flight

Multirotor UAVs and helicopters work by similar principles. A manned helicopter uses large rotor blades to push air downwards and create an upwards lift to stay airborne. The high rotational energy of the rotor creates a torque on the body, and a smaller rotor is attached to the aircraft's tail to compensate and keep the helicopter aligned. In a multirotor UAV, the only moving part is the fixed horizontally oriented rotors. As they rotate, they push air downwards like a manned helicopter. To manoeuvre in the air, the speed of the individual rotors is adjusted to orient the UAV as intended.

2.4.1.2 Multirotor coordinate system

Back at the 16th century (Learn Robotix, u.d.), a system for describing the orientation of rigid bodies was developed, and is still in use to this date. It describes the orientation around 3 axes, pitch, roll and yaw.

Table 6 Description of UAV coordinate system (Learn Robotix, u.d.)

| | |
|-------|---|
| Roll | Describes how the right and left side are elevated with respect to each other. If the left side is pushed down, and the right side is pushed up, the UAV will move to the left. |
| Pitch | Describes how the front and back are elevated with respect to each other. If the front of a drone is moved down, and the back up, it will move forward. |
| Yaw | Describes the rotation of the drone. If the front, back, and both sides are levelled, it can turn around the yaw axis without shifting position. |

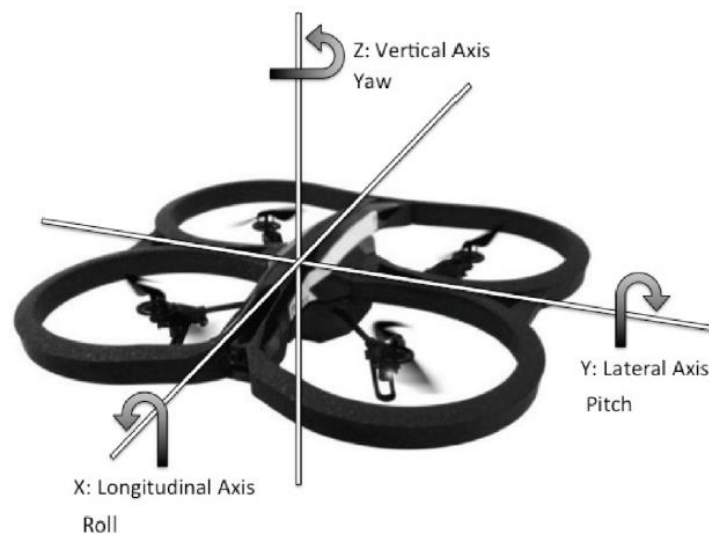


Figure 2-23 UAV coordinate system. Roll, pitch and yaw. (Hansen, et al., 2014)

2.4.1.2.1 Roll and pitch

Roll and pitch of the quadcopter is achieved by the same principle, increasing the speed of the rotors on the opposite side of the direction you want to fly. If the pilot, for example wants to fly forward (pitch), he must increase the speed of the back rotors and reduce the speed of the front rotors, elevating the back relative to the front. For a rolling motion, the same principle applies.

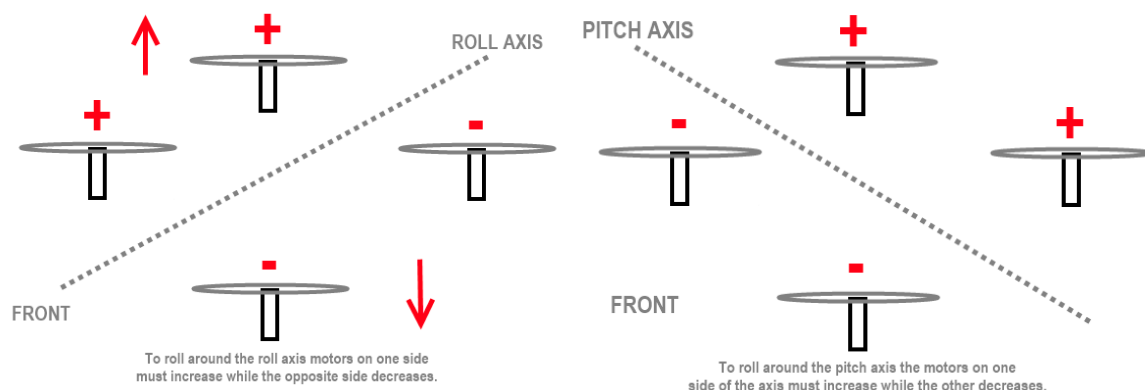


Figure 2-24 Roll and pitch, engine control (Learn Robotix, u.d.)

2.4.1.2.2 Yaw

To achieve a yaw motion on a quadcopter, it must be assembled with clockwise (CW) and counter clockwise rotors (CCW). This is also important for keeping the quadcopter stable during flight. When this criterion is met, the quadcopter can rotate by adjusting the speed of diagonal rotors. Depending on which rotors have the highest speed, CW or CCW, it will rotate left or right around the yaw axis. (Learn Robotix, u.d.)

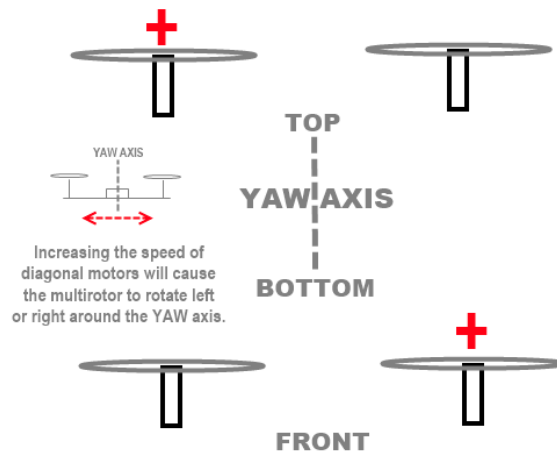


Figure 2-25 Yaw, engine control (Learn Robotix, u.d.)

2.4.1.3 Limitations of multirotor UAV

Despite high levels of stability, there are some severe limitations to the multi-rotor design. These UAVs are fundamentally very inefficient regarding energy consumption. The small rotors require a large amount of power just to keep the UAVs in the air. Due to the need of precise thrust control, they currently only run on electrical motors. This puts great limitations on the expected flight time, and with the current battery technology, they are limited to approximately 20-30 minutes depending on the models. The high weight-to-power ratio of batteries also gives little potential of reaching longer flight times (Chapman, 2016).

2.4.2 Fixed-Wing

Fixed-wing drones get their lift from fixed wings, like normal manned airplanes. This allows the engines to solely provide the forward thrust needed, making them much more efficient than the multi-rotors. It also allows for the use of petrol engines, which have a much higher weight to power capacity than electrical motors and batteries. Due to their efficiency, they can stay in the air for much longer periods of time and fly at higher speeds. Some fuel based fixed-wing drones can stay airborne for as much as 16 hours or more, making them ideal for mapping large areas.

2.4.2.1 Limitations of fixed-wing UAV

As opposed to the multi-rotor design, there are more limitations to take-off and landing conditions. Big UAVs that carry heavy equipment, such as high definition cameras and lasers, cannot be launched straight from the hand. Often, a launchpad or runway is needed to launch the plane, and a runway, parachute or net to land the drone. These drones are also much harder to control, as it cannot hover like the multi-rotor. They do not have the same manoeuvrability as for example a quadcopter where 4 motors can thrust independently. To operate heavy fixed-wing drones, the pilot must have a lot of experience and expensive equipment to keep the plane

stable. There are however continuous developments in this market, and September 2016 Parrot launched a commercial easy-to-use fixed-wing drone. (Chapman, 2016)

2.4.3 Other designs

The purpose of the drone determines the best suitable design. For example, the single-rotor helicopter is an option when it is needed to carry heavy loads with hover capabilities. Due to a single large rotor blade, the helicopter is much more efficient in energy consumption than the multi-rotor drones, and can use fuel powered engines. These drones are harder to control than multi-rotor models, and bring serious challenges such as vibration. They are also dangerous to operate due to the high kinetic energy of the blades, which can cause serious injuries. In 2013, the New York Post reported a fatal accident from a high-powered model helicopter. The experienced pilot had received fatal wounds from an impact with the rotor blades (Conley, 2013). Another interesting concept is the fixed-wing hybrid. This design is intended to allow for vertical take-off, and uplift from the fixed-wings during long flights. These designs have been tested in manned flight in the 1950s and 1960s, but due to their instability and complexity, the results were disastrous. With the current development in gyro and autopilots, the designs are emerging again. For example, Amazon are developing drones with this design for package delivery (Chapman, 2016).

2.4.4 Norwegian Aviation Law and Regulations

The rapid rise in popularity for commercial drones has brought on legal and moral challenges. Drones have been featured in international media for quite some time, where cases such as stalking and espionage have been in the focus. Camera technology has reached a high quality to weight ratio, where small drones can take highly detailed pictures. This has led to situations where commercial drones can spy on neighbours, take unflattering or revealing pictures, which breaches a person's privacy. UAVs may also pose a threat when operated in public areas, where dropped equipment or failure can lead to damages to people and property. There are also reported cases where UAVs fly into commercial airspace and have near-collisions with air traffic. Collision with manned air-traffic can lead to engine failures in helicopters and airplanes, which can lead to catastrophic accidents. To cope with the emerging risks and challenges, CAA has developed regulations for unmanned aerial operations. Today, UAV operations must follow the regulations set in "Regulations concerning aircraft without a pilot on board etc." These regulations are based on paragraph 15-1 in the Norwegian aviation act, and came into effect 01.01.2016.

The following chapters will briefly present the Norwegian aviation law and regulations. Because it only applies in Norway, it cannot be used as an absolute consideration for UAV usage in non-destructive testing. However, because the regulations were released in 2016, they may be considered relevant as to how UAV regulations may develop in other countries as well.

2.4.4.1 Model airplanes

RPAS Reg. distinguishes between model airplanes and drones, which is determined by the intention of the flight. Model airplane flights are defined as activities that are for recreational, sport or competition purposes. Some regulations do not apply to model airplanes, especially if the flight is conducted with an approved model airplane club. These regulations are not relevant to this thesis, as model airplanes cannot be applied for physical contact non-destructive testing.

2.4.4.2 General requirements and limitations for all RPAS-operators

UAV flights can only be conducted if the business has a responsible leader, operation leader and technical leader. However, one person can fulfil one, two or three roles, depending on the magnitude of the operation. These regulations are in place in to distribute responsibility and ensure a safe and legal operation, and can be found in chapter 3 of RPAS Reg. (Lovdata, 2015)

To preserve the safety of the public, aviation traffic and military security, the RPAS regulations states prohibited flight zones, where flight is only possible through special permissions. The regulations state that no UAV may exceed a height of 120 meters from ground level during the flight. All drones are required to carry a sensor, or other accurate means of height measurement, to uphold these regulations.

All rotary powered systems must have a system for fail-safe in place. The drones must be able to land unassisted in the case of technical errors or loss of communication. In cases of fixed-wing design aircrafts, there must be a system in place to ensure contact when the main radio fails so that the UAV can land in a controlled manner.

2.4.4.3 Operational provisions for all RO-operators

In addition to the responsibilities for the pilot and aircraft supervisor, chapter 7 in RPAS Reg defines safety distances for all RO-operators. Per § 51., all flight must happen in a considerate (“hensynsfull”) manner, which are not bothersome (“sjenanse”) and does not pose a risk to aircrafts, people, birds, animals or property.

The regulations require a certain gentleness for RPAS flights which cannot exceed the threshold paragraph 51 implies. The threshold can be hard to define, and will be dependent on the surroundings and situation.

2.4.4.4 Safety distances and no-flight zones

§ 51. Defines the following safety distances:

It is not allowed to fly:

- Higher than 120 meters over the ground or water.
- Closed than 150 meters from groups of more than 100 people.
- Closer than 50 meters from people, vehicles or buildings which are not under the pilot's control.

§ 54. Defines the following no-flight zones:

It is not allowed to fly:

- In proximity to, or over, military areas, embassies or prisons.
- Closer than 5 km to an airport, unless the flight has been cleared with the local flight control service or flight information service.

2.4.4.5 RPAS-operator categories (R01, R02, R03)

In addition to the general requirements and limitations for all RPAS-operators, the RPAS regulations has divided UAV flight licences into three categories. The purpose of the RO system is to define requirements for the complexity of operations, in addition to the weight and speed of the drones. The required documentation for each RO category varies greatly, where R01 operation does not require a risk analysis before flight, R02 does. A brief summary of the technical requirements for each category is listed below:

RO1 is needed for aircrafts with a MTOM of up to 2,5 kg and a maximal speed of 60 knots. The flight also must be carried out in daylight and within VLOS.

RO2 is needed for aircrafts with a MTOM of up to 25 kg and a maximal speed of 80 knots. The flight can be operated with VLOS, or EVLOS and BLOS if requirements are met.

RO3 is needed for aircrafts with MTOM of over 25 kg or speeds of over 80 knots. RO3 is also required if the aircraft is run by a turbine engine, operated BLOS, flies in controlled airspace at more than 120 meter heights, or in proximity of large crowds.

:

2.5 RISK MANAGEMENT

UAV flight, like regular aviation, have a series of related risk during operation. The machines are delicate, and simple system errors can lead to total system failure. As reviewed in chapter 2.3.2 Norwegian Aviation Law and Regulations, UAVs of MTOM of over 2,5 kg requires a risk analysis before flight. In our case, the UAVs are intended for flight in proximity and direct contact with the wind turbine rotor blades. Damage to the blades would be directly against the purpose of this thesis, and a risk analysis must be carried out to investigate the hazards of the intended operation. In this chapter, a theoretical framework of basic risk management will be presented. A risk analysis will be carried out in chapter 4.1, and discussed in chapter 5.

The term risk is often used in everyday speech with a varied definition. It originates from the Italian word “risicare” and means “to dare”. In modern technical terms it is often described as a combination of probability and consequence (Gjellestad, 2011). Risk is involved in our lives daily, and in many cases, must be taking in to account. Risk management is a tool for identifying hazards, analysing probabilities and consequences, addressing dangerous situations, and implementation of preventive measures. Risk management is used by organizations and businesses for a vast number of operations and systems. The level of detail and effort put in to risk management must be proportional to the complexity of the operation or system (Insitute of Risk Management, 2016).

The parameters of probability and consequence can either be qualitative or quantitative, or a combination of the both, with varied levels of details. Normally, a risk analysis aims to answer:

- What unwanted incidents can occur?
- What are the causes and probability of each unwanted incident?
- What are the consequences if unwanted incidents do occur?

2.5.1 Risk Analysis

A risk analysis is an effective tool for carrying out operations and operating systems in a safe manner. By identifying potential accidents before they happen, we can implement barriers that reduce the probability of unwanted events occurring, or reduce the consequences if they do occur. There are many ways of performing a risk analysis, but we can identify some main characteristics in the process. The figure 2-26 shows a general model for risk analysis (Gjellestad, 2011).

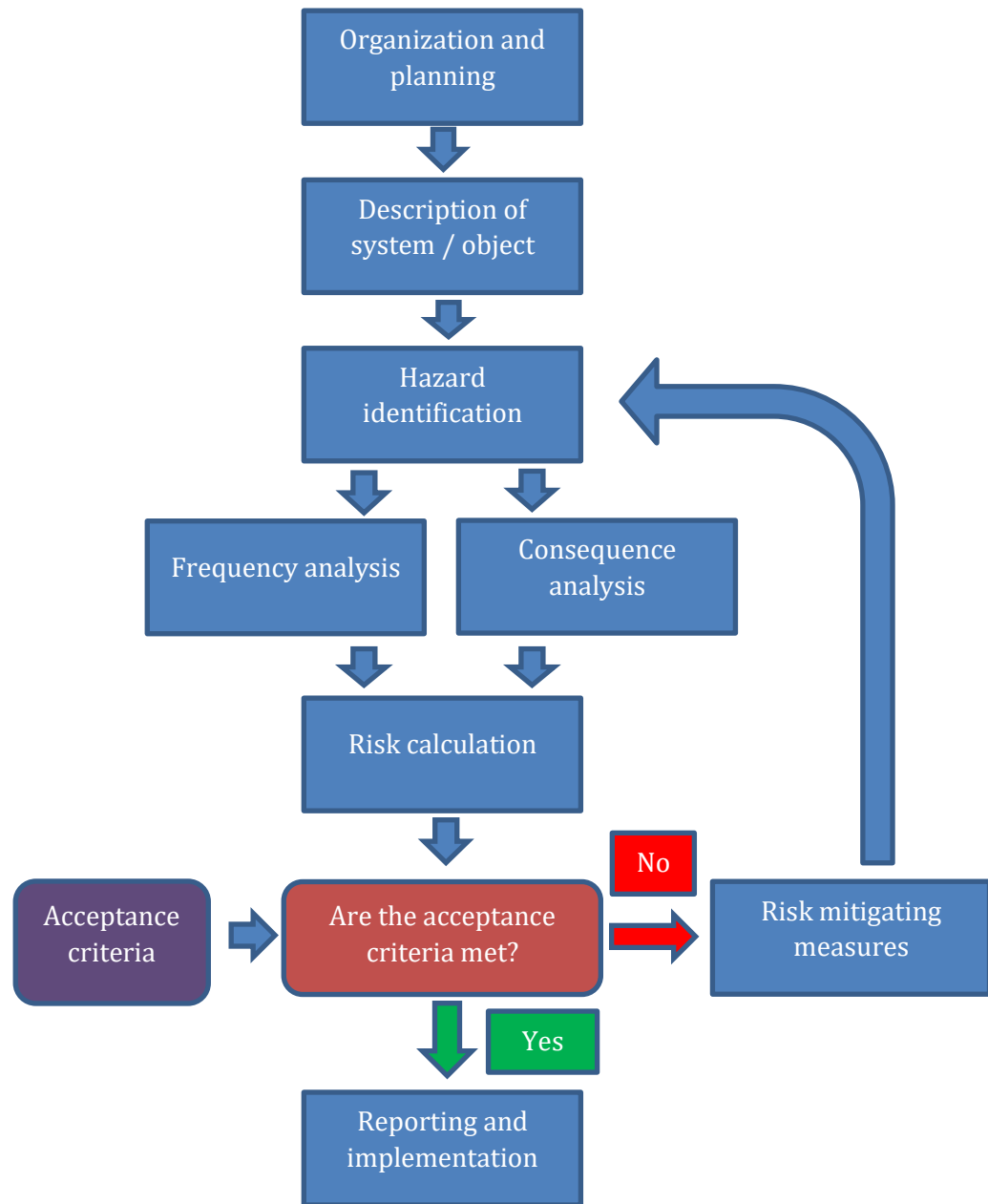


Figure 2-26 Risk analysis procedure (Gjellestad, 2011)

Organization and planning

Before a risk analysis can commence, it is important to establish a plan for how the analysis is to be carried out. Which resources are at disposal, which personnel will be involved, and what level of detail is needed for sufficient results.

Description of the system/object

To carry out a good risk analysis, the system or object of interest must be clearly defined. For large systems, such as an oil and gas separator, it is helpful to divide the system in to sub-systems. This ensures focus on critical components and makes the analysis easier to handle.

Hazard-identification

“A Hazard is something in, around or part of the organisation which has the potential to cause

damage” (CGE Risk Management Solutions, u.d.). It is a creative process which identifies scenarios that can be broken down into probability and consequence. Brainstorming with qualified personnel is a typical strategy for hazard identification.

Frequency-analysis

The purpose of the frequency analysis is to identify how often causes for unwanted events occur. These values can be numbered mathematical probabilities (quantitative) or simply defined as low, medium and high (qualitative). Quantitative values allow for a complex analysis, but requires more data.

Consequence-analysis

The purpose of the consequence analysis is to identify the consequences of an unwanted event. Consequences are normally categorized into personnel, environment and material, because a loss of human life cannot be directly compared to financial losses. As with frequencies, consequences can have quantitative and qualitative values, normally in the same level of detail.

Risk-calculation

Once the frequency and consequence of the identified hazards have been defined, they are combined to make a “picture” of the risks. Risk is a product of frequency (probability) and consequence, and the correlation of the two factors determine the risk.

$$\text{Risk} = \text{Frequency} \times \text{Consequence}$$

A normal technique is to construct a risk matrix. Depending on the quality of the data used in the analysis, the matrixes resolution is determined. For a qualitative risk analysis, it is common to use a 5x5 matrix. To clearly separate the factors, probability is rated by numbers 1-5 and consequence with the letters A-E, where A equals 1 and E equals 5 in numeric values. The risk matrix used in this thesis is a 5 by 5 matrix which splits the hazards into risk categories. High consequence and high probability will result in high-risk, and low consequence with low probability is low-risk. The matrix also provides a good visual presentation of all the hazards in question.

Table 7 5x5 risk matrix

| Risk Matrix | | | Consequence | | | | |
|-------------|---|----------------|-------------|--------|----------|--------|--------|
| | | | A | B | C | D | E |
| | | | Minimal | Minor | Moderate | Major | Severe |
| Probability | 5 | Almost certain | Yellow | Yellow | Red | Red | Red |
| | 4 | Likely | Green | Yellow | Yellow | Red | Red |
| | 3 | Possible | Green | Green | Yellow | Yellow | Red |
| | 2 | Unlikely | Green | Green | Green | Yellow | Yellow |
| | 1 | Rare | Green | Green | Green | Green | Yellow |

Acceptance criteria

At this stage of the analysis, we compare our values of risk against our acceptance criteria. The acceptance criteria may come from a standard, experience or company policy. This comparison will determine whether preventive measures must be taken to reduce the risk.

We can normally categorize acceptance criteria in 3 categories, acceptable risk, tolerable risk (ALARP - As Low As Reasonably Practicable), and unacceptable risk. We aim to push all activities and systems in to the acceptable area with risk mitigating measures. However, in cases where the activity is highly important but the means of risk reduction is impossible or have unreasonable costs, we accept ALARP tolerances. The following picture is a visual representation of the acceptance criteria assessment.

Report and implementation

The results from the risk-analysis must be documented, and the preventive measures must be implemented in the operation protocols.

2.5.2 SWIFT-Analysis

“A SWIFT-analysis is a structured brainstorm where people with extensive experience of the object in question ask questions as to what can go wrong, and answer these questions” (Rausand & Utne, 2009). A SWIFT-analysis is different from “what-if” analysis, which have been used in risk analysis for a long time, by working through a structured checklist. The checklist is developed in the planning phase of the risk analysis, and is often based of early risk assessments of similar operations. A good and well-thought checklist will help the analyst to stay creative and work efficiently, as well as reducing the risk of missing significant hazards. (Rausand & Utne, 2009).

2.5.2.1 Advantages

The SWIFT-analysis is easy to carry out, yet effective, for simple operations and systems. It is easy to understand and can be used for a wide range of topics. Due to its simplicity, it can be carried out at many stages of operation. It also produces quick results, and measures are often easy to implement. (Rausand & Utne, 2009)

2.5.2.2 Limitations

The SWIFT-analysis is highly dependent on the competence of personnel, and it is more subjective than other options. The analysis is not recommended for complex systems, and high-risk objects should be analysed in greater detail.

2.5.2.3 Methodology

SWIFT analysis can be carried out with simple tools, and an excel sheet will in most cases be sufficient. In the example bellow is a typical form used for the SWIFT-analysis. It is created in excel and demonstrates the methodology (Rausand & Utne, 2009).

Table 8 SWIFT-analysis (Rausand & Utne, 2009)

| Nr. | What if? | Potential causes | Effects and consequences | Existing barriers | Risk | | | Risk reducing measures | Responsible | Post-barrier risk | | |
|-----|----------|------------------|--------------------------|-------------------|-------|-------|-----|------------------------|-------------|-------------------|-------|-----|
| | | | | | Freq. | Cons. | RPN | | | Freq. | Cons. | RPN |

| | |
|---------------------------------|--|
| Nr. | Each of the analysed cases should be given an identification number for future reference. |
| What if? | The analysts ask themselves questions. For example, what if the quadcopter loses propulsion? These questions lay the grounds for the next steps of the analysis. |
| Potential causes | The analysts list potential causes to the “what if” scenario. |
| Effects and consequences | The analysts list the effects and causes of the “what if” scenario. |
| Existing barriers | The barriers to the “what if” scenario is listed here. These are barriers that are already in place to reduce the probability or consequence of the scenario happening. This gives insight to whether more preventive measures need to be implemented. |
| Frequency | To calculate the risk, the frequency (probability) is needed. The analysts use their best judgement and intuition, or mathematical models if data is available, to determine the frequency. |
| Consequence | As with frequency, the consequences are determined by the analysts. |
| RPN | This is the risk index. The index is often calculated using a risk matrix, and depending on our acceptance criteria, we may need to introduce preventive measurements. |
| Risk reducing measures | For high RPN scenarios, we need to introduce preventive measures to reduce the risk. In this thesis, we will be using a bow-tie method for risk-reducing measures. |
| Responsible | The person responsible signs off for the specific ID number. |
| Post-barrier risk | In the post-barrier risk section, the risk after the bow-tie analysis is presented. |

2.5.3 The Bow-tie Method

In combination with the SWIFT-analysis, the bow-tie method can be a powerful tool in risk management. It can be used for a more thorough analysis of high-risk scenarios from the SWIFT-analysis, eliminating weaknesses from our results. It is a method which visualizes the risk we are analysing in one single picture (CGE Risk Management Solutions, u.d.). It is based on the hazards, or unwanted events, identified in the SWIFT-analysis, where the potential threats are analysed individually. The potential threats can have one of more causes and consequences, and the method aims to identify preventive and consequence reducing measures. The name bow-tie originates from its appearances, which looks like a bow tie.

2.5.3.1 Top Event

The Top Event is determined based on the hazard. We start the analysis by choosing a hazard to analyse and set the top event as the event that leads to consequences. This is the moment when control of the hazard is lost (CGE Risk Management Solutions, u.d.). No consequence has occurred yet, it is however, imminent.

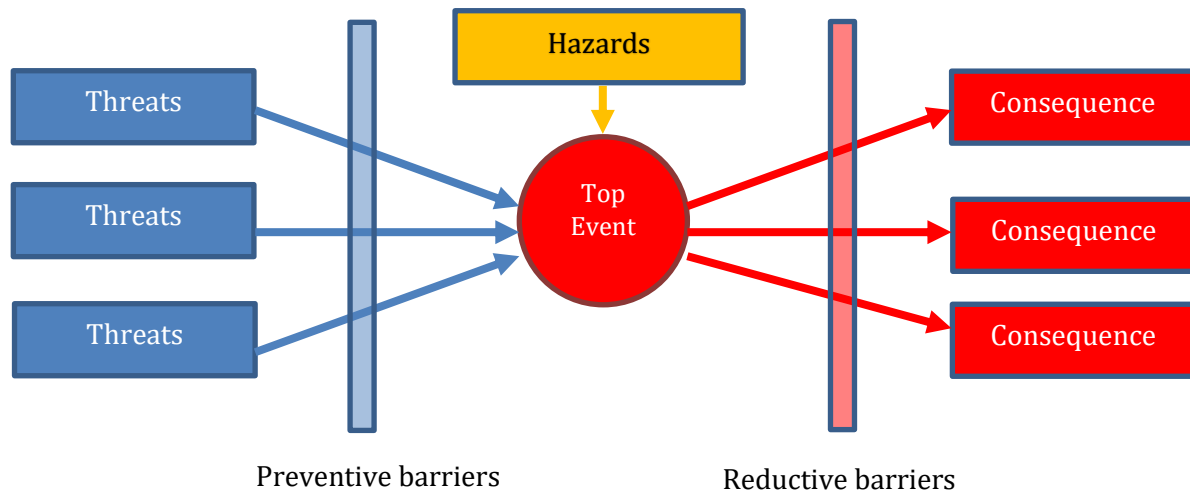


Figure 2-27 Bow-tie diagram

2.5.3.2 Threats

Threats are causes that lead to the Top Events. One Top Event can have multiple threats, and a good bow-tie analysis will have well defined threats. Examples such as “human error” or “equipment failure” will in many cases be too generic (CGE Risk Management Solutions, u.d.). However, we should avoid being too specific, as 100 threats can be unnecessary.

2.5.3.3 Preventive barriers

Preventive barriers are meant to reduce the risk of a top event occurring. By looking at the threats, we can identify and implement measures that “stop” the threats from happening. Depending on the original probability of a threat, we can introduce one or more preventive barriers to each.

2.5.3.4 Consequences

The outcome of the top event is referred to as consequences. As with threats, one top event can have more than one consequence, and the correct level of detail is important. We want to avoid generic as well as over-specific consequences.

2.5.3.5 Reductive barriers

Unlike preventive barriers, reductive barriers are in place after the top event has occurred. They are meant to reduce the consequences by either reducing the degree of impact, or increasing the recovery rate of the operation or object in question. It is important to keep in mind that barriers are never perfect, and barriers can be extended to barrier effectiveness (CGE Risk Management Solutions, u.d.). Effectiveness can be included in quantitative risk analysis to give a better estimation of probabilities.

2.6 ULTRASONIC TESTING

Ultrasonic testing has been a valued means of material evaluation for a long time, and experimental work can be traced back as far as the 1930s. The first ultrasonic flaw detector was introduced in 1945 by Sperry Products, and over the next decades, the testing technique grew greatly in popularity. Until 1984, all ultrasonic testing instruments used analogue signal processing. However, with the arrival of microprocessors, NDT suppliers started digitalizing the technique. Today, the ultrasonic flaw detectors are available from simple transducers to highly advanced systems (Olympus, 2017).

Ultrasound can be used for inspection and testing of most materials and the echo technique only require surface contact of one side, which makes it a highly versatile non-destructive technique. The method uses directional beams of sound which propagate through the sample in question. Cracks, discontinuities and changes in material properties can be measured by their influence on the soundwaves. The soundwaves can be dissipated or reflected which will be picked up by a receiver which listens for the returning soundwaves. Typically, ultrasonic testing uses high frequency soundwaves that range from 1 to 10 Mega Hertz.

2.6.1 Basic principles of soundwaves

Soundwaves are mechanical vibrations that propagate through a material like a wave. For sound to propagate, it must pass through a medium, such as air, water or metal. The rate of which the wave travels depend on the type of wave and the medium it passes through. The direction of wave propagation is predictable, and when wave enter a boundary to a different medium, or the same medium of different chemical composition, the wave is either reflected, dissipated or transmitted.

Sound waves, as with other types of waves, oscillates at a specific frequency. Frequency is defined as the number of oscillations per unit time. The image bellow shows the properties of a wave, that is the frequency, amplitude, wavelength and period.

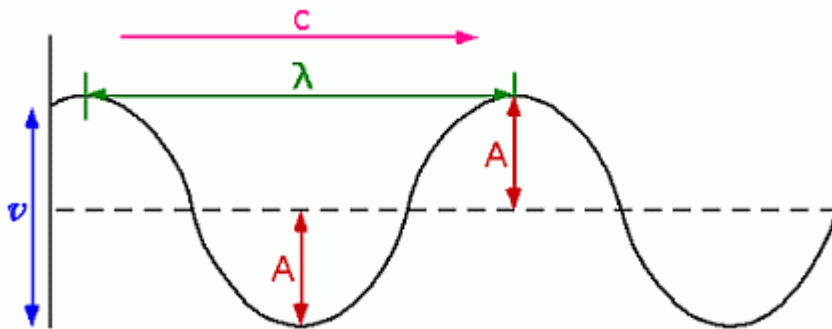


Figure 2-28 Wave properties (CBSE Portal, u.d.)

The wavelength is the distance from crest to crest and is often denoted as λ . A is the amplitude, which is the distance from the level (dotted line) to the crest. The period of a wave is the time between crests, in other words, the time it takes the wave to travel one wavelength. And lastly, the frequency is the rate of oscillation per unit time. For example, 10 oscillations per second gives a frequency of 10 Hz, and a period of 0,2 seconds gives a frequency of 5 Hz. The relationship between frequency and period is shown in the following equation.

$$f = \frac{1}{T} \quad (2.5)$$

Where f is the frequency and T is the period.

Humans can hear sounds with frequencies between approximately 20 Hz and 20 kHz. The rest of the spectrum is defined outside this range, where ultrasound is sound with frequencies above 20 kHz. Soundwaves with frequencies below 20 Hz are called infrasound. The image below shows the spectrum of sound.

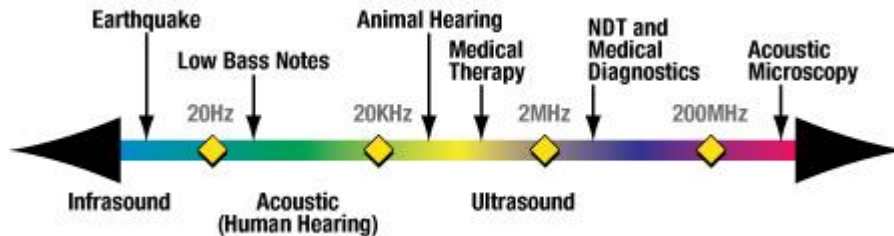


Figure 2-29 Sound spectrum (Olympus, 2017)

Soundwaves can be classified depending on their mode of vibration through a medium. There are 3 classes: longitudinal waves, transverse waves and surface waves.

2.6.1.1 Longitudinal waves

Longitudinal waves are the most usual form of soundwaves. This is the type of sound humans create when speaking and exists everywhere around us. Figure 2-31 illustrates how a soundwave propagates through gas. The black dots are gas molecules and the wave above illustrates the waveform of sound. As we can observe, there is a variation in molecule density, also known as pressure. The molecules in the high-pressure area will push each other into the low-pressure area, resulting in lower and higher pressure respectively. This cycle between high and low pressure comes through the compressional and dilutive forces in play, and drives the waves forward. The molecules in the material oscillate back and forth, but the wave propagates in one direction. However, the wave will not travel infinitely. Because of internal forces such as friction, the pressure differences will reduce with each cycle and eventually, the gas will reach equilibrium.

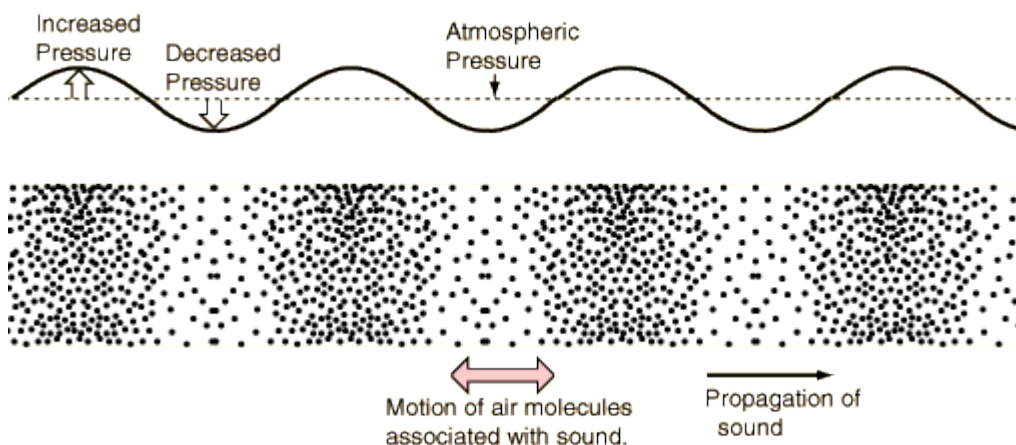


Figure 2-30 Longitudinal soundwave propagation in air (Nave, 2016)

Gas is a relatively bad medium for soundwaves to propagate. Because air and other gasses have a low molecule density, the transition of pressure from high to low and low to high happens more slowly than in denser materials such as water or metals.

Longitudinal waves are most common in ultrasonic testing. Because these waves can propagate in all types of medium that carry sounds, instruments utilizing this wave class have a wide range of application.

2.6.1.2 Transverse wave

Transverse waves, also known as shear waves, are types of waves that can only travel in solid materials. The wave depends on strong bonds between particles to propagate. Unlike longitudinal waves, the motion of particles is at right angles, or transverse to the motion of the wave itself. A good example of a transverse wave is a rope that is shaken up and down. Each rope molecule only moves up or down, and as a molecule moves, it pulls its neighbours with it.

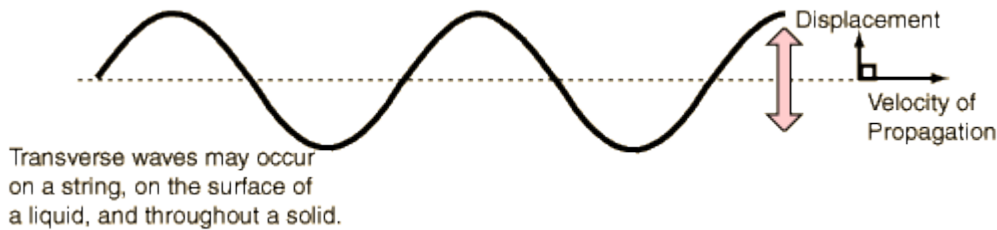


Figure 2-31 Transverse wave propagation (Nave, 2016)

2.6.1.3 Surface waves

Surface waves, also known as Rayleigh waves, are a type of wave that can only travel along the surface of a solid material. To propagate, one side of the surface must be bounded by strong elastic forces, while the other side must have nearly zero elastic forces between gas molecules (Baldev, et al., 2007). These waves have very little application in the case of ultrasonic testing because the waves lose their intensity more quickly than longitudinal waves. In addition, these waves only travel in the top layer of the sample surface. At a depth of approximately the wavelength of the wave from the surface, the strength of the wave has dropped to about 4%. Thus, surface waves can only detect cracks and discontinuities at the surface of the sample (Baldev, et al., 2007).

2.6.2 Behaviour of ultrasonic waves

It is important to understand the fundamentals of ultrasonic wave behaviour before the instrumentation of ultrasonic testing can be covered. This chapter present the velocity of ultrasonic sound waves, how they behave upon hitting a boundary and the fundamentals of wave weakening. These aspects are important when designing ultrasonic instrumentation for the testing of a specific material.

2.6.2.1 Ultrasonic sound velocity

The wave velocity of ultrasonic waves is dependent on the wave type, the density of the material and the E-modulus of the material. Longitudinal waves travel faster than transverse waves, and waves generally travel faster in liquids or solids than in gas. The elastic properties of the sound medium are very important for its wave speed. Because stiffness is a materials ability to resist deformation during applied force, rigid materials have a strong “spring effect” which pull the atoms and molecules quickly back in place during vibration. The strong intermolecular bonds allow the material to vibrate faster than in materials of less stiffness.

A second important parameter is the density of a material. For two samples with different density, but the same elastic properties, sound will travel faster in the low-density material. This is due to the size of the molecules in the material. Larger molecules require more force to be

dislocated and vibrate, thus sound travels slower. The following equations can be used to calculate the wave velocity in a material (Baldev, et al., 2007).

$$V_{Longitudinal} = \sqrt{\frac{E(1 - \mu)}{\rho(1 + \mu)(1 - 2\mu)}} \quad (2.6)$$

$$V_{Transverse} = \sqrt{\frac{E}{\rho 2(1 + \mu)}} \quad (2.7)$$

$$V_{Surface} = 0.9V_{Transverse} \quad (2.8)$$

Where E is Young's modulus, ρ is the density of the medium and μ is Poisson's ratio. It is important to keep in mind that the speed of sound is temperature dependent. This effect is included in the formula in the density term, as the density is also temperature dependent. For example, in air, sound travels at 343 m/s at 20°C and at 331 m/s at 0°C. The following table shows the speed of sound in a selection of common materials (Nave, 2016).

Table 9 Velocity of sound in common gases, liquids and solids (Nave, 2016)

| Gases | m/s | Liquids at 25°C | m/s | Solids | m/s |
|-----------------------|------------|------------------------|------------|---------------|------------|
| Hydrogen (0°C) | 1286 | Glycerol | 1904 | Diamond | 12000 |
| Helium (0°C) | 972 | Sea water | 1533 | Pyrex glass | 5640 |
| Air (0°C) | 343 | Water | 1493 | Glass | 3950-5000 |
| Air (20°C) | 331 | Mercury | 1450 | Aluminium | 5100 |
| | | Methyl alcohol | 1143 | Brass | 4700 |
| | | | | Copper | 3560 |
| | | | | Gold | 3240 |
| | | | | Lead | 1322 |
| | | | | Rubber | 1600 |

The velocity of sound in glass fibre composites depends on the mixture of glass and epoxy or polymer. A paper by (Wróbel & Pawlak, 2006) presents the average speed of sound (m/s) per the percentage of glass by weight (%). The tests were conducted on glass fibre epoxy, and shows that average speed of sound increases with an increase in glass fibre content.

Table 10 Velocity of sound in glass fibre epoxy per glass fibre content

| Average thickness (mm) | Percent glass by weight (%) | Average speed of sound (m/s) |
|-------------------------------|------------------------------------|-------------------------------------|
| 9.1 | 31.0 | 2461 |
| 9.3 | 37.2 | 2581 |
| 15.1 | 55.1 | 2744 |
| 13.8 | 55.9 | 2818 |
| 12.5 | 56.8 | 2950 |
| 13.1 | 57.3 | 2964 |
| 11.2 | 60.9 | 3014 |
| 10.7 | 65.2 | 3045 |
| 10.3 | 69.1 | 3169 |

2.6.2.2 *Transmission, reflection and refraction*

In practise, the substance of which sound travels is limited. A powerful sound wave can travel long distances, especially in water and solid materials. However, the wave will eventually hit a boundary. Upon hitting this boundary, the sound wave can behave in a variety of ways, depending on the angle of impact and the type of boundary. If sound hits a boundary to empty space (vacuum), the sound wave cannot travel further and will be reflected in some form. If a material is adhered to the boundary, the particle vibration may carry on through to the next medium, potentially at a changed angle, energy and wave type.

In the case of a wave hitting the boundary at a right angle, with an adhered medium on the other side, the transmission and reflection of the wave can be calculated. The amount of energy that is transmitted to the next medium is dependent on the difference in acoustic impedance of the two materials. The following equations can be used to calculate the reflection and transmission of sound waves when hitting the boundary at right angles.

$$R = \frac{(Z_2 - Z_1)^2}{(Z_2 + Z_1)^2} \quad (2.9)$$

$$T = \frac{4Z_2Z_1}{(Z_2 + Z_1)^2} \quad (2.10)$$

Where R is the reflection coefficient, T is the transmission coefficient and Z_1 and Z_2 is the acoustic impedance of medium 1 and 2 respectively. Because these are coefficients, and the total energy coefficient can be set to 1, we also have that $R = 1 - T$.

There are significant differences in the acoustic impedance of gas, liquids and solids. In the case of sound propagating in water and hitting a steel surface, only about 12% of the energy will be transmitted into the steel (Baldev, et al., 2007). Per the formula, $R = 1 - T$, 88% of the wave energy will be reflected. In comparison, sound waves propagating in air and hitting a steel surface will be almost entirely reflected. Thus, air can in most cases be considered as vacuum because of the very low acoustic impedance of gasses, which results in a reflection coefficient of almost 1.

Refraction occurs when the beam of sound hits a barrier between two mediums of different acoustic impedance at an angle. Snell's law determines how the waves are reflected and refracted, and depends on the relative velocities in the mediums.

$$\frac{\sin \alpha}{\sin \beta} = \frac{V_1}{V_2} \quad (2.11)$$

Where α is the angle of the reflected wave and β is the angle of refracted waves. V_1 and V_2 is the velocity of sound in the mediums.

2.6.2.3 *Attenuation*

Attenuation is the weakening of sound waves as they propagate through a medium. Sound waves are weakened by two reducing effects: scattering and absorption. As previously mentioned, sound waves are not infinite, and the reduction of wave strength is dependent on material composition. In an ideal material, wave strength (signal amplitude) would only be reduced by the spreading of the wave.

Absorption is the conversion of sound energy into heat. Because of forces such as internal friction, heat conduction, elastic and magnetic hysteresis, the signal strength is weakened.

Absorption is closely related to the frequency of the wave and usually increases with higher frequencies (Baldev, et al., 2007). Because absorption only weakens the signal strength, we can compensate by increasing the transmitter voltage and amplification. It is also possible to reduce the frequency of the signal to reduce absorption.

Scattering comes from inhomogeneities and anisotropic material properties, as most materials often include pores or inclusions. These impurities have grain boundaries which reflect the sound waves in directions different from its original path, which chips away at the signal as it propagates. Scattering cannot be handled like the absorption effect, as increasing the signal strength also increases the strength of the signals that are reflected in different direction. These reflected signals cause a disturbance which can mask the signals reflected from flaws. The only way to reduce the disturbance, also known as the “grass effect” is to reduce the frequency, which makes it harder to detect small defects.

The attenuation of sound waves in a material can be calculated with the following formula:

$$A = A_0 e^{-\alpha r} \quad (2.12)$$

Where A_0 is incident amplitude, A is the value of the amplitude after traveling the distance r in the material and α is the attenuation coefficient (Baldev, et al., 2007).

2.6.3 Ultrasonic instrumentation

This chapter presents the most basic instrumentation required for ultrasonic pulsed testing. There is a vast number of possible instrumentation configurations. However, ultrasonic instrumentation can be grouped into wave generation, probe and means of display.

2.6.3.1 Wave generation

Ultrasonic waves can be created by oscillating mechanical movement, also known as vibration. There are several ways to achieve this movement, however, one method stands out in ultrasonic testing. The most popular solution is to convert electrical pulses into movement using piezoelectric ceramic or composites. Piezoelectricity means electricity resulting from pressure (Wikipedia, 2017), and there are a broad range of materials which have this property. Their ability to generate electricity through mechanical stress and vice versa comes from its lattice molecular structure. When the piezoelectric material is cut with respect to its crystallographic axes, it can expand or contract according to the electric field it is subjected to.

Quartz, a naturally occurring piezoelectric material, is highly popular for ultrasonic flaw detection. Quartz have a high mechanical strength and stability as well as great piezoelectric properties, and can be used in temperatures reaching 773K. Today, there is a wide range of both naturally occurring and artificial piezoelectric materials available. Depending on the parameters of the test, the choice of material in the ultrasonic instrumentation can be of great significance. For example, produced crystalline ceramics such as Barium titanate which has a low mechanical resistance is a good transmitter, while the naturally occurring Lithium sulphate has much better sensitivity. By using materials with different properties for transmitting and receiving the ultrasonic waves, better results may be achieved. The piezoelectric materials can be cut in the shape of a thin disk, a square or a rectangle. This is the element that converts the electrical energy into sound waves and is called the transducer.

2.6.3.2 Probe

The probe is a vessel for the transducer, and its job is to protect it from external damage as well as facilitate optimal measurement results. It also functions as shock protection and hinders the risk of electric shock for the operator. In addition, ultrasonic flaw detection is popular for

underwater applications and the electrical components must be protected, especially the electrical cables. The probe is also installed with a component of dampening material, which quickly dampens the vibration in the piezoelectric material after the soundwave has been generated. Thus, the piezoelectric material can be used for transmission and receiving of the signal. There is a range of different probe configurations, and figure 2-33 shows a single element transducer (left) and a dual element transducer(right).

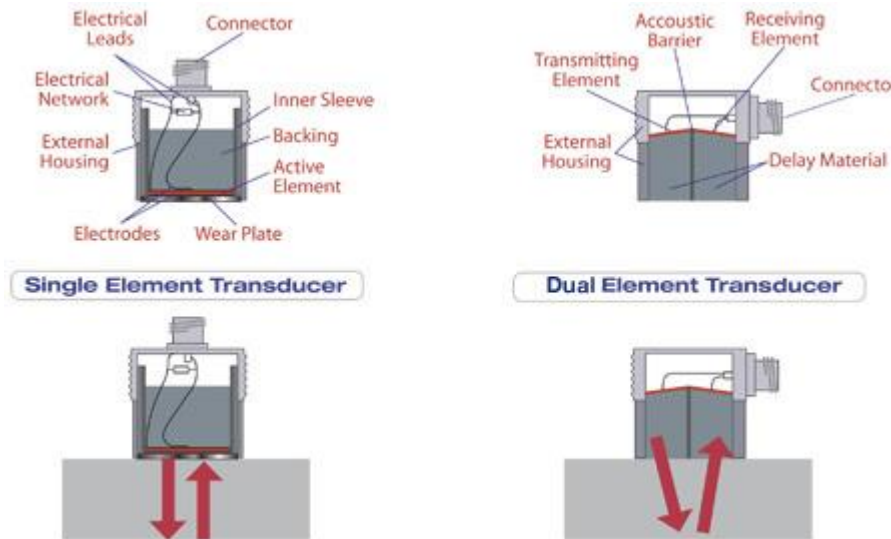


Figure 2-32 Single element and dual element ultrasonic transducers (Olympus, 2017)

This basic design is commonly used for contact measurements, such as crack detection or thickness measurements. The dual element transducer uses two piezoelectric materials with separate functions and is commonly used for corrosion surveys (Olympus, 2017).

2.6.3.3 Block diagram of ultrasonic instrumentation

In ultrasonic instrumentation, we are dealing with mechanical movement, electrical analogue signals, digital signals and precise timing. It is imperative that the instrumentation is set up correctly. Figure 2-34 presents a basic block diagram of ultrasonic instrumentation.

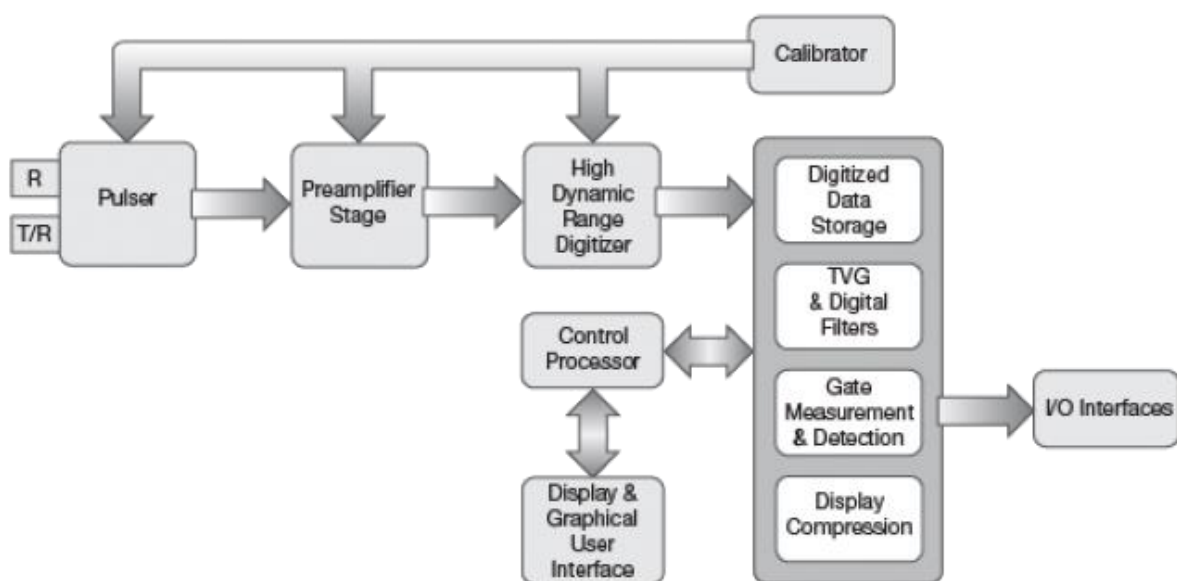


Figure 2-33 Block diagram of ultrasonic instrumentation (Olympus, 2017)

The “Pulser” at the left produces high voltage pulses to the piezoelectric element at the desired frequency, which in turn creates the ultrasonic wave with specific properties. Echoes from the output wave are also received by the piezoelectric material. The soundwaves are transformed into electrical signals that must be processed to facilitate proper interpretation. After being fed into the receiver, the signal is amplified in the “Preamplifier Stage” before becoming digitalized in the “High Dynamic Range Digitalizer”. This unit can handle a wide range of signal amplitudes, which varies greatly in ultrasonic testing.

Throughout the signal processing, a calibrator is implemented. It provides instrument linearity and unit to unit repeatability, in addition to ensuring drift free operation. By calibrating DC offset, phase, gain and the frequency response through the digitalizer, it creates the major advantage of digital ultrasonic testing. After the signal has been digitalized, it may be processed or stored. There are several ways of analysing and displaying results, and it depends on the interests of the operator. In this thesis, the results are presented with an oscilloscope.

2.6.3.4 Oscilloscope

As previously mentioned, we utilized an oscilloscope for signal interpretation in this thesis. The main purpose of this instrument is to graph an electric signal as it varies over time. A bulk of information can be extracted from the waveform measurements, depending on the oscilloscope.

Table 11 Waveform measurements of oscilloscopes

| | |
|-----------------------------|--|
| Frequency and period | Each repeating signal, such as soundwaves, has a frequency and thus a period. An Oscilloscope can accurately measure the frequency of the input signal. |
| Voltage | Voltage is the amount of electric potential between two points in a circuit (Tektronix, 2000). In case of ultrasonic testing, the voltage-time graph tells the story of the soundwave. The changes in amplitudes can identify backwall echoes and signal strength reduction. In addition, the difference in amplitudes can pinpoint specific points of interests, such as internal cracks in the sample. |
| Phase | Phase can be described as a difference in timing of two signals, otherwise similar. As a soundwave hits a boundary, its phase can be delayed. Thus, valuable information about the boundary can be extracted based on the phase. |

3 METHODOLOGY

This chapter presents the methodology used in this thesis. This is an interdisciplinary study and it was important to, in detail, review extensive literature on UAV's, ultrasonic testing and condition monitoring. The thesis is based on an UAV experiment to support the discussion with results. The methodology used in this thesis is a combination of theory and experiments, to investigate the feasibility of UAV application in ultrasonic testing of wind turbine rotor blades.

3.1 IN DEPTH LITERATURE REVIEW

The in-depth literature review presented in this thesis is collected from a variety of sources. Books such as (D. C. Quarton, 1998) and (Baldev, et al., 2007) were used as the main sources for facts on wind turbines and non-destructive testing, respectively. Because this study is dependent on the most recent technology in wind turbines, UAVs and ultrasonic sensors, research articles from the last 5 years have been prioritized due to their relevance. Wind turbines are continuously researched, especially in recent years due to increased investment in the industry. Thus, there is a lot of information available, despite a lack of available product specifications from the manufacturers. This thesis has focused on large-scale wind turbine, thus the literature discussing small-scale turbines has been filtered out, eliminating concerns regarding the size-scaling of the reviewed data.

Due to the experiments involved in this paper, UAV's and ultrasonic sensor technology has been researched. There is a wide range of available UAVs at different prices and specifications. In this thesis, we carried out the UAV experiments with a privately-owned UAV. Ultrasonic testing is covered at a basic level because the authors background does not facilitate a technical review of the available sensor technology, and the appropriate sensors are not available within this project's budget.

3.2 RISK MANAGEMENT

Risk management accounts for the most significant challenges related to our intended operation. The feasibility of UAV ultrasonic testing depends on safe and economically beneficial operation. The author has carried out the risk analysis. The risk analysis is qualitative and based on the knowledge and experiences of the author.

The focus of the risk analysis is safety of operation. Environmental and economic challenges have been covered at basic level. In the authors opinion, collision avoidance is the primary challenge of UAV application for ultrasonic wind turbine rotor blade inspection, which is reflected in the analysis. The author opted for a SWIFT-analysis, because it requires little technical knowledge about the specific systems and is based on a generic checklist. The results ensure a good overview of the hazards related to the operation. A bow-tie diagram analysis was applied to high-risk events to reduce the overall risk of the operation to acceptable levels. The end results can be viewed as a good indicator for the severity of the hazards, it should however be completed in higher detail.

3.3 ULTRASONIC NON-DESTRUCTIVE TESTING - GROUND EXPERIMENTS

In (Galleguillos, et al., 2014), a feasibility study on thermographic non-destructive inspection using UAV was conducted. The study was completed in two steps, firstly the feasibility of thermography for wind turbine rotor blade testing was confirmed during experiments on the ground, before the test was attempted via an UAV. This approach generated interesting results, and in this thesis, we will be attempting a similar methodology. Before conducting experiments with UAVs, the sensors, materials and instrumentation was tested to prove its functionality by testing for a simulated skin/adhesive debonding (type 1 and 2 damage) and induced delamination (type 4 damage).

The skin/adhesive debonding defect was simulated by creating an imperfect adhesion between two samples of glass fibre. In cases where the adhesive layer between the skin and the spar is damaged (type 1 damage), the material can be viewed as non-continuous. The defects can be of small magnitudes, and to increase the quality of the experiments, the surfaces of the glass fibre samples was polished using a rotary water polisher to create a smooth surface for the best possible non-adhesive connection. An ultrasonic echo-pulse was fired into the sample, and the returning echoes was analysed to identify the artificial defect.

3.3.1 Instrumentation

For the experiments presented in this thesis, the following ultrasonic instrumentation was used. A model 5077PR is an ultrasonic square wave pulser/receiver unit. It can be used in combination with an appropriate transducer and oscilloscope for low-cost ultrasonic measurements (PANAMETRICS-NDT, 2004). The instrument can be applied for flaw detection, thickness gaging, sound velocity measurements, spectrum analysis amongst other measurements. For signal processing, the Agilent InfiniiVision DSO-X 2002A oscilloscope was used. This model has the capabilities to present both the pulsed and received signals and has a range of signal processing options available. In addition, screen captures can be saved directly to an USB, which is how the results are presented in this thesis.



Figure 3-1 Ultrasonic pulser/receiver (left) and oscilloscope (right)

The transducer we used for our measurement is a large diameter case immersion unfocused transducer. We used model V397-SU with a nominal element size of 1.125 inches or 29 mm (Olympus, u.d.). The 2.25 MHz transducer proved to be a good compromise between resolution and penetration depth for our choice of samples and experiments. For other types of samples, thickness and defect types, higher resolution might be necessary.



Figure 3-2 V397-SU 29mm element transducer (Skaga, 2017)

3.3.2 Experimental set-up

We received samples of 4 different thicknesses from Lyngen Plast A/s, where one sample also had a coating on one side. Because of the rough surfaces of the samples, we grinded the surfaces of some samples using a water based rotation grinder, with P125, P500 and lastly, P1000. These samples had to be of no more than 50 mm x 100 mm to fit in the safety mould used to hold the samples during grinding. We used a pressure controlled gauge for 3-point bending tests on the remaining material and measured the displacement. The intention of the test was to run a sample to failure, and look for variations in the ultrasonic measurements. We had to ensure that the sensor can detect internal damages in glass fibre materials before conducting the UAV-based experiments.

3.4 ULTRASONIC NON-DESTRUCTIVE TESTING – UAV EXPERIMENTS

The second experimental study in this thesis investigates the potential for UAVs to be used as a carrier of ultrasonic instrumentation. We aim to test whether UAVs have the capability to carry out the testing without significant risks, thus saving time compared to using climbers. The experiment was carried out using the same equipment for ultrasonic measurements as we did in the handheld experiment.

3.4.1 Experiment set-up

We did not have access to handheld pulsers/receiver and equipment for wireless signal transmission, and the available equipment was too heavy to be carried by the drones we had at our disposal. To solve this, only the transducer was carried by the drone. It was connected to the transducer and UAV using a long wire. This meant that the experiment had to be carried out just above ground level, yet in the air. To deliver the ultrasonic pulse without damaging the drone or the glass fibre, the probe was mounted on a hollow aluminium rod. By attaching the rod to the UAV via rubber bands, some dampening was introduced to the system.

3.5 CRITICISM OF METHODOLOGY

This section covers criticism of the methodology used in this thesis. Due to the scope of work, the experiments can be viewed as preliminary, and more research must be conducted to conclude whether ultrasonic non-destructive testing can be carried out by UAVs. The following list presents some concerns regarding the methodology.

- The literature review presented in this thesis does not cover maintenance statistics of wind turbines. For an in-depth study of UAV application in condition monitoring of a wind turbine, current inspection practises should be reviewed in detail. Statistical data would be site or turbine specific, interfering with the general approach of this thesis.
- The glass fibre samples are not of equal quality to that used in wind turbine rotor blades. However, the material is similar in many ways. It has not been produced using vacuum moulding, thus the samples contain air. Air is bad for ultrasonic testing and can complicate our experiments. Ideally, the tests should be conducted on parts from a real wind turbine rotor blade.
- In this thesis, only type 4, 5 and 7 damage detection has been tested. Due to limitations in both time and resources, we could not produce these damages in a reliable fashion. Ultrasonic testing can apply to more types of defects in rotor blades, and more experiments should be conducted to identify defects such as damage formation in adhesive layers.
- The UAV used in this thesis is not optimal for ultrasonic testing of wind turbine rotor blades, especially due to its collision vulnerability. In addition, the UAV flight tests was conducted in wind-free indoor conditions. The results would be more conclusive if the flight had been conducted in site-representative weather conditions.
- The risk analysis presented in this thesis is subjective and for preliminary purposes. It does not include quantitative data, nor field experts' opinion. The results are valid to some degree, but in case of an in-depth risk assessment, financial and environmental risks must be included.
- The transducer used in the experiments is specifically designed for testing of partially or fully submerged test pieces. We did not have ideal sensors available, nor the funds to purchase operation specific transducers. Although we were able to produce promising results, better instrumentation can yield significantly more information.

4 RESULTS

4.1 RISK ANALYSIS

This chapter presents a preliminary risk-analysis. The complete SWIFT-analysis is briefly presented in a risk-matrix. However, the full analysis is attached in Appendix A. Unwanted events with high-risk index will be discussed in detail, and a bow-tie diagram will be applied to further reduce either the probability or consequence, which in turn reduces the risk.

4.1.1 SWIFT-analysis

From the SWIFT-analysis, we first developed a checklist of potential “what-if” scenarios. This checklist is used when the analysts attempts to derive possible unwanted events (causes of the “what-if” scenario), and supports a structured review of the operation. In this paper, we initially developed the checklist presented in table 12.

Table 12 SWIFT-analysis "what-if" checklist

| Category | What if? | General comment |
|-----------------|--------------------------------------|--|
| 1 | The UAV loses propulsion | Loss of UAV propulsion is defined as loss of power in one or all electric motors, resulting in loss of control or no lift at all. |
| 2 | We lose radio contact with the drone | Loss of radio contact is defined as loss of manual control. The pilot or ground station has no influence on the UAV flight. |
| 3 | A participant makes a human error | Human error occurs in all industries and must be accounted for. |
| 4 | The UAV has a mechanical failure | Mechanical failure can be loss of structural integrity of the platform, or automated features. |
| 5 | The UAV has a sensor failure | In case of sensor failure, vital UAV systems can fail. Sensor is defined as UAV flight control sensors, not the ultrasonic transducer. |
| 6 | The UAV collides mid-air | UAV collision is defined as impact with any object. |
| 7 | The battery fails | The battery is the UAVs only power supply, there are no redundant systems in place. |
| 8 | The weather changes | The weather is unpredictable to some extent and sudden changes must be accounted for. |
| 9 | Issues with surroundings | Issues with surroundings is defined as third-party conflicts, such as legal concerns, excessive noise etc. |
| 10 | Take-off and landing. (UAV handling) | The take-off and landing procedure involves human contact with the UAV. This section covers the risks related to launch and landing. |

The consequence and probability parameters were defined for use in a 5x5 risk matrix. The consequences have been defined regarding the safety of people and personnel, and the probability follows an exponential distribution. This SWIFT-analysis does not include financial and environmental consequences, but they have been informally considered during “what-if?” evaluation.

Table 13 Definition of consequence and probability parameters

| Consequence | | | Probability | | |
|-------------|----------|---|-------------|----------------|-----------------------------------|
| A | Minimal | Hazard or near miss requiring reporting and follow-up action. | 1 | Rare | Less than once per 10000 flights. |
| B | Minor | Potential first aid injury. | 2 | Unlikely | Once in 1000-10000 flights. |
| C | Moderate | Potential medical treatment injury or illness. Non-permanent. | 3 | Possible | Once in 100-1000 flights. |
| D | Major | Potential major injury with permanent disability. | 4 | Likely | Once in 10-100 flights. |
| E | Severe | Potential fatality and multiple injuries. | 5 | Almost Certain | More than once in 10 flights. |

By using the “what-if” checklist, we derived the following risk ratings presented in the risk matrix below. More than half of the unwanted events are within the acceptance area, and will require no further risk mitigation. However, 2 unwanted events are in the not-acceptable category, and 15 are in the ALARP area.

Table 14 Risk matrix post SWIFT-analysis

| Risk Matrix | | | Consequence | | | | |
|-------------|---|----------------|-------------|---------------|--|--|-------------------------|
| | | | A | B | C | D | E |
| | | | Minimal | Minor | Moderate | Major | Severe |
| Probability | 5 | Almost certain | | | | | |
| | 4 | Likely | | | | | 6.3 |
| | 3 | Possible | 2.4 | | | | 8.2 |
| | 2 | Unlikely | 2.5, 5.2 | 5.3 | 3.8, 6.1, 8.1, 10.1, 10.2 | 1.1, 1.2, 1.4, 3.2, 3.7, 4.3, 5.1, 7.1 | 3.5 |
| | 1 | Rare | 9.1 | 7.2, 9.2, 9.3 | 2.1, 2.2, 2.3, 4.1, 6.2, 8.3, 8.4, 8.5, 10.3 | 1.3, 3.4, 4.2, 7.3, 7.4 | 2.6, 3.1, 3.3, 3.6, 6.4 |

The identified unwanted events are extracted from the SWIFT-analysis and presented in table 15. We will attempt to apply preventive and reductive barriers beyond what already exists to further reduce the risk. The goal is to implement measures that are financially and practically applicable.

Table 15 Identified ALARP risks

| Nr. | Potential causes | Effects and consequences |
|------------|---|--|
| 6.3 | Uncontrolled impact with wind turbine rotor blade | Can destroy the UAV and severely damage the rotor blade. |
| 8.2 | Unpredictable wind gusts | The wind can throw the UAV out of course. The UAV can crash and damage wind turbine rotor blade. |
| 1.1 | Exhausted battery | Complete loss of control. The UAV will crash |
| 1.2 | Control system fails | Complete loss of control. The UAV will crash. |
| 1.4 | Engine failure | Complete or reduced loss of control. The UAV will descend unpredictably, depending on how many engines fail. |
| 2.6 | Hacking | Complete loss of control, and the UAV can be used to cause harm to others. |
| 3.1 | Insufficient pilot training | Loss of control of UAV, unaware of surroundings and potentially dangerous flight. |
| 3.2 | Communication failure between pilot, ground station and other personnel | Unawareness can lead to collision, mission abort and/or loss of control. |
| 3.3 | Intoxicated personnel | Unawareness and loss of control. Can lead to reckless flying. |
| 3.5 | Failure to spot obstacles in flight path. | Impact with obstacle, potentially destroying the UAV and causing damage to third-party equipment. |
| 3.6 | Failure to spot people | Can lead to severe and potentially lethal damage. |
| 3.7 | Insufficient pre-flight check | Can cause failure in critical components. Potentially temporary or complete loss of control of the UAV. Uncontrolled crash. |
| 4.3 | Faulty payload attachment | Uneven weight distribution. Leads to high power consumption, mission abort or emergency landing. Potential for equipment detachment. |
| 5.1 | Gyro fails | Complete loss of UAV control. |
| 6.4 | Manned aircraft traffic | Can potentially damage the helicopter or airplane and lead to multiple fatalities. |
| 7.1 | Fire in the battery | Complete loss of UAV control. Fiery crash landing. Fire can spread once the UAV is on the ground. |

4.1.2 Bow-tie analysis

From the listed unwanted events, we derived the following barriers. The barriers are also included in the SWIFT-analysis attachment. Some barriers, both preventive and protective will appear in multiple events. Preventive barriers are noted as P and reductive barriers are noted as R. The existing barriers presented in the SWIFT-analysis are not mentioned in this analysis, as they were taken into consideration during the initial risk assessment. This analysis aims to implement new risk-reducing measures for increased overall risk.

Table 16 Barriers identified from Bow-Tie method

| NR. | Preventive barrier | Reductive barrier |
|-----|---|--|
| 6.3 | | R1: Design UAV for impact with turbine blades. |
| 8.2 | P1: Develop statistical data on wind conditions at wind turbine site, calculate low-risk dates for flight. | R:1 Design UAV for impact with turbine blades. |
| 1.1 | P2: Use recommended settings and follow instructions issued by the UAV manufacturer. P3: Keep batteries heated until flight. | R1: Design UAV for impact with turbine blades. R2: Control ground below flight to prevent people directly underneath the drone. |
| 1.2 | P2: Use recommended settings and follow instructions issued by the UAV manufacturer. | R1: Design UAV for impact with turbine blades. R2: Control ground below flight to prevent people directly underneath the drone. |
| 1.4 | P4: Thoroughly examine the propellers and battery before flight. | R1: Design UAV for impact with turbine blades. R2: Control ground below flight to prevent people directly underneath the drone. |
| 2.6 | P5: Use firewalled computes. P6: Take computer offline for flight. | R1: Design UAV for impact with turbine blades. |
| 3.1 | P7: Check pilot experience and qualifications before flight. | R1: Design UAV for impact with turbine blades. R2: Control ground below flight to prevent people directly underneath the drone. |
| 3.2 | P8: Pre-flight briefing with all participants. Test communication equipment before flight. | R1: Design UAV for impact with turbine blades. R2: Control ground below flight to prevent people directly underneath the drone. |
| 3.3 | P9: Establish a zero-tolerance of drugs and alcohol. Abort if personnel are under the influence. | R1: Design UAV for impact with turbine blades. R2: Control ground below flight to prevent people directly underneath the drone. |
| 3.5 | P10: Keep VLOS, have additional personnel dedicated to spotting obstructions. | R1: Design UAV for impact with turbine blades. |
| 3.6 | P11: Have enough participants in the operation to control the entire flight zone. | |
| 3.7 | P2: Use recommended settings and follow instructions issued by the drone manufacturer. | R1: Design UAV for impact with turbine blades. R2: Control ground below flight to prevent people directly underneath the drone. |
| 5.1 | P2: Use recommended settings and follow instructions issued by the drone manufacturer. | R1: Design UAV for impact with turbine blades. R2: Control ground below flight to prevent people directly underneath the drone. |
| 6.4 | P12: Land immediately if aircrafts can be seen or heard flying low. | |
| 7.1 | P2: Use recommended settings and follow instructions issued by the drone manufacturer. | R2: Control ground below flight to prevent people directly underneath the drone. R3: Keep a fire extinguisher ready for immediate firefighting. |

4.1.2.1 Reductive barriers

Despite defining consequences as personnel safety concerns, it is imperative for UAV ultrasonic testing that the operation does not damage the wind turbine rotor blade. Two unwanted events have been placed in the unacceptable risk area due to potential damage to rotor blades. From the SWIFT and bow-tie analysis, the UAV must be designed for impact with the rotor blades to carry out the operation. It is, to the authors knowledge, not possible to reduce the risk of impact to tolerable levels. Thus, the UAV must be specifically designed to not inflict damage to the rotor blade in case of impact, to reduce the consequences to acceptable levels. The barrier “R1: Design UAV for impact with turbine blades” was introduced, and is considered implementable for the rest of the risk assessment. The means of achieving this barrier will be discussed in chapter 5.

From the table above, we can see that the preventive barrier R2: “Control ground below flight to prevent people directly underneath the drone” is a very effective measure of risk reduction for UAV flight operations. The reoccurring potential consequences “loss of UAV control” and “UAV crash”, will be reduced from D: “Potential major injury with permanent disability” to C: “Potential medical treatment injury or illness. Non-permanent.” if there are no unaware people

underneath the UAV. The consequences of “Uncontrolled automatic flight” is also reduced if there are no people or vehicles under the UAV’s flight path.

The third reductive barrier R3: “Keep a fire extinguisher ready for immediate firefighting” is meant to reduce the impact of an incinerated UAV. It is used in combination with R2 to ensure that no people are harmed in case of the unwanted event 7.1.

4.1.2.2 Preventive barriers

UAVs have available safety functions programmed in its software, and because the UAV will be flying VLOS, failure of automatic flight or camera functions has redundancies with manual pilot control. It is also expected that the personnel of the operation follow the RPAS Reg. issued by CAA, and the risk analysis does not consider events that are caused due to illegal or inconsiderate flight. A UAV specific pre-flight checklist must be developed and applied to the operation. Most of the preventive barriers are related to the pre-flight check, and P2 states: “Use recommended settings and follow instructions issued by the drone manufacturer.” P12 is included to keep awareness, however, the probability of low flying airplanes and helicopters can be considered extremely low.

“P1: Develop statistical data on wind conditions at wind turbine site, calculate low-risk time tables for flight” is an important measure for UAV flight at wind turbine sites. The risk of unpredictable wind is considerable, and a major concern for the safety of the UAV, personnel and wind turbine. For the post-barrier risk analysis, it is assumed an implemented P1 barrier. The means of achieving this barrier will be discussed in chapter 5.

4.1.3 Post-barrier risk matrix

After implementing the barriers formulated in the bow-tie analysis, we could reduce the unwanted events in the unacceptable area from 2 to 0, and the unwanted events in the ALARP area from 16 to 6. The remaining risks will be discussed in chapter 5.

Table 17 Post-barrier risk matrix

| Risk Matrix | | | Consequence | | | | |
|-------------|---|----------------|-------------|--|--|-------|--------------------|
| | | | A | B | C | D | E |
| | | | Minimal | Minor | Moderate | Major | Severe |
| Probability | 5 | Almost certain | | | | | |
| | 4 | Likely | | 6.3 | | | |
| | 3 | Possible | 2.4 | | | | |
| | 2 | Unlikely | 2.5, 5.2 | 1.1, 1.2, 1.4, 5.3, 6.1 | 3.2, 3.5, 3.7, 4.3, 5.1 | 8.2 | |
| | 1 | Rare | 9.1 | 1.3, 2.1, 2.2, 2.3, 3.8, 4.1, 6.2, 7.2, 8.1, 8.3, 8.4, 8.5, 9.2, 9.3 | 3.1, 3.4, 4.2, 7.1, 7.3, 7.4, 10.1, 10.2, 10.3 | | 2.6, 3.3, 3.6, 6.4 |

4.2 ULTRASONIC HANDHELD MEASUREMENTS

The first ultrasonic measurement was conducted on a glass fibre sample, with a thickness of 29.9mm. From the following edited screen capture, we can clearly observe the voltage-time response presented in the oscilloscope. A single pulse was sent into the material, propagated through its thickness, hit the backwall and returned to the transducer. As the wave returns, the soundwaves hit the piezoelectric material which in turn generates voltage. The echo effect can be observed 3 times, with diminishing amplitudes. To reduce the effect of random noise, we repeat the pulse echo over several measurements. Typically, 8-16 averages proved to yield a stable, noise free result within 16-32ms.

In the following figures, $t = 0$ is defined by the vertical orange cursor on the left, while the yellow cursors mark the backwall echoes. At $t = 0$ the transceiver starts to pull the transducer and prepares it for a 2.25 MHz pulse. The Model 5077PR user's manual (PANAMETRICS-NDT, 2004) informs of an expected delay between external triggers and main bang pulse of approximately $2\mu\text{s}$. With our trigger and cursor placement, the pulse transmission is initiated at $t = 1.0\mu\text{s}$. The first echo occurs at $t = 24,4\mu\text{s}$, while the second and third echo occurs at $t = 47,8\mu\text{s}$ and $t = 71,2\mu\text{s}$ respectively.

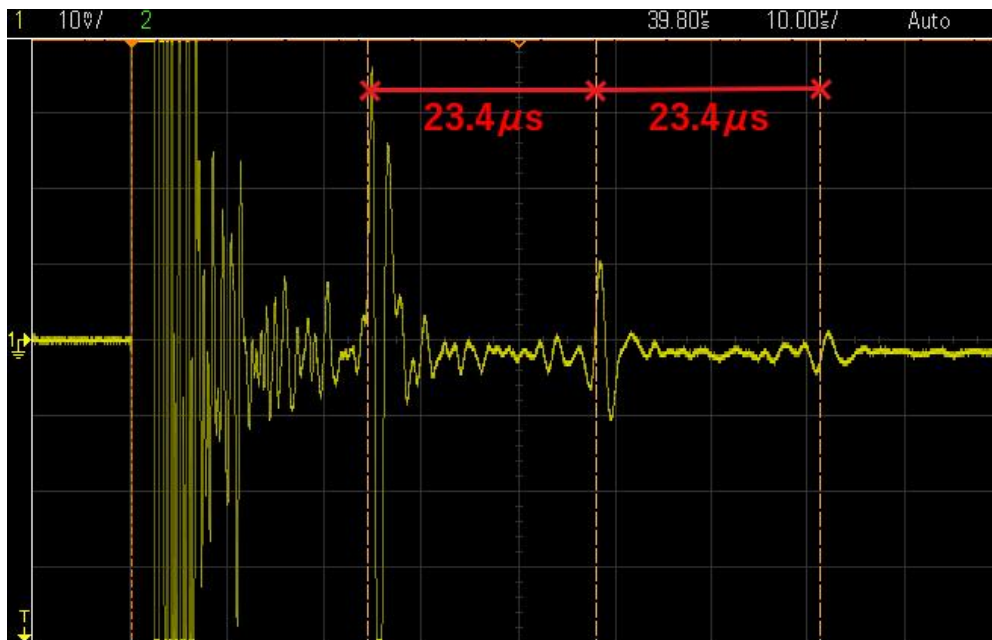


Figure 4-1 Triple echo response from ultrasonic pulse in 29.9mm thick glass fibre sample

The time of soundwave propagation through the material and back, can be calculated by using the time difference between the pulse and echoes. Thus, $71,2\mu\text{s} - 47,8\mu\text{s} = 23,4\mu\text{s}$, $47,8\mu\text{s} - 24,4\mu\text{s} = 23,4\mu\text{s}$, and $24,4\mu\text{s} - 1,0\mu\text{s} = 23,4\mu\text{s}$. By including the known thickness of the plate, we can calculate the sound velocity in the given material. Because the time between the echoes is the time the soundwaves take to travel back and forth in the material, we must use half its value, or twice the thickness.

$$v = \frac{l}{\frac{1}{2}t} \quad (4.1)$$

$$v_{\text{sound in sample}} = \frac{29.9\text{mm} * 10^{-3} \frac{m}{mm}}{\frac{1}{2} * 23.4\mu\text{s} * 10^{-6} \frac{s}{\mu\text{s}}} = 2555.55 \frac{m}{s}$$

A velocity of sound of 2555.55 m/s falls in the range (2461-3169) of the speeds of sound identified in the paper by (Wróbel & Pawlak, 2006). Because we do not know the exact material composition, not the exact method of production, we do not attempt to calculate the percentage of glass by weight.

4.2.1 Measurement of crack simulation

To simulate a crack caused by adhesive debonding of skin or joints in the composite, we placed a piece of glass fibre with a thickness of 9mm at the back of the thick block from the previous experiment, as seen in figure 4-2. The contact between the pieces was increased by adding a thin layer of water, this reduced the amount of trapped air and allows for the transmission of ultrasonic waves.

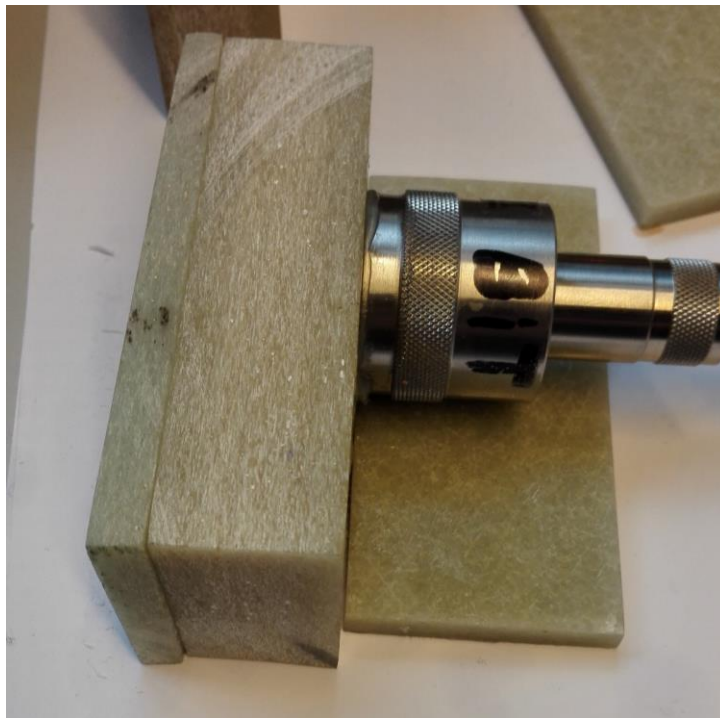


Figure 4-2 Simulation of crack due to debonding in glass fibre sample (Skaga, 2017)

The response from the ultrasonic pulse clearly shows a different result, compared to the first experiment. In figure 4-3, the orange cursor shows the echo from the backwall of the thick piece. This occurs at the same time $t = 24,4\mu\text{s}$, as in the first test. However, in this case, the echo is significantly weaker. In addition, a stronger response occurs shortly after.

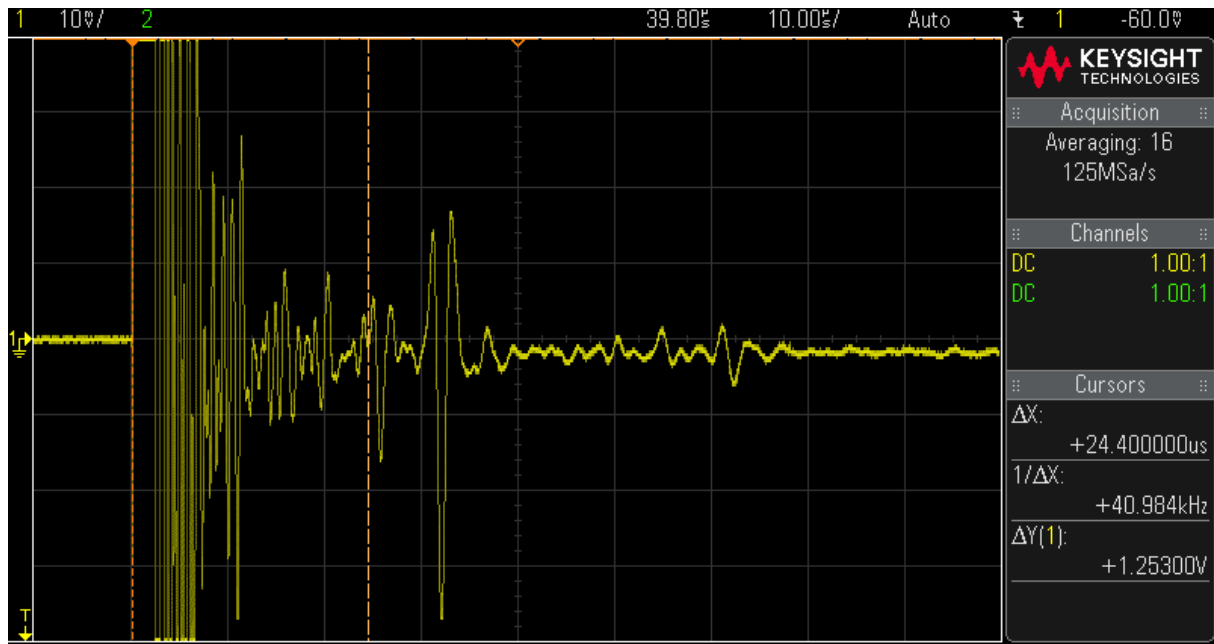


Figure 4-3 Echo response from ultrasonic pulse in simulated crack, first backwall echo

The second echo is from the backwall of the 9mm piece. This can be confirmed by using the velocity of sound from the previous experiment. The time difference between the echoes is $30.8\mu\text{s} - 24.4\mu\text{s} = 6.4\mu\text{s}$, which should correlate with the expected time for the sound to travel back and forth in 9mm of the sample.

$$t_{back\ and\ forth} = \frac{2 * 9\text{mm} * 10^{-3} \frac{m}{mm}}{2555.55 \frac{m}{s}} = 7.04\mu\text{s}$$

From our calculations, there is a difference of $7.04\mu\text{s} - 6.4\mu\text{s} = 0.64\mu\text{s}$. This error is due to the inaccuracy of our cursor placement, thickness measurements or variation in material composition. The small error indicates that this is the backwall echo of the 9mm piece.



Figure 4-4 Echo response from ultrasonic pulse in simulated crack, second backwall echo

4.2.2 Measurement of induced damage

To carry out measurements on real internal damages in the glass fibre composite, we had to apply sufficient stress for the material to be permanently deformed. We used a 3-point bending test to subject the sample with enough force for it to break. The sample was 99mm wide, 250mm long and 27mm thick. This sample had a coating on one side, this is where we applied the load. The instrument used was controlled by a pressure gauge, and load was applied by a hydraulic pump.

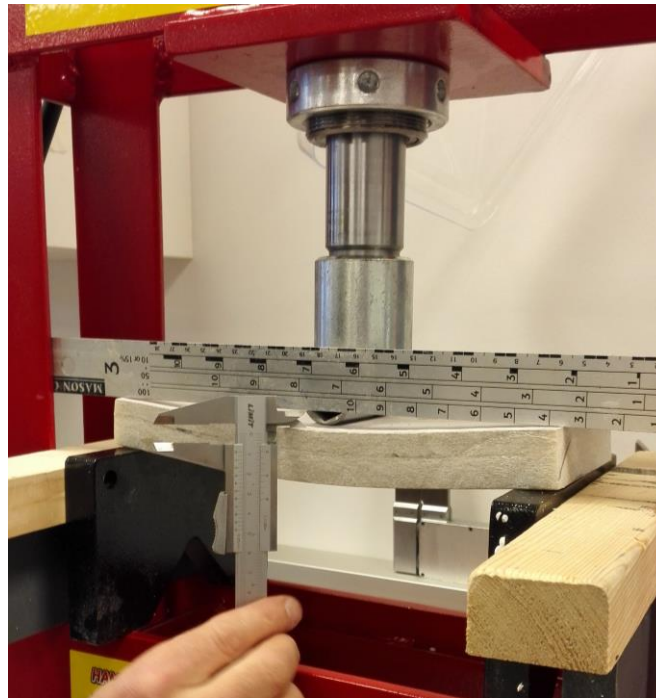


Figure 4-5 Set-up for 3-point bending test (Skaga, 2017)

From the 3-point bending test, we noted down the displacement and some observations, as seen in table 18.

Table 18 3-point bending test, pressure, displacement and observations

| Pressure | Displacement | Observation |
|-------------|--------------|--|
| 1.8 tonnes | 1 mm | No observation. We removed the load, and the sample returned to 0 displacement. |
| 2 tonnes | 2.7 mm | We could hear some cracking noises coming from the material. We removed the load, and the sample returned to 0 displacement. |
| 3 tonnes | 5.4mm | We could hear cracking noises that sounded like breaking glass. |
| 4 tonnes | 6.5mm | The cracking noises intensified. |
| 5 tonnes | 8.4 | In addition to intensified cracking noises, we could observe smoke coming from the material. |
| 5.75 tonnes | | The sample broke and a large surface crack formed at the bottom of the sample. The crack made a loud sound and small glass fibre pieces could be felt flying off the sample. |

Figure 4-6 show the resulting damage. Because the sample is a solid piece, we do not expect adhesive failures (type 1 and 2 damage). In addition, the sample does not have a sandwich structure, excluding type 3 damages. On the uncoated side of the sample (left), we can observe splitting along the fibres (type 5 damage) at the very surface. In addition, we can observe delamination (type 4 damage) below the extruding fibres. On the coated side, we can observe cracks in the gelcoat (type 7 damage) at the top, and delamination (type 4 damage) at the bottom.



Figure 4-6 Image of visual damage induced in 29mm glass fibre sample by 3-point bending test. Uncoated surface (left) and coated surface (right)

We carried out ultrasonic measurements at 3 separate locations from the side without coating. Figure 4-7 indicates the positions where we carried out our measurements.

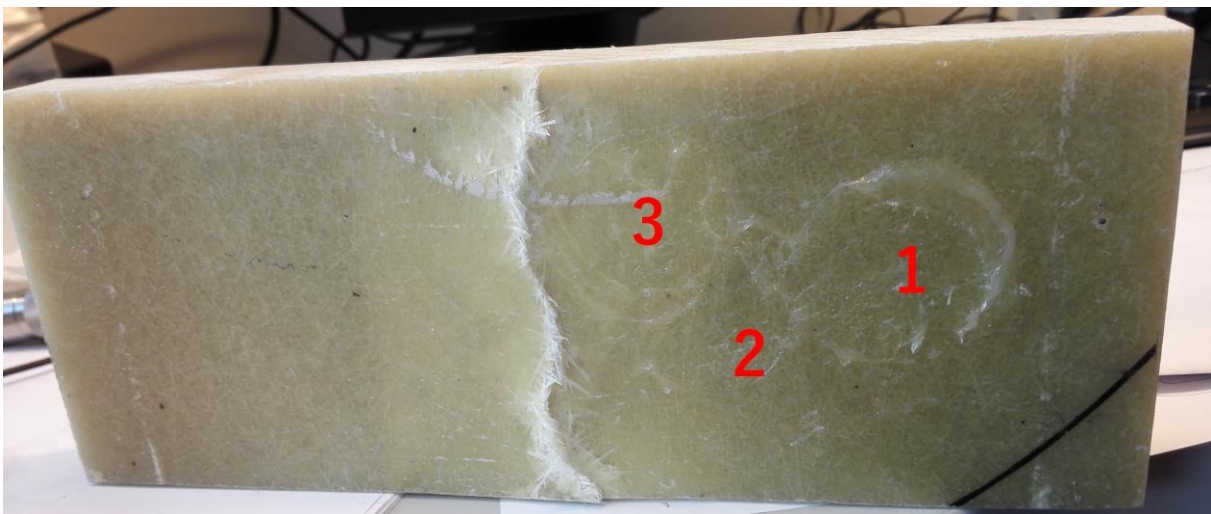


Figure 4-7 Position of ultrasonic measurements on damaged glass fibre sample (Skaga, 2017)

The results from the various locations were different, and as we measured closer to the crack, the backwall echo became weaker. The following captures show the results from location 1, 2 and 3 respectively. Figure 4-8 from position 1 shows a clear backwall echo. This indicates little to none internal damage because the soundwaves can propagate well in the material. We can also observe the second backwall echo on the far right of the graph. From our sample images in figure 4-6, we cannot observe surface damage (type 5 & 7) or delamination at this location.

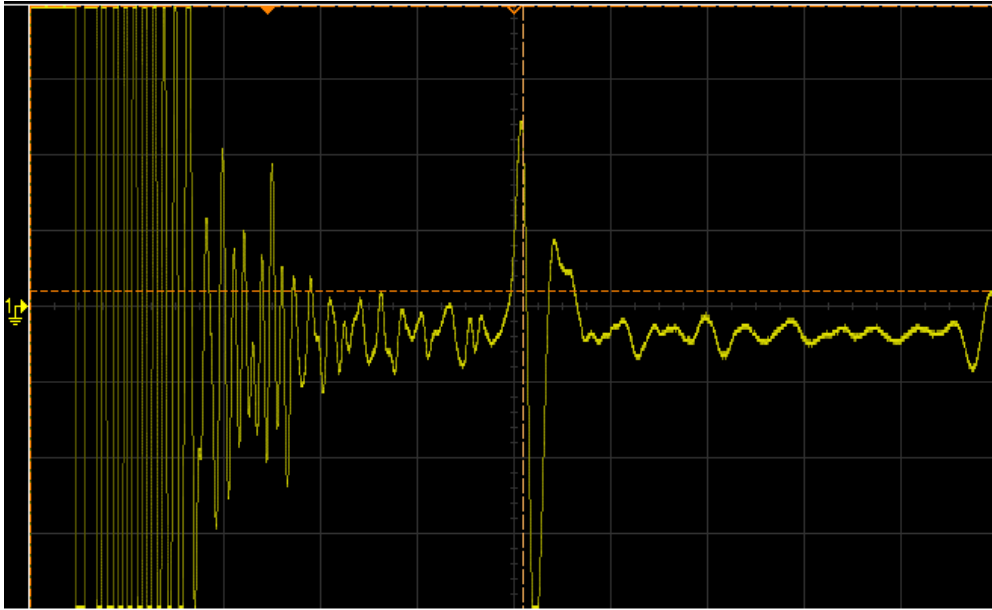


Figure 4-8 Echo response from measurement 1.

The second measurement (figure 4-9) shows a significantly reduced echo strength. It is much weaker than in the first sample, which indicates pockets of air or lack of continuous material for the sound to propagate in. In addition, we cannot observe a second echo, which means that the wave has been scattered and lost in the material. From our sample images in figure 4-6, we can observe surface damage on the coated side (type 7 damage), which reduces the reflection of the backwall surface. We could not observe delamination at this point of the sample.

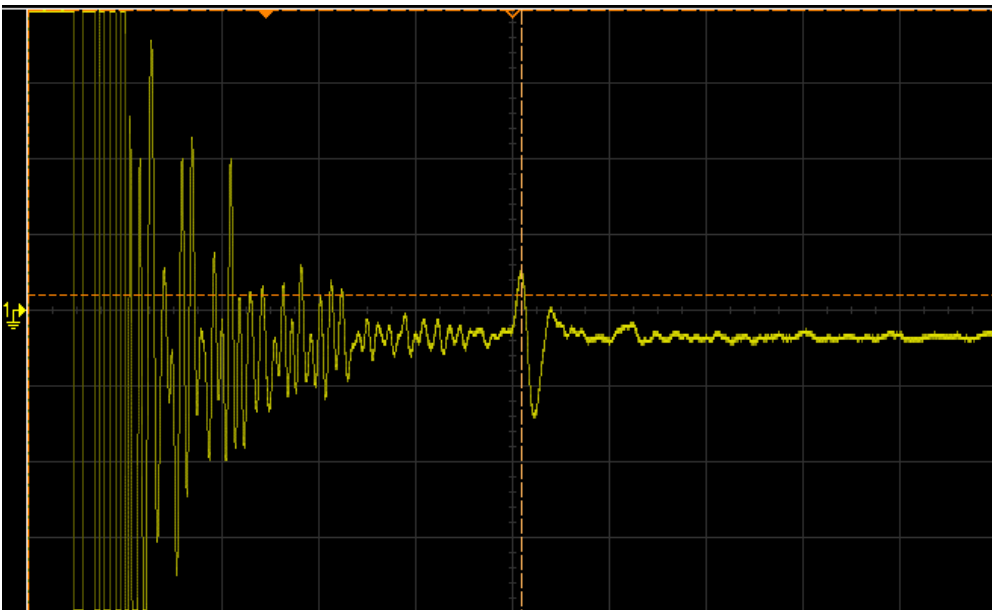


Figure 4-9 Echo response from measurement 2.

The last measurement (figure 4-10) was taken very close to the crack. The material has suffered severe damage in this location because there is no sign of a backwall echo. By observing the material from the sides as seen in figure 4-6, we could see a large crack running perpendicular to the direction of the ultrasonic waves. This delamination (type 4 damage) has created a void inside of the material, which completely stops the wave from propagating further into the material. In case of a clean crack, we could expect an early echo. In this example however, the

crack is not clean, and has splitting along the fibres (type 5 damage). This internal damage scatters or absorbs the ultrasonic wave completely. The orange cursor indicates where the echo is expected to appear, per the previous echo measurements.

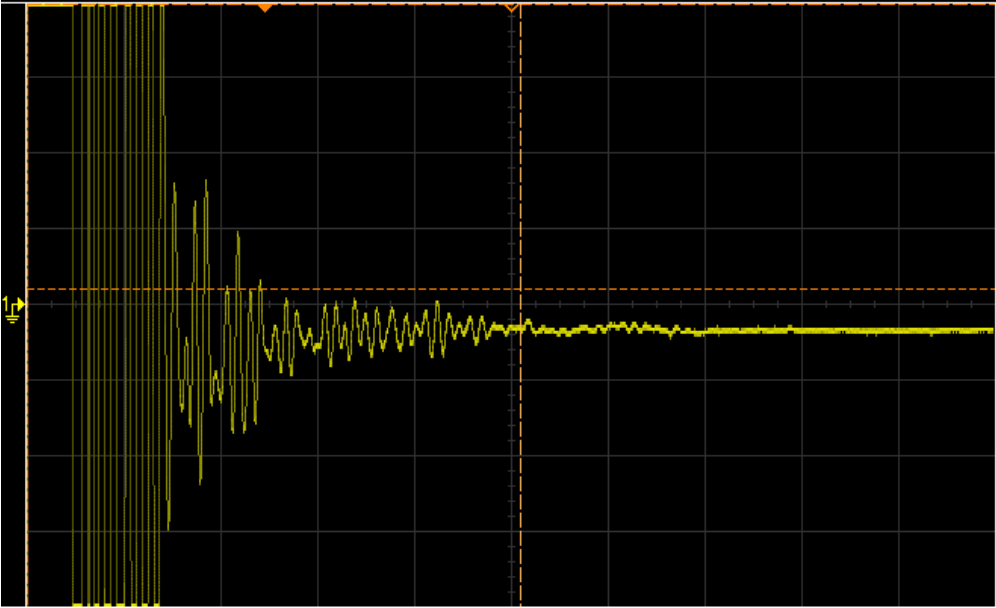


Figure 4-10 Echo response from measurement 3.

4.3 ULTRASONIC MEASUREMENT WITH UAV

The ultrasonic experiments of fibre glass composites using UAV was completed in two stages. Firstly, we tested a simple contact mechanism in flight using two different UAVs. The initial test was conducted to determine the choice of UAV for the final experiment, UAV ultrasonic measurements. We flew with privately owned drones, specifically the Storm AntiGravity platform and a Storm Racing Drone 260 (Helipal, 2017) (Helipal, 2017).





Figure 4-11 Small racing UAV (Helipal, 2017)

Figure 4-12 Medium UAV (Helipal, 2017)

| | | |
|---------------------------|---|--|
| Body-weight | 546g | 1201g |
| All-up-weight | 736g | 1830g |
| Dimension | 240mm x 218mm x 60mm | 500mm x 520mm x 170mm |
| Radio system | RadioLink AT9 2.4Ghz | RadioLink 2.4Ghz AT9 w/ R9D 9-Ch Receiver |
| Flight Time | With stock 14.8V 1800mah 35C battery: 9-19 minutes | With 6S 4200mAh: 35 minutes. |
| Brief description: | This is a racing drone, designed for high speed first person view (FPV) flight. It is not built to carry extra measurement equipment. | The Storm AntiGravity is designed for long duration flight with modified equipment. It is a versatile drone with a wide range of applications. |

4.3.1 Preliminary flight test

The test flight was conducted in a locked room indoors. Thus, the only people involved had complete control over the operation. In addition, factors such as wind and rain was removed. We used a hollow white aluminium rod to represent the device that carries the sensor and puts the transducer in contact with the surface of the test material. The table below shows our flight observations.

| Type of observation | Storm Racing Drone 260 V2 | Storm AntiGravity |
|--------------------------------------|---|--|
| |  |  |
| | <p data-bbox="584 577 979 663"><i>Figure 4-13 Preliminary flight test with Storm Racing Drone 260 V2 (Skaga, 2017)</i></p> | <p data-bbox="1011 577 1362 663"><i>Figure 4-14 Preliminary flight test with Storm AntiGravity (Skaga, 2017)</i></p> |
| UAV could hit the target | No | Yes |
| Pilot's opinion of stability | Unstable in flight with the attached rod. This drone has limited flight control programming because it is intended for racing activities. | Stable with rod. The drone was in altitude hold mode, which made a controlled flight easy for the pilot under controlled conditions. |
| Pilot's experience of control | The drone acted wobbly during flight, and in an environment with more obstacles, it was at risk of collision. | The drone was very steady in position. However, upon approaching the wall, the drone was pushed back by the airflow reflected from the wall. |

Based on our results, we opted to use the Storm AntiGravity drone for the ultrasonic measurements.

4.3.2 Ultrasonic measurements using UAV

This experiment was conducted under the same circumstances as the preliminary UAV flight. The sensor was attached to the UAV via a rod, with a similar sensor attached on the back for counterweight and balance. Flexibility was added to the rod by using rubber bands as UAV attachment, which dampened the impact when the transducer hit the sample. In this experiment, we used the same damaged glass fibre sample from chapter 4.2.2 "Measurement of induced damage", and aimed for the location 1 from experiment 4.2, where minor to none damage is expected. Thus, backwall readings were possible and the pulsed echo test could function as proof of concept.

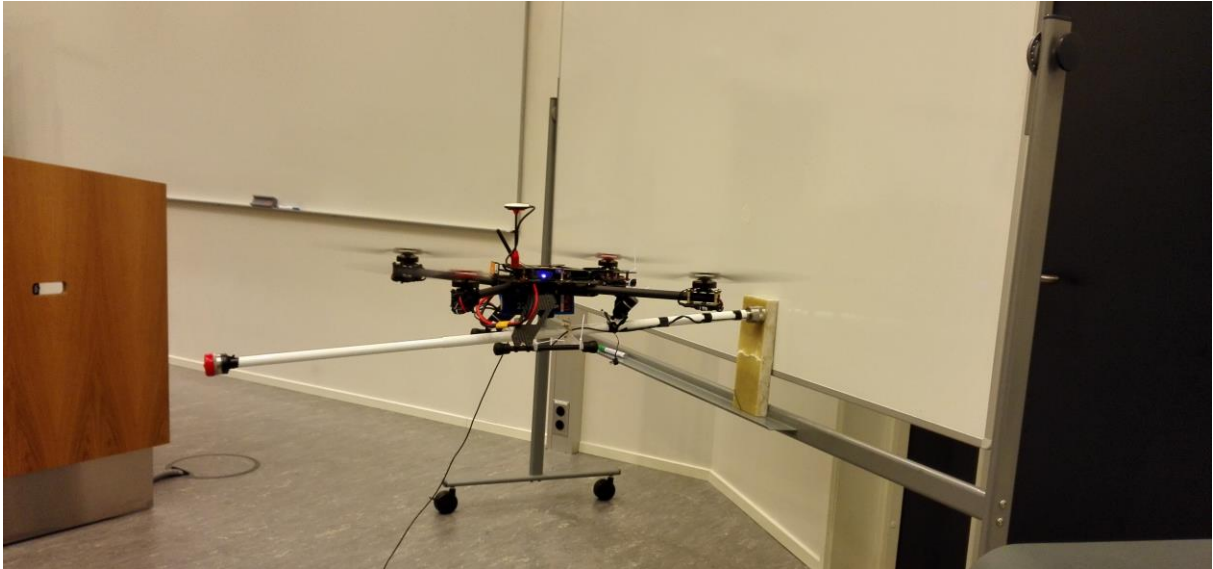


Figure 4-15 Ultrasonic measurement using Storm AntiGravity (Skaga, 2017)

For the UAV experiment, we used a mask trigger function to trig and stop the measurement. The mask was generated with the transducer in free air, and any measurement outside the mask (light grey area in figure 4-16), such as echoes from the back wall or a defect, will trig and stop the measurement. Figure 4-16 and figure 4-17 show the results of two separate flights. Both flights showed a clear echo response, which indicates that ultrasonic non-destructive testing equipment can be carried and applied using a UAV.

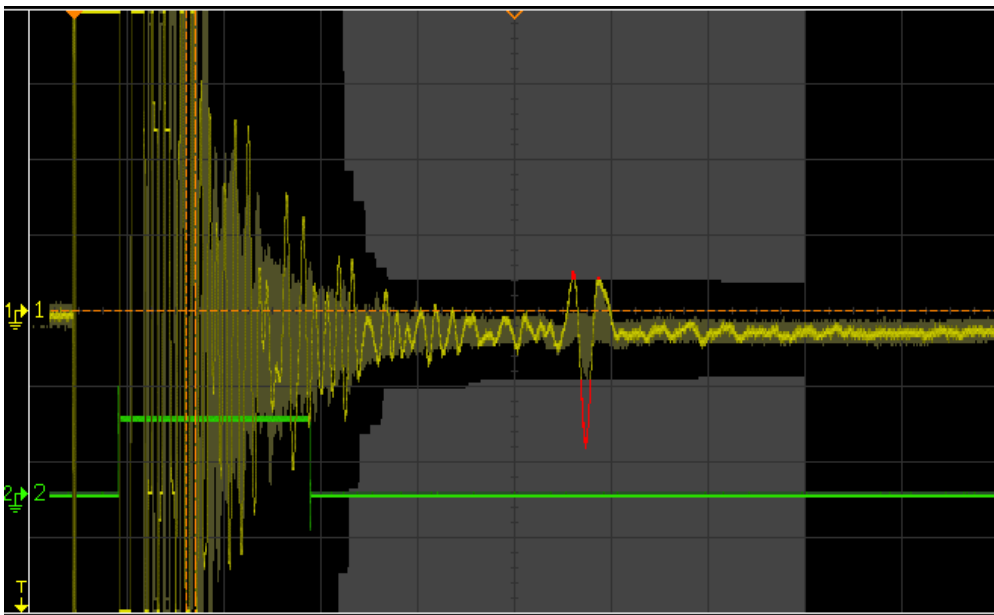


Figure 4-16 Echo response from ultrasonic measurement using Storm AntiGravity, test nr. 1.

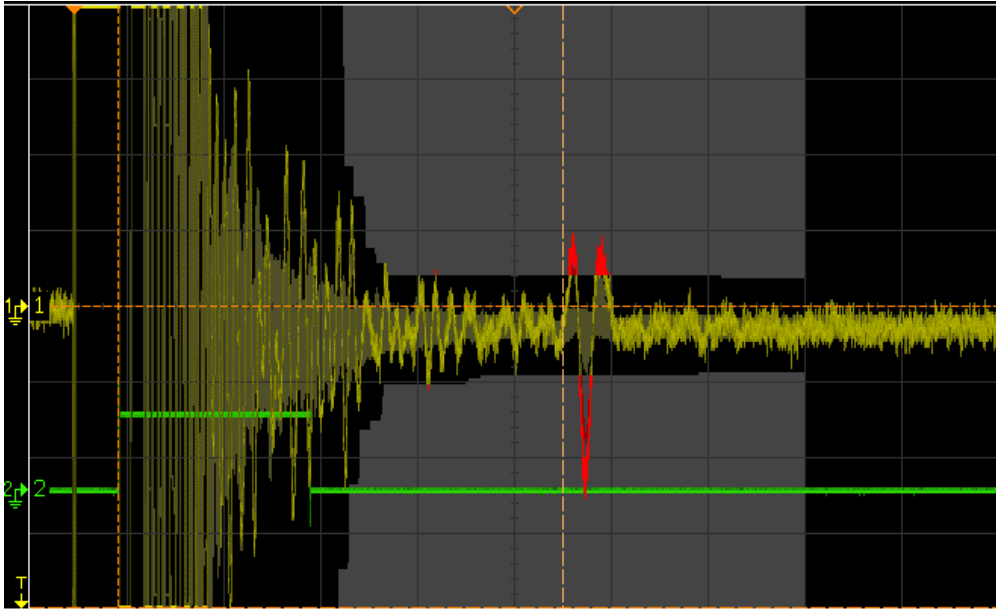


Figure 4-17 Echo response from ultrasonic measurement using Storm AntiGravity, test nr. 2.

5 DISCUSSION

This chapter will discuss the objectives specified in chapter 1.2 Aim and Objectives. For the structure of the report, this chapter has been sectioned according to the objectives, which are repeated here:

- d) Review the current UAV technology regarding stability, high windspeed flight and risks associated with direct contact measurements of wind turbine rotor blades.
- e) Review the typical causes for wind turbine rotor blade damage and the resulting failure modes. Investigate the potential of the ultrasonic echo pulse technique for damage detection through literature review and handheld experimental studies.
- f) Conduct ultrasonic experiments using an UAV, identify advantages and challenges from the results.

5.1 REVIEW OF UAV TECHNOLOGY AND FLIGHT CHALLENGES

When considering the challenges related to UAV flight in proximity to wind turbines, wind is the most obvious concern. Wind turbines are built in places where the wind speeds are high throughout most of the year. Naturally, this is desired, but high windspeeds can complicate the use of UAVs. In addition to undesirably high windspeeds, strong gusts and turbulence due to the wake of the turbine is a substantial risk. By looking at previous experiences of UAV flight in challenging environments and research on state-of-the-art stabilizing technology, we aim to produce a solution to this issue.

If we can solve the wind related challenges, there are still unresolved problems for this project. To carry out ultrasonic testing of the rotor blades, the drone needs to make physical contact with the blade. As our experiments in chapter 4 indicated, the time required to make the measurements is minimal, and a <1 second impact should be sufficient. We must design a device that can put the ultrasonic probe in contact with the blade without a UAV collision. UAVs are delicate, and any damage to the aircraft can result in a crash. As a worst-case scenario, impact with the wind turbine blade can lead to severe damage, resulting in extremely high unwanted costs.

Lastly, UAV flight can be hazardous to personnel and the environment. One must consider the safety of the wind turbine, the environment and people working on site. This calls for a detailed risk analysis, with preventive and consequence reductive measures.

5.1.1 Applicable UAV designs

As presented in chapter 2.2 Unmanned Aerial Vehicle (UAV), there are a series of available designs for UAVs. An important property of the UAV design for ultrasonic testing of wind turbine blades is hover capabilities. The UAV must fly with precision to approach the blade in a controlled manner. By considering the current technology, and excluding various untested design concepts such as fixed-wing drones with hover capabilities, we are limited to multirotor and single rotor drones. Due to independently controlled rotors, the multirotor can achieve high precision flight. However, the multirotor drone has limitations to flight time and maximum load. Single rotor drones can use combustion engines and are fundamentally more energy efficient, and can generally carry more payload. Multirotor drones can only operate with electrical motors. Because it runs on electricity, the engine thrust can be controlled with precision and power can be applied to the rotors instantaneously. The number of rotors in multirotor designs commonly range from 3 to 8, depending on the size and intended purpose of the UAV. In cases with many rotors, the thrust is distributed over the engines, reducing the size and RPM

(rotations per minute) of the rotors. In our case, this is advantageous, as in case of impact with a wind turbine blade, less force is stored in the rotational energy of the individual rotor blades of the UAV.

In case of single rotor drones, the high rotational energy of the rotor can cause greater damage during impact. Because the risk of impact can be considered one of the greatest hazards in this thesis, as shown in the risk analysis, reducing the consequences is a significant factor in our choice of UAV platform. We can deal with the restricted flight time by keeping extra charged batteries on hand during operation, reducing the concerns on time efficiency. In addition, the instrumentation for ultrasonic testing can be designed for minimal payload weight through handheld instrument technology. Flight precision and reduced potential impact energy is a valuable trade-off for flight time and payload capacity, making multirotor drones the most promising option.

5.1.2 Metrological conditions for UAV flight

The degree of acceptable wind conditions of UAV flight will depend on the drone design and the experience of the pilot. Most consumer market multirotor UAVs are not designed for flight in challenging weather. For example, in the preflight checklist for 3D Robotics drones (Robotics, 2017), it is advised against flight in snow, rain or windy conditions. Generally, drones are not made watertight to spare unnecessary weight, however, a wide range of drones available for flight in both rain and snow (Dronelli, 2017).

Wind is a more difficult environmental challenge. It can change speed and direction in minutes, and it is not always possible to forecast the weather with accuracy. A major advantage of flying at wind turbine sites is the availability of continuous wind speed data. The wind direction and velocity is monitored to optimize production by adjusting the rotor blades and rotor hub. The data also ensures the safety of the wind turbines, because at excessive winds, it is imperative that the production is shut down to prevent damages to the wind turbine. Thus, reliable information of the flight conditions is readily available before and during flight.

Chapter 2.1.2 presented some examples of wind conditions at wind turbine sites. Figure 2-4 showed a distribution of hourly wind speeds at a location in the UK, where the mean was centred around 10 m/s. Wind speeds of 5 m/s had a density of 0.06, indicating that low-speed wind is not a common occurrence. In addition, the height of the wind turbine must be considered because wind speed increases with height. Table 1 presented some wind speed measurements at different heights under various conditions. A wind speed of 1.8 m/s at 1 meters above ground, can increase to 8.5 m/s at heights of 117. During clear nights, the weather is particularly stable and wind speeds of 1.7 can increase to 10.9 at 117 meters height. Thus, it is important to consider the wind speed at the level of the rotor blade, and not plan according to measurements at ground level.

Choosing the best UAV design for windy conditions is a complex aerodynamic problem. Designs that deal well with strong steady winds, may not function well in crosswinds or turbulence. Generally, small UAVs with light wing loads are especially sensitive in windy conditions (DeGarmo, 2004). UAV response in wind depends on factors such as drone weight, shape, number of rotors, stabilizing software and thrust. To cope with the complex problem, one may draw from the experience of UAV pilots to identify acceptable wind thresholds. The internet flourishes with active drone hobby forums, where wind condition discussion is a popular topic. The opinions on acceptable windspeeds vary greatly, as their individual drones vary in design and the pilots have different opinions of acceptable risk. Some users claim to fly comfortably in winds of 30 km/h, while others experience scary situations at 20 km/h. Because flight in this

thesis is planned to take place with high precision, the acceptable wind speeds drop significantly from that of unobstructed hobby flight.

5.1.3 UAV stability

The onboard controllers and engine precision technology of UAVs have reached extraordinary levels in the recent years. UAVs can be programmed to follow predetermined GPS coordinates with impressive accuracy and hover steadily in good conditions with very little deviation. However, carrying out ultrasonic testing requires the sensor to stay completely still while the soundwave propagates through the material and returns as an echo. If the sensor is moved in any way, the results may be inaccurate and useless. As mentioned in chapter 2.6 ultrasonic testing, the transducer also requires a liquid medium to transfer the soundwaves into the material in question. If the instrument is not kept still, this liquid may be smeared over the sample and cease to function as intended, thus giving insufficient results. These requirements put high demands to the stability of UAVs, possibly outside the capabilities of today's technology.

In our experiments, we coped with the stability challenges by attaching the sensor to a rod with rubber band dampening, and intentionally "crashed" the UAV into the sample in a controlled fashion. By using this technique, the forces applied to the sample is minimal because the rubber bands absorbed most of the impact, yet the transducer was in direct contact with the surface for the time required for the measurements. Thus, the stability challenges in this operation is related to the effect of the instrumentation and payload of the UAV.

5.1.4 RPAS Regulations

The RPAS regulations, which was briefly presented in chapter 2.2.2, regulates UAV flights regarding location, height, personnel and weight. Depending on the intended operation, the required licence is one of the three categories: R01, R02 and R03. These regulations increase the safety of the operation by introducing risk-analysis requirements for UAVs of more than 2.5 kg, restricting the airspace, and demanding communication with nearby air traffic control in cases of flight in proximity to airports. This section discusses the requirements that are expected for ultrasonic non-destructive testing with UAVs.

The MTOB of the drone in this operation will fall within the 2.5 kg to 25 kg range. The ultrasonic instrumentation and the physical contact arrangement is expected to contribute with a payload of approximately 1 kg. This places requirements on the UAV's payload capacity, which in turn requires larger drones. Other important parameters to consider is the nature of the flight, whereas the regulations places higher safety requirements when UAVs fly BLOS (Beyond line of sight). In this case, the drone will be flying at relatively high altitudes and manoeuvre through a camera mounted on this UAV. The pilot will be able to maintain VLOS (Visual Line of Sight) during the ultrasonic testing, however, if the drone reaches heights of more than 400 ft. AGL, which is 121.92 meters above ground level, the flight is defined as BLOS (Luftfarttsynet, 2016). The top of the rotor blades can exceed this height for the largest offshore wind turbines, and will require special permissions.

Due to the expected weight of the UAV, a detailed risk-analysis will be required. This must be attached in the UAV's operations manual which must be approved by the CAA. A preliminary analysis was carried out in this paper. If UAV application for ultrasonic testing proves feasible, a more detailed risk analysis should be carried out with experienced UAV pilots, as well as engineering specialists in the following fields: electrical, mechanical, computer and atomization science.

5.1.5 Future of UAV technology

When presenting the future of UAV technology, one cannot exclude the recent developments in computer capability, artificial intelligence and machine learning. The developments in computer reasoning has exponentially increased in the last decade, and mankind is facing a revolution. It has already influenced the everyday life of the common man, through smartphone apps such as Siri and Cortana, or self-driving cars from manufacturers such as Tesla (Adams, 2017). The connectivity of today's technological devices causes immense amounts of valuable data, which is processed and shared throughout a company's network. Thus, autonomous vehicles can learn from one another. The potential of this technology is unprecedented, and can change the way most industries work today. Regarding wind turbine rotor blade inspection, non-destructive testing could be carried out by an army of autonomous UAVs. Docking for power, launch and the inspection itself could be carried out by an onshore computer, resulting in an effortless, economic and effective process. The process of ultrasonic testing can be highly automated, involving proximity sensors, an array of intelligent laser and camera technology. Thus, the UAV can stabilize and position itself in an optimal fashion, increasing the quality of the measurements.

5.1.6 Risk evaluation

The risk analysis initially identified 2 unacceptable and 15 ALARP unwanted events. After implementing preventive and reductive barriers, the risk assessment was reduced to 7 ALARP unwanted events. These values of risk assume that the barriers have been successfully implemented. This section will discuss the risks and barriers presented below, aiming to evaluate if it is possible to apply UAVs for ultrasonic non-destructive testing regarding operational safety. The table below recaps the results presented in chapter 4.1, with brief comments on whether the risk can be accepted or not.

Table 19 Brief review of 7 identified ALARP unwanted events with implemented barriers and comments.

| Nr. | | Implemented barriers | Comments |
|------------|---|--|---|
| 6.3 | Uncontrolled impact with wind turbine rotor blade | R1: Design UAV for impact with turbine blades. | This event has been evaluated to high probability because many factors can contribute to reduced control. The risk will be discussed. |
| 8.2 | Unpredictable wind gusts | P1: Develop statistical data on wind conditions at wind turbine site, calculate low-risk dates for flight. R:1 Design UAV for impact with turbine blades. | This event is hard to predict, and the risk will be discussed. |
| 2.6 | Hacking | P5: Use firewalled computes. P6: Take computer offline for flight. R1: Design UAV for impact with turbine blades. | The probability of hacking is neglectable due to the remote location of wind farms and low range communication. The risk is accepted. |
| 3.3 | Intoxicated personnel | P9: Establish a zero-tolerance of drugs and alcohol. Abort if personnel are under the influence. R1: Design UAV for impact with turbine blades. R2: Control ground below flight to prevent people directly underneath the drone. | The risk of intoxicated personnel occurs in any industry and will not be considered further in this thesis. The risk is accepted. |
| 3.6 | Failure to spot people | P11: Have enough participants in the operation to control the entire flight zone. | Personnel safety is the top priority, but with sufficient mission planning and adequate manpower, the probability is significantly low. The risk is accepted. |

| | | | |
|-----|---------------------------|---|--|
| 6.4 | Manned helicopter traffic | P12: Land immediately if helicopters can be seen or heard flying low. | The probability of low flying helicopters is extremely low, and the height of the turbines themselves pose a bigger threat. The risk is accepted. |
| 6.5 | Manned airplanes traffic | P13: Land immediately if airplanes can be seen or heard flying low. | The probability of low flying airplanes is extremely low, and the height of the turbines themselves pose a bigger threat. The risk is accepted. |

5.1.6.1 R1: Design UAV for impact with wind turbine rotor blades.

The probability of uncontrolled impact with wind turbine rotor blades is high. Because the operation depends on repeated surface contact for the transducer, the UAV will be very close to the rotor blades throughout the entire operation. At close distances, small disturbances in the UAV's position can lead to impact. Wind gusts or turbulence can push the UAV into the rotor blade. There is little margin for pilot error, and instruments such as GPS, gyro and altimeter are not precise at a millimetre level. Combined, these factors make it difficult to reduce the probability of impact. Thus, the only way to reduce the risk is to design the UAV with the expectance of impact.

When designing the UAV for impact with rotor blade, the size and weight of the UAV becomes highly relevant. The kinetic energy applied to the blade is proportional with UAV weight and its impact velocity, per the kinetic energy of rigid bodies formula 5.1 (Wikipedia, the free encyclopedia, 2017) .

$$E_k = \frac{1}{2}mv^2 \quad (5.1)$$

A heavy UAV, which is less susceptible to sudden changes in wind due to its weight per surface area, will have a lower velocity due to the wind than lighter UAVs. It will, however, gain kinetic energy due to its mass. Light UAVs will have a larger increase in kinetic energy due to the wind, because of the v^2 term. Thus, the relationship between mass, surface area and expected wind speed must be carefully considered.

It is important to protect the propellers and keep objects outside their rotational field. In today's consumer marked, many UAVs are designed for flight by inexperienced pilots, and both small and large UAVs come with propeller protection. Two popular solutions are the propeller guard and propeller cage.



Figure 5-1 Example of UAV propeller guard (left) (DJI Store, 2017) and UAV propeller cage (right) (UAV Expert News, 2017)

The propeller guard protect the propellers in the horizontal direction, while the propeller cage encases the propellers completely. The best solution will depend on the UAV in question and the aerodynamic influence of the guard/cage. In addition, increased protection leads to added weight and surface area, which makes the UAV more susceptible to wind. There will be an optimal relationship between payload capacity for ultrasonic equipment, flight time, control systems, thrust, weight and protection. In addition, the contact mechanism for the ultrasonic equipment can add a protective factor to the UAV.

We can distinguish between UAV damage and rotor blade damage, as the magnitude of the consequences are vastly different. The costs related to a damaged blade will make UAV ultrasonic testing non-viable, whereas the UAV can be repaired or replaced at much lower costs. Thus, the UAV can be designed to fail, and protect the rotor blade in case of collision.

5.1.6.2 P1: Develop statistical data on wind conditions at wind turbine site, calculate low-risk dates for flight.

As presented in chapter 5.1.2 Metrological conditions for UAV flight, the operation appears feasible based on wind statistics. Although wind turbines are built at wind exposed sites, there are wind free days throughout the operational year (Dowell, et al., u.d.). It should be possible to manoeuvre in steady low-wind speeds, especially with the reductive barrier R1 implemented. Due to the availability of wind data at wind turbine sites, it is possible to derive optimal date and times for the UAV operation. In addition, due to the speed of UAV ultrasonic testing, the tests can be conducted within little time and in short notice. This is one of the major advantages of UAV application for non-destructive testing, and with careful consideration of when and where to fly, the probability of lost control due to high winds will be significantly reduced. However, the wake of the wind as it hits the wind turbine induces some complex wind patterns of turbulence. Computer simulations can be used to calculate the airflow of the wind as it hits the wind turbine at different angles. This will identify dangerous zones where the UAV should keep distance to the rotor blades during the operation.

5.2 HANDHELD ULTRASONIC EXPERIMENTS

The handheld ultrasonic experiments showed that the ultrasonic pulse technique can be used for non-destructive testing of the glass fibre material we received from Lyngen Plast A/S. We simulated a Type 1 “Damage formation and growth in the adhesive layer joining skin and main spar flanges” by holding two samples together and observing their separate echoes. The void, or reduced uniformity, between the two blocks of glass fibre disrupted the ultrasonic signal, which resulted in partial reflection of the signal. It was possible to carry out thickness measurements of the material, which can be used to accurately specify the depth of the damage. Type 1 damage

occurs inside the material and can be impossible to visually detect before it grows to the surface. At this point, it may be too late, and the turbine must be shut down. Type 1 damage will significantly affect the structural integrity of the rotor blade as it occurs at the load-bearing spar. The simulation also shows that ultrasonic testing can be used to identify type 2 “Adhesive joint failure”. Voids in the material will generally disrupt the soundwave, and disruption can easily be detected with simple readings on an oscilloscope.

The second handheld ultrasonic experiment was conducted on a damaged block of glass fibre. It was broken during a 3-point bending test, and the damages could be observed by visual inspection. In the images presented in chapter 4.3.2, we can clearly observe the following damages.

Table 20 Damage types visually observed in broken glass fibre sample

| Type | Comment |
|---------------------------------------|--|
| Type 7: Cracks in gelcoat | The coating on the top of the sample broke, and crack channels could be observed. The coating broke off across the breadth of the sample, where the compression load was concentrated. |
| Type 5: Splitting along fibres | We could clearly observe splitting along fibres on both sides of the sample, and as we observed during the bending test, small fibres were launched from the sample. |
| Type 4: Delamination | When we observed the sample from the sides, clear delamination could be observed. It appeared like layered cracks. |

The ultrasonic measurements on the damaged sample clearly indicated internal damage in the material. We measured the sample in 3 places, as seen in figure 4-7. The first measurement was taken where we expected little to none internal damage, and the measurement showed a clear backwall echo. This indicates that the ultrasonic waves could propagate efficiently throughout the material, with relatively little scattering and absorption. The second measurement was taken closed to the visible crack, at the edge of a zone where the colour of the fibre sample had changed. Once again, we could observe a backwall echo, but significantly weaker than in the first measurement. This indicates air and discontinuities in the material, when comparing to first measurement for reference. The third measurement showed no backwall echo, as seen in figure 4-10. This is the expected response, as the measurement were taken perpendicular to the visible delamination in the material. Ultrasonic soundwaves cannot travel from solid, into air and back into the solid due to the differences in acoustic impedance. However, in cases of clear cracks with an even surface, we can expect an early backwall echo from the surface of the crack. There are several potential reasons as to why we did not observe this. The material could be internally damaged and have many air inclusions and voids, this would explain excessive scattering, essentially dispersing the soundwave in all directions. Another cause could be the noise at the start of the pulse. Because the delamination was located very closely to the surface, the low-dampening transducer used in the experiments was unable to clearly distinguish an echo from its internal oscillations post-pulse. Ultrasonic equipment specifically designed to detect damages in wind turbine rotor blades could be used for better measurements.

5.3 UAV ULTRASONIC EXPERIMENTS

The ultrasonic experiments using an UAV were of a basic nature. The engineering challenges regarding contact delivery mechanism, UAV modification and custom sensor equipment has not been covered. We used a very preliminary solution, consisting of a transducer, rubber bands and a hollow aluminium rod for putting the ultrasonic equipment in contact with the sample surface. The pulser/receiver and oscilloscope was located on the ground, connected to the UAV via a long wire. The main goal of the experiment was to prove that ultrasonic NDT contact measurements can be done using a UAV, and by looking at the results, we could send and receive an ultrasonic pulse in the sample. The echo from the backwall of the sample could be easily be observed in figure 4-16 and figure 4-17, indicating that with proper instrumentation, UAVs can carry out ultrasonic testing.

By using the Storm AntiGravity UAV, we hit the target with relative precision. Each attempt could put the transducer in contact with the sample, within a 20cm circle. In addition, both our handheld and UAV ultrasonic measurements were conducted within milliseconds of direct contact, due to the repeated pulse echo measurements and averaging functions. Thus, the UAV requires contact for a brief period (<1 second) to carry out ultrasonic pulse echo testing.

Larger UAVs that are less susceptible to airflow reflecting from the surface of the sample/wall, should be capable of better accuracy and stability. There is a significant potential for improvement of the instrumentation, and from our experimental experiences, the following aspects need more consideration.

5.3.1 Transducer surface contact mechanism

In this thesis, we did not attempt to engineer a reliable solution for setting the transducer in surface contact with the sample. Because of the vibration from the UAV, the delivery mechanism must include some sort of dampening. The mechanism must be well balanced around the UAV's centre of mass for flight stability. To measure at a wide range of positions on the blade, it should include remote control functions, so that it can be oriented at different angles during one flight, facilitating fast and reliable results. To carry out ultrasonic contact measurements, a coupling medium between the surface and transducer is required, thus a system for gel injection must be developed. As mentioned in chapter 5.1.6 Risk evaluation, the transducer surface contact mechanism can function as increased protection from UAV collision. Because it must be built as an extension with dampening functions, extending outside the range of the UAV rotor blades, it can absorb much of the collision energy. Thus, reducing the consequences of collision.

5.3.2 Ultrasonic instrumentation

The ultrasonic instrumentation must be as lightweight as possible to reduce the size of the UAV, resulting in less kinetic energy, reducing the consequences of impact with the blade. Through ultrasonic testing of rotor blades on the ground, reference data can be established, and measurements can be interpreted on site. It would be beneficial with wireless transmission of the measurements to the ground station, because a live feed of the ultrasound can increase the quality of the results. Handheld ultrasonic pulse equipment is available for a wide range of application, where measurement of wind turbine blades is already a documented application. From (Olympus, u.d.), a selection of suitable transducer can be found, such as single element contact transducers and dual element transducers. The choice of transducer depends on the thickness of the material, desired resolution, durability and damages of interest. For example, dual element transducer is more suitable for near-surface damages, as it does not require the pulsing piezoelectric crystal to be dampened before echoes can be observed. However, the soundwaves are fired at an angle, placing a range on depth of penetration.

6 CONCLUSION

The findings presented in this feasibility study of UAV application for ultrasonic non-destructive testing has indicated considerable potential. We initially derived the following research questions from the aims and objectives presented in the introduction.

- a) Can UAV's fly near wind turbine rotor blades with acceptable risk?
- b) Is ultrasonic echo testing suitable for wind turbine rotor blades, built from fibre glass laminates?
- c) Can UAVs be used to carry out ultrasonic non-destructive testing?

We identified no concerns of UAV application for ultrasonic testing regarding the RPAS Regulations. The risks of the UAV flight operation were considered very important, thus both SWIFT-analysis and the bow-tie barrier method was appropriate. The results were two barriers that must be implemented for the risk to reach acceptable levels. Risk reductive "Design UAV for impact with turbine blades," and preventive: "Develop statistical data on wind conditions at wind turbine site, calculate low-risk dates for flight." Weather conditions must be ideal for UAV flight near wind turbine rotor blades, in addition, the UAV must be designed for impact because an uncontrolled collision is inevitable.

In figure 4-3, we can observe the results from an ultrasonic pulse at $2555.55 \frac{m}{s}$, propagating through a simulated glass fibre laminate delamination. A voltage-time graph tells the story of the soundwave in the laminate. We carried out measurements on echo amplitudes and thus, the thickness and the degrees of damage in the material could be identified. With the instrumentation that was available short-handly, a considerable quality was achieved. In combination with the existing literature on ultrasonic non-destructive testing of wind turbine rotor blades, our experiments clearly indicate that the technique is suitable for testing of glass fibre laminates.

Next, we attempted to acquire comparable results using the Storm AntiGravity UAV, a privately-owned drone. The test was conducted indoors which facilitated wind-free flight conditions. We also had complete control of the room and could fly with the pulser/receiver & oscilloscope on the ground. Despite the basic nature of the test, an echo response could easily be observed. This confirms that UAVs can indeed be used for ultrasonic testing of wind turbine rotor blades. The extent and quality of our measurements does not confirm that UAV ultrasonic testing can be a viable means of non-destructive testing for wind turbine rotor blades, it does however, warrant a detailed and continued study of the application. The author recommends the following future studies.

Future studies

- The risk analysis presented in this paper is a preliminary approach. The method was conducted by the author which recommends a detailed quantitative risk assessment. Future study is recommended an interdisciplinary team, including programmers, electrical-/ atomization engineers and expert pilots.
- The ultrasonic instrumentation necessary for non-destructive testing of wind turbine rotor blades must be studied. From the measurements, one should know the details of the damage. Future study is recommended that development of UAV payload technology is considered, thus designing the transducer-surface contact mechanism.
- Develop statistical data on wind conditions at wind turbine site, calculate low-risk dates for flight. - The preventive barrier that requires well-developed algorithms and in-detail

computer simulation. Future study is recommended to investigate wind conditions at the coast of England, specifically offshore.

- A study should be made on the consequences of UAV impact or loss of control. A series of trials of UAV collision with wind turbines could produce data that could improve the UAV design or contact mechanism. Data on UAV collision could also benefit general awareness amongst the commercial drone manufacturers and owners.

7 REFERENCES

- Adams, R., 2017. *Forbes - 10 Powerful Examples Of Artificial Intelligence In Use Today*. [Internet] Available at: <https://www.forbes.com/sites/robertadams/2017/01/10/10-powerful-examples-of-artificial-intelligence-in-use-today/#66a06c87420d> [Funnet 23 05 2017].
- Amenabar, I. et al., 2011. Comparison and analysis of non-destructive testing techniques suitable for delamination inspection in wind turbine blades. *Composites: Part B*, Issue 42, pp. 1298-1305.
- Baldev, R., Jayakumar, T. & Thavasimuthu, M., 2007. *Practical Non-Destructive Testing*. Third Edition red. Oxford, U.K.: Alpha Science International Ltd..
- Business Insider Nordic, 2016. *Business Insider Nordic*. [Internet] Available at: <http://nordic.businessinsider.com/sweden-is-to-use-100-renewable-energy-by-2040---but-no-expiration-date-has-been-set-for-nuclear-energy-2016-6> [Funnet 07 04 2017].
- CBSE Portal, u.d. *Important Topics Physics: Properties of Electromagnetic waves*. [Internet] Available at: <http://cbseportal.com/Important-Topics/Physics-Properties-of-Electromagnetic-Waves> [Funnet 26 May 2017].
- CGE Risk Management Solutions, u.d. *The Bowtie Method*. [Internet] Available at: [CGE Risk Management Solutions](http://www.cge-risk.com/) [Funnet 18 10 2016].
- Chapman, A., 2016. *Australian UAV*. [Internet] Available at: <http://www.auav.com.au/articles/drone-types/> [Funnet 30 09 2016].
- Chia Chen, C., Jung-Ryul, L. & Hyung-Joon, B., 2008. *Measurement Science and Technology*, Volum 19.
- Conley, K., 2013. Toy helicopter slices off top of man's head. *New York Post*, 5 09.
- D. C. Quarton, G. H. a. P. L. T. C. H. F. L. L. A., 1998. The Evolution of Wind Turbine Design Analysis - A Twenty Year Progress Review. *John Wiley & Sons, Ltd*, p. 20.
- Darby, M., 2016. *The Guardian*. [Internet] Available at: <https://www.theguardian.com/environment/2016/jan/26/solar-panel-costs-predicted-to-fall-10-a-year> [Funnet 07 04 2017].
- DeGarmo, M. T., 2004. *Issues Concerning Intergration of Unmanned Aerial Vehicles in Civil Airspace*, s.l.: McLea, Virginia: Center for Advanced Aviation System Development.
- DJI Store, 2017. *Phantom 3 - Propeller guard*. [Internet] Available at: <http://store.dji.com/product/phantom-3-propeller-guard> [Funnet 26 May 2017].
- DNV GL AS, November 2016. Loads and site conditions for wind turbines. I: *Standard DNVGL-ST-0437*. Edition November 2016 red. s.l.:s.n.

Dongsheng, L. et al., 2015. A review of damage detection methods for wind turbine blades. *Smart Materials and Structures*, Issue 24.

Dowell, J. et al., u.d. *Analysis of Wind and Wave Data to Assess Maintenance Access to Offshore Wind Farms*. Glasgow, University of Strathclyde.

Dronelli, V., 2017. *Drones Globe*. [Internett]
Available at: <http://www.dronesglobe.com/guide/waterproof/>
[Funnet 26 04 2017].

Dvorak, P., 2014. *Why not more vertical-axis wind turbines?*. [Internett]
Available at: <http://www.windpowerengineering.com/design/vertical-axis-wind-turbines/>
[Funnet 19 01 2017].

Eastlake, C. N., 2002. An Aerodynamicist's View of Lift, Bernoulli, and Newton. *The Physics Teacher*, Volum Vol. 40.

European Commission, 2017. *Climate Action - Paris Agreement*. [Internett]
Available at: https://ec.europa.eu/clima/policies/international/negotiations/paris_en#tab-0-0
[Funnet 07 04 2017].

Galleguillos, C. et al., 2014. *Thermographic non-destructive inspections of wind turbine blades using unmanned aerial systems*. Seville, Spain, European conference on composite materials.

Gjellestad, O. J., 2011. *Drifts- og vedlikeholdsledelse - For bærekraftig utnyttelse av maskiner, anlegg og utstyr*. v05.12.2012 red. Bergen: Høgskolen i Bergen.

Hansen, J. P., Alapetite, A., MacKenzie, I. S. & Møllenbach, E., 2014. The Use of Gaze to Control Drones. *Proceedings of the ACM Symposium on Eye Tracking Research and Applications*, pp. 27-34.

Helipal, 2017. *STORM Drone AntiGravity GPS Flying Platform (BNF / NAZA V2)*. [Internett]
Available at: <http://www.helipal.com/storm-drone-antigravity-gps-flying-platform-bnf-naza-v2.html>
[Funnet 20 05 2017].

Helipal, 2017. *STORM Racing Drone (RTF / SRD260 Pro V2)*. [Internett]
Available at: <http://www.helipal.com/storm-racing-drone-rtf-srd260-pro.html>
[Funnet 20 05 2017].

ifm, u.d. *Pitch drive electric in a gearless wind turbine*. [Internett]
Available at: https://www.ifm.com/ifmuk/web/apps-by-industry/cat_060_010_010.html
[Funnet 26 May 2017].

Institute of Risk Management, 2016. *Risk Management*. [Internett]
Available at: <https://www.theirm.org/the-risk-profession/risk-management.aspx>
[Funnet 18 10 2016].

Jiles, D. C., 2007. *Introduction to the Principles of Materials Evaluation*. Cardiff, U.K.: CRC Press.

Jüngert, A., 2008. Damage Detection in Wind Turbine Blades using two Different Acoustic Techniques. *NDT.net - The e-Journal of Nondestructive Testing*, Issue December 2008.

KNMI Hydra Project, 1998 - 2005. *Wind speed profile*. [Internett]
Available at: <https://projects.knmi.nl/hydra/faq/profile.htm>
[Funnet 27 May 2017].

Lading, L. et al., 2002. *Fundamentals for Remote Structural Health Monitoring of Wind Turbine Blades - a Preproject*, Roskilde, Denmark: Risø National Laboratory.

Layton, J., 9 August 2006. *How Wind Power Works*. [Internett]
Available at: <http://science.howstuffworks.com/environmental/green-science/wind-power2.htm>
[Funnet 26 May 2017].

Learn Engineering, u.d. *Wind turbine design*. [Internett]
Available at: <http://www.learnengineering.org/2013/08/Wind-Turbine-Design.html>
[Funnet 26 May 2017].

Learn Robotix, u.d. *Learn Robotix*. [Internett]
Available at: <http://learnrobotix.com/uavs/quadcopter-basics/how-do-quadcopters-fly.html>
[Funnet 18 10 2016].

Lombardo, T., 2014. *The World's Most Powerful Wind Turbine*. [Internett]
Available at:
<http://www.engineering.com/ElectronicsDesign/ElectronicsDesignArticles/ArticleID/7874/Worlds-Most-Powerful-Wind-Turbine.aspx>
[Funnet 19 01 2017].

Lovdata, 2015. *Lovdata*. [Internett]
Available at: <https://lovdata.no/dokument/SF/forskrift/2015-11-30-1404>
[Funnet 18 10 2016].

Luftfartstilsynet, 2016. *Generelt om droner/RPAS*. [Internett]
Available at: http://luftfartstilsynet.no/selvbetjening/allmennfly/Droner/Om_Droner
[Funnet 03 05 2017].

Martinez-Luengo, M., Kolios, A. & Wang, L., 2016. Structural health monitoring of offshore wind turbines: A review through the Statistical Pattern Recognition Paradigm. *Renewable and Sustainable Energy Review*, Issue 64, pp. 91-105.

Mobley, R., 1990. *An introduction to predictive maintenance*. New York: Van Nostrand Reinhold.

mpower, u.d. *Aerodynamic Lift and Drag and the Theory of Flight*. [Internett]
Available at: http://www.mpoweruk.com/figs/flight_theory.htm
[Funnet 26 May 2017].

Nave, C. R., 2016. *HyperPhysics*. [Internett]
Available at: <http://hyperphysics.phy-astr.gsu.edu/hbase/Tables/Soundv.html>
[Funnet 22 03 2017].

Nave, R., u.d. *Sound waves in air*. [Internett]
Available at: <http://hydrogen.physik.uni-wuppertal.de/hyperphysics/hyperphysics/hbase/sound/tralon.html>
[Funnet 26 May 2017].

Nex, F. & Remondino, F., 2013. *Springer Link*. [Internett]
Available at: <http://link.springer.com/article/10.1007/s12518-013-0120-x>

Olympus, 2017. *Ultrasonic Flaw Detection Tutorial*. [Internett]
Available at: <http://www.olympus-ims.com/en/ndt-tutorials/flaw-detection/ultrasound/>
[Funnet 26 May 2017].

Olympus, 2017. *Ultrasonic Flaw Detection Tutorial 1.2 History of Flaw Detection*. [Internett]
Available at: <http://www.olympus-ims.com/en/ndt-tutorials/flaw-detection/history/>
[Funnet 17 03 2017].

Olympus, 2017. *Ultrasonic Flaw Detection Tutorial 2.2 Generating Ultrasound (Transducers)*.
[Internett]
Available at: <http://www.olympus-ims.com/en/ndt-tutorials/flaw-detection/generating-ultrasound/>
[Funnet 20 03 2017].

Olympus, u.d. *Ultrasonic Transducers*. [Internett]
Available at: <http://www.sintrol.fi/images/Esitteet/Ultraaniluotaimet.pdf>
[Funnet 18 05 2017].

PANAMETRICS-NDT, 2004. *User's manual model 5077PR*. United States of America: Olympus NDT.

Rausand, M. & Utne, I. B., 2009. *Risikoanalyse - teori og metoder*. Trondheim: Tapir Akademisk Forlag.

Robotics, 3., 2017. *Preflight Checklist*. [Internett]
Available at: <https://3dr.com/support/articles/preflight-checklist/>
[Funnet 26 04 2017].

Ruizhen, Y., Yunze, H. & Hong, Z., 2016. Progress and trends in nondestructive testing and evaluation for wind turbine composite blade. *Renewable and Sustainable Energy Reviews*, Issue 60, pp. 1225-1250.

Skaga, S. K., 2017. *Unpublished photograph*. UiT, Tromsø: s.n.

Sørensen, B. F. et al., 2004. *Improved design of large wind turbine blade of fibre composites based on studies of scale effects (Phase 1) - Summary Report*, Roskilde, Danmark: Risø National Laboratory.

Spera, D. A., 2009. *Wind Turbine Technology - Fundamental Concepts of Wind Turbine Engineering*. 2nd red. New York: ASME.

Statoil, 2017. *Our offshore wind projects*. [Internett]
Available at: <https://www.statoil.com/en/what-we-do/new-energy-solutions/our-offshore-wind-projects.html>
[Funnet 07 04 2017].

Tangler, J. L., 2000. *The Evolution of Rotor and Blade Design*. Golden, Colorado, NREL, National Renewable Energy Laboratory.

Tchakoua, P. et al., 2014. Wind Turbine Condition Monitoring: State-of-the-Arth Review, New Trends, and Future Challenges. *Energies*, Issue 7, pp. 2595-2630.

Tektronix, 2000. *XYZs of Oscilloscopes*. s.l.:Tektronix.

The Worlds of David Darling, u.d. *Nacelle*. [Internett]
Available at: http://www.daviddarling.info/encyclopedia/N/AE_nacelle.html
[Funnet 26 May 2017].

Tractica, 2016. *Tractica*. [Internett]
Available at: <https://www.tractica.com/newsroom/press-releases/consumer-drone-sales-to->

increase-tenfold-to-67-7-million-units-annually-by-2021/
[Funnet 25 09 2016].

UAV Expert News, 2017. *Tag: Propeller Cage*. [Internett]
Available at: <http://www.uavexpertnews.com/tag/propeller-cage/>
[Funnet 26 May 2017].

Wallenberger, F. T. & Bingham, P. A., 2010. *Fiberglass and Glass Technology Energy-Friendly Compositions and Applications*. s.l.:Springer.

Wikipedia, the free encyclopedia, 2017. *Kinetic energy, Wikipedia*. [Internett]
Available at: https://en.wikipedia.org/wiki/Kinetic_energy
[Funnet 31 May 2017].

Wikipedia, t. f. e., 2017. *Piezoelectricity*. [Internett]
Available at: <https://en.wikipedia.org/wiki/Piezoelectricity>
[Funnet 20 03 2017].

Wróbel, G. & Pawlak, S., 2006. Ultrasonic evaluation of the fibre content in glass/epoxy composites. *Journal of Achievements in Materials and Manufacturing Engineering*, 18(1-2), pp. 187-190.

Xiao, C., Wei, Z., Xiao Lu, Z. & Jian Zhong, X., 2014. Preliminary failure investigation of a 52.3 m glass/epoxy composite wind turbine blade. *Engineering Failure Analysis*, Issue 44, pp. 345-350.

8 APPENDIX A

The following appendix contains the worksheet used in the SWIFT-analysis. An explanation of the columns is presented in chapter 2.5.2 SWIFT-analysis.

The appendix has been developed in the period 1. November 2016 to 20. May 2017, through the course of a pre-project and the writing of this thesis. The analysis has been produced by the author, currently completing a MSc in Technology and Safety in the High North at the University in Tromsø.

The appendix is 9 pages long, including this preface.

| Nr. | What if? | Potential causes | Effects and consequences | Existing barriers | Risk | | | Risk reducing measures | Responsible | Post-barrier risk | | |
|-----|--------------------------------------|--------------------------|--|---|-------|-------|-----|--|-------------|-------------------|-------|-----|
| | | | | | Freq. | Cons. | RPN | | | Freq. | Cons. | RPN |
| 1.1 | The drone loses propulsion | Exhausted battery | Complete loss of control. The UAV will crash vertically. | Modern UAVs have safety barriers, and will return to launch before battery is depleted. | 2 | D | 6 | Examine battery before flight. Use recommended margins. | Simon | 2 | B | 4 |
| 1.2 | | Control system fails | Complete loss of control. The UAV will crash. | If possible, pilot can take manual control. | 2 | D | 6 | Make sure the UAV firmware and software is up to date. | Simon | 2 | B | 4 |
| 1.3 | | Electrical failure | Complete loss of control. The UAV will crash. | Many UAVs have well protected electronics. | 1 | D | 5 | Use a platform which encases the UAV electronics. | Simon | 1 | B | 3 |
| 1.4 | | Engine failure | Complete or reduced loss of control. The UAV will descend unpredictably, depending on how many engines fail. | | 2 | D | 6 | Thoroughly examine propeller and engine before flight. | Simon | 2 | B | 4 |
| 2.1 | We lose radio contact with the drone | Drone out of range | Uncontrolled automatic flight | Modern UAVs have automatic hover or slow decent functions in case of contact loss. | 1 | C | 4 | Ensure good radiolink and GPS contact before lift-off. Monitor signal strengths throughout the operation. Program good failsafe. | Simon | 1 | B | 3 |
| 2.2 | | Exhausted remote battery | Uncontrolled automatic flight | Modern UAVs have automatic hover or slow decent functions in case of contact loss. | 1 | C | 4 | Control the battery before lift-off. Monitor GPS contact throughout the operation. | Simon | 1 | B | 3 |

| | | | | | | | | | | | | | |
|-----|-----------------------------------|---|---|---|---|---|---|--|--|-------|---|---|---|
| 2.3 | | Signal interference | Temporary or permanent loss of control. If not restored, uncontrolled automatic flight. | Modern UAVs have automatic hover or slow decent functions in case of contact loss. | 1 | C | 4 | Ensure good radiolink and GPS contact before lift-off. Monitor signal strengths throughout the operation. Program good failsafe. | Simon | 1 | B | 3 | |
| 2.4 | | Loss of GPS signal | The UAV loses automatic functions. | Modern UAVs display errors and refuse to lift-off in case of bad or no GPS signal. | 3 | A | 4 | Set standard settings to slow decent, so that the operation crew can control the landing. Do not plan the operation based on GPS auto functions. | Simon | 3 | A | 4 | |
| 2.5 | | Ground station failure | Sensor readings and automatic flight will be unavailable. Only VLOS flight. | | | 2 | A | 3 | Keep software up-to-date and a reliable power supply. | | 2 | A | 3 |
| 2.6 | | Hacking | Complete loss of control, and the UAV can be used to cause harm to others. | Due to the location of wind turbines, it is very unlikely that hackers are in range of the UAV. | | 1 | E | 6 | Use firewalled computers, stay unconnected to the internet during flight. | Simon | 1 | E | 6 |
| 3.1 | | Insufficient pilot training | Loss of control of UAV, unaware of surroundings and potentially dangerous flight. | | | 1 | E | 6 | Check the pilot's qualifications and experience before flight. Ensure good training. | Simon | 1 | C | 4 |
| 3.2 | A participant makes a human error | Communication failure between pilot, ground station and other personnel | Unawareness can lead to collision, mission abort and/or loss of control. | | 2 | D | 6 | Plan the flight will all participants. Test communication equipment, develop communication routines and protocols. | Simon | 2 | C | 5 | |

| | | | | | | | | | | | | |
|-----|--|---|---|--|---|---|---|---|-------|---|---|---|
| 3.3 | | Intoxicated personnel | Unawareness and loss of control. Can lead to reckless flying. | | 1 | E | 6 | Establish a zero-tolerance of drugs and alcohol. Abort if personnel are under the influence. | Simon | 1 | E | 6 |
| 3.4 | | Insufficient mission planning | Impact with obstacles or people. Bad scan results | | 1 | D | 5 | Carry out detailed reconnaissance of the site in question and thoroughly plan the mission in teams. | Simon | 1 | C | 5 |
| 3.5 | | Failure to spot obstacles in flight path. | Impact with obstacle, potentially destroying the UAV and causing damage to third-party equipment. | | 2 | E | 7 | Keep VLOS, have additional personnel dedicated to spotting obstructions. | Simon | 2 | C | 5 |
| 3.6 | | Failure to spot people | Can lead to severe and potentially lethal damage. | | 1 | E | 6 | Keep VLOS, have additional personnel dedicated to spotting obstructions. | Simon | 1 | E | 6 |
| 3.7 | | Insufficient pre-flight check | Can cause failure in critical components. Potentially temporary or complete loss of control of the UAV. Uncontrolled crash. | | 2 | D | 6 | Develop mandatory safety protocols and follow instructions issued by the UAV manufacturer. | Simon | 2 | C | 5 |
| 3.8 | | Stressed or fatigued pilot | Can lead to inaccurate flying and loss of focus. Potential for reckless flight. | | 2 | C | 5 | Have the operation team evaluate each other's health and condition. Plan the operation well in advance. | Simon | 1 | B | 3 |
| 4.1 | The drone has a mechanical or electrical failure | Insufficient rotor attachment | Can make the UAV difficult to fly, potentially complete loss of control or emergency landing | Modern UAVs have self-tightening rotor blades. | 1 | C | 4 | Evaluate the rotors in the pre-flight check-list. | Simon | 1 | B | 3 |

| | | | | | | | | | | | | |
|-----|---------------------------------|---------------------------|--|---|---|---|---|--|-------|---|---|---|
| 4.2 | | Production defect | The drone platform can experience induced vibrations and potentially collapse. Complete loss of control and crash landing. | | 1 | D | 5 | Carry out test-flights before using the UAV in a operation. Inspect all UAVs for production defects before flight. | Simon | 1 | C | 4 |
| 4.3 | | Faulty payload attachment | Uneven weight distribution. Leads to high power consumption, mission abort or emergency landing. Potential for equipment detachment. | | 2 | D | 6 | Design reliable payload attachment. Have no personnel directly under the UAV, and test flight with payload before operation. | Simon | 2 | C | 5 |
| 5.1 | The drone has a sensor failure. | Gyro fails | Complete loss of UAV control. | Pre-flight check | 2 | D | 6 | Test the gyro during pre-flight checklist. | Simon | 2 | C | 5 |
| 5.2 | | Gimbal failure | The camera and video is useless. FPV or video results unavailable. | | 2 | A | 3 | Test gimbal during pre-flight checklist. | Simon | 2 | A | 3 |
| 5.3 | | Altimeter failure | The autopilot can lose track of current height. | VLOS allows pilot to take control if the UAV behaves suspiciously. | 2 | B | 4 | Test altimeter during pre-flight checklist. | Simon | 2 | B | 4 |
| 6.1 | The drone collides mid-air | Birds | Impact with a bird can cause temporary or permanent damage to the UAV. Lead to emergency landing or complete loss of control. | During VLOS flight, the pilot will control of UAV and the surrounding airspace. | 2 | C | 5 | Abort if birds fly in proximity to the UAV. | Simon | 2 | B | 4 |
| 6.2 | | Other UAVs | Can cause temporary or permanent damage to the drone. Will lead to emergency landing or complete loss of control. | During VLOS flight, the pilot will control of UAV and the surrounding airspace. | 1 | C | 4 | Abort if other drones are spotted or heard. | Simon | 1 | B | 4 |

| | | | | | | | | | | | | |
|-----|-------------------|---|---|--|---|---|---|--|-------|---|---|---|
| 6.3 | | Uncontrolled impact with wind turbine rotor blade | Can destroy the UAV and severely damage the rotor blade. | The pilot will have visual contact with the drone and the surrounding airspace at all times during flight. | 4 | E | 9 | Use rotor blade protection. Have advanced control systems. | Simon | 4 | B | 6 |
| 6.4 | | Manned air traffic | Can potentially damage the aircraft and lead to multiple fatalities. | RPAS Reg. does not permit flight in manned air traffic. Communicate with air traffic control at the airport. | 1 | E | 6 | Land immediately if helicopters or airplanes can be seen flying low. | Simon | 1 | E | 6 |
| 7.1 | The battery fails | Fire in the battery | Complete loss of UAV control. Fiery crash landing. Fire can spread once the UAV is on the ground. | Instructions issued by the UAV manufacturer states procedures of battery maintenance and pre-flight checks. | 2 | D | 6 | Keep a fire extinguisher ready for immediate firefighting. | Simon | 1 | C | 4 |
| 7.2 | | Damaged battery due to wrongfull use (charge/discharge) | Can greatly reduce battery life and capacity. Resulting in less airtime. | Instructions issued by the UAV manufacturer states procedures of battery maintenance and pre-flight checks. | 1 | B | 3 | | Simon | 1 | B | 3 |
| 7.3 | | Faulty readings on remaining battery capacity. | Battery can deplete unexpectedly. Will cause complete loss of control and crash. | Instructions issued by the UAV manufacturer states procedures of battery maintenance and pre-flight checks. | 1 | D | 5 | | Simon | 1 | C | 4 |

| | | | | | | | | | | | | |
|-----|---------------------|--------------------------------|---|---|---|---|---|---|-------|---|---|---|
| 7.4 | | Physical damage to the battery | The battery can have reduced capacity, catch fire or explode. | Instructions issued by the producer states procedures of battery maintenance and pre-flight checks. | 1 | D | 5 | | Simon | 1 | C | 4 |
| 8.1 | The weather changes | Wind suddenly increases | Reduced UAV control, emergency landing. | | 2 | C | 5 | Monitor the wind continuously. Abort if the windspeed increases. Check weather forecasts. Always have an emergency landing zone prepared. | Simon | 1 | B | 3 |
| 8.2 | | Unpredictable wind gusts | The wind can throw the UAV out of course. The UAV can crash and damage wind turbine rotor blade. | | 3 | E | 8 | Monitor the wind continuously. Abort if the windspeed increases. Check weather forecasts. Always have an emergency landing zone prepared. | Simon | 2 | D | 6 |
| 8.3 | | Precipitation | Can cause short-circuits and crash landing | All electronics are confined in a shell. | 1 | C | 4 | Pay attention to the skies and abort if participation occurs or is expected. Check weather forecasts. Always have an emergency landing zone prepared. | Simon | 1 | B | 3 |
| 8.4 | | Icing | Icing on drone can occur which will affect its stability. It may also cause electrical failure and lead to crash landing. | | 1 | C | 4 | If temperatures drop and the air is moist or foggy, land immediately. | Simon | 1 | B | 3 |

| | | | | | | | | | | | | |
|------|---------------------------------------|---|---|--|---|---|---|---|-------|---|---|---|
| 8.5 | | Temperature drops to extremely cold | Operation participants may find it uncomfortable and lose focus. The battery can have reduced performance. | | 1 | C | 4 | Keep the UAV in room temperature before flight. If icing is likely, abort mission. Make sure all participants are sufficiently dressed for the expected weather. Check weather forecasts and do not fly in very cold weather. Always have an emergency landing zone prepared. | Simon | 1 | B | 3 |
| 9.1 | Issues with surroundings | Excessive noise | Third-party can find the operation uncomfortable. | Noise from the UAV will be neglectable compared to wind turbine noise. Operation at remote location. | 1 | A | 2 | | Simon | 1 | A | 2 |
| 9.2 | | Conflict with landowner | Can cause social and legal complications | | 1 | B | 3 | | Simon | 1 | B | 3 |
| 9.3 | | Scaring third-party | People can find drones frightening and uncomfortable. | | 1 | B | 3 | Make sure everyone on-site is informed about the UAV operation. | Simon | 1 | B | 3 |
| 10.1 | Take-off and landing (drone handling) | Propellers spin while UAV is being handled. | Propellers can cut of fingers and do considerable damage to personnel. | The drone's propellers will not spin unless armed. | 2 | C | 5 | Do not arm the UAV before everything is ready for flight and people are at safe distances. | Simon | 1 | C | 4 |
| 10.2 | | People are too close to the UAV | During take-off and landing, the UAV can be unstable. Propellers or the kinetic energy of the drone can cause serious harm. | | 2 | C | 5 | Do not arm the drone before everything is ready for flight and people are at safe distances. | Simon | 1 | C | 4 |

| | | | | | | | | | | | | |
|------|--|--------------------------------|---|--|---|---|---|--|-------|---|---|---|
| 10.3 | | Bad take-off and landing site. | If the take-off and landing site has limited visibility and limited control, personnel may be harmed. | | 1 | C | 4 | Make sure the take-off and landing site is completely under control and has good visibility. | Simon | 1 | C | 4 |
|------|--|--------------------------------|---|--|---|---|---|--|-------|---|---|---|